1-1-2011

Base excision repair, folate deficiency and cancer

Archana Unnikrishnan
Wayne State University,

BASE EXCISION REPAIR, FOLATE DEFICIENCY AND CANCER

by

ARCHANA UNNIKRISHNAN

DISSERTATION

Submitted to the Graduate School

of Wayne State University,

Detroit, Michigan

in partial fulfillment of the requirements

for the degree of

DOCTOR OF PHILOSOPHY

2011

MAJOR: NUTRITION AND FOOD SCIENCE

Approved by:

_____
Advisor   Date

_____

_____

_____

_____

DEDICATION

This manuscript is dedicated in loving admiration to my father and mother, Unnikrishnan and Sarala, whose solid support and continued encouragement gave me the foundation and strength to pursue my research. Words cannot express my thanks to my husband, Prabhu and son Sachin, for their love, support, trust and more than anything else for their patience, over these past few years. I would like to express my thanks to my aunt, Maheshwari and brother, Nirmal for their constant motivation in my endeavor. Finally, I would like to extend my thanks to my parents-in-law, Mani and Rukmani, for their enthusiasm and support.

ACKNOWLEDGEMENTS

TABLE OF CONTENTS

LIST OF FIGURES

Chapter 1

Introduction

Genomic Stability:

Maintenance of genomic stability is an essential feature in preventing development of cancer. Prevention of DNA damage accumulation is also very vital in delaying the aging phenotype. When damages occur in the genome through replicative processes and /or through transcription associated mutagenesis, this damage becomes permanent, in the form of mutations which could potentially lead to chromosomal breakage and genomic instability. This increased genomic instability negatively alters both the carcinogenic and aging processes. There are many types of DNA repair mechanisms that have evolved to help maintain genomic integrity. Different types of damages encountered by DNA are repaired via specialized repair mechanism evolved to repair that specific damage. Most of the repair pathways and the enzymes functioning in these pathways are stress inducible genes and can be upregulated during stress.

DNA damages and mechanism of DNA repair:

Genomic integrity depends on the speed and fidelity with which the damages to DNA are repaired. As mentioned above, there are specific repair pathways for the different types of damages encountered by the DNA. The different kinds of damages to DNA and the types of repair mechanisms are briefly discussed below (1,2). The various insults the genomic DNA are exposed to can be classified as endogenous and exogenous damages. The *endogenous damages* include mainly replication errors, alkylating damages, Oxidative and hydrolytic damages arising from the surrounding water and cellular metabolism. Some of the hydrolytic damages encountered by the DNA are,

(i) Depurination/Depyrimidination of the nucleotides

(ii) Deamination of nitrogenous bases (e.g. Cytosine Deamination to Uracil).

The <u>oxidative damages</u> to the DNA include,

    (i) Ring-saturated pyrimidines like thymine glycols and cytosine hydrates

    (ii)Ring-opened purines forming FaPy products (formamidopyrimidine),

    (iii)8-oxoguanine,

    (iv)Damages arising from lipid peroxidation products like M_1G and etheno adduct

The various *exogenous insults* to the DNA are introduced by Physical and Chemical agents. Some of them are,

    (1) <u>Physical agents</u> like ionizing radiations (e.g. oxidative damages), Ultraviolet rays (e.g. Cyclobutane dimers and DNA double strand breaks) and Heat

    (2) <u>Chemical agents</u>: (i) direct acting – Alkylating agents, (ii) Indirect acting requiring activation like Benzopyrene.

Despite the large exposure of the DNA to these damages, only a few accumulate as stable heritable mutations. This lower frequency for mutations shows the existence of Extensive repair mechanisms which very efficiently removes the damages to the DNA. Different caretaker/repair pathway has evolved to deal with all types of insult suffered by the DNA. The biological response pathway to DNA damage can be classified as,

    (1) Reversal of damage

    (2) Excision of damage

    (3) Tolerance of damage

Reversal of Damage: Simplest repair mechanism requiring no knowledge of genetic information. Repairs both single and double stranded DNA. This mechanism involves single enzyme that catalyzes

direct reversal of damage. This is a highly specific, error free energetically expensive repair mechanism. Few examples are as follows,

A) Reversal of cyclobutane pyrimidine dimers and (6-4) photoproduct by photolyases utilizing light of a specific wavelength. Hence the reaction called as Photoreactivation. This process is absent in eukaryotes.

B) Reversal of O^6alkyl guanine and other related alkylated products (e.g. MGMT)

C) Reversal of N^1 alkyl A and N^3 alkyl C (ABH2 & ABH3)

Excision of Damage/ Excision repair: The pathway for most type of damages incurred by the DNA. Excision repair deals with double stranded DNA. In this pathway, the damaged/incorrect nucleotides will be excised out and replaced with appropriate nucleotides using the genetic information from the complementary DNA strand. There are three kinds of excision repair pathway,

(i) Base Excision repair

(ii) Nucleotide excision repair and

(iii) Mismatch excision repair

All three excision pathways involve five steps to execute the repair. They are: 1) Damage recognition, 2) Incision of the DNA strand on either side of the damage, 3) Excision of the damaged nucleotide/oligonucleotide, 4) Replacement synthesis of new DNA, 5) Ligation

Base excision repair pathway (BER): BER pathway is involved in the repair of endogenous damages that arise spontaneously in the living cell. This pathway repairs nucleotides with small base adducts like oxidized bases (e.g. 8-oxoG), hydrolytically deaminated bases (e.g. Cytosine to Uracil) and alkylated bases (e.g. 3-methyl adenine). BER usually replaces a single damaged nucleotide and sometimes can replace up to 6 nucleotides hence classified as short patch and long patch BER.

The initial step in BER involves highly specific DNA glycosylases which recognizes and removes altered bases creating an abasic site (AP site). AP site can also arise due to spontaneous hydrolysis of the N-glycosidic bonds linking the purine/pyrimidine base to the deoxyribose residue. The second step occurs with the help of apurinic/apyrimidinic endonucleases which creates an incision 5' to the abasic site. The resulting sugar phosphate is removed by a deoxyribophosphodiesterase and the gap created is filled with a new appropriate nucleotide by DNA polymerase. Many studies with cells/tissues show that DNA polymerase β is responsible for the gap filling reaction. After the repair synthesis of the DNA the nick is sealed enzymatically by ligase which marks the completion of the repair pathway.

Mismatch Repair pathway (MMR): This pathway predominantly repairs replication errors and also when there is insertion or deletion of nucleotides in DNA. The mismatch repair system is efficient enough to discriminate the incorrect base from the correct base in a mispair as both the bases would be a normal base of the DNA. Mismatch repair involves five main events in its pathway. They are: i) Recognition of the mismatch (e.g. Mut S or Msh), ii) Strand discrimination to identify the incorrect base in the daughter strand. Unmethylated daughter strand in prokaryotes and daughter strands with nicks arising during replication in eukaryotes act as markers for strand discrimination, iii) Incision on either 5' or 3' side of the mismatch (Eukaryotic Mlh and prokaryotic Mut L and Mut H help in this process), iv) Unwinding of DNA by helicase and Excision of the damage by Exonuclease (e.g. Exo1) and v) Resynthesis of the DNA by Polymerase (e.g. pol δ) and Ligation by Ligase leading to completion of repair.

Nucleotide Excision repair (NER): NER repairs large and bulky helix distorting adducts to DNA like the ones created by carcinogens (e.g. Benzopyrene, Cis-platin), UV (e.g. cyclobutane pyrimidines dimers) and some oxidative adducts. The enzymes involved in BER and MMR have strict substrate specificity whereas the enzymes in NER have a very broad specificity accommodating a large number of substrates. NER also involves five distinct steps ,they being : i) Recognition of damage by DNA binding protein which also unwinds the DNA , ii) Incision of the damaged DNA strand on either side of the bulky adduct by endonucleases. One incision is made at 22nd or 24th phosphodiester bond 5' to the damage and the

second incision made at the 5th phosphodiester bond 3' to the damage, iii) Excision of a 27-29 oligomer containing the damage creating a gap, iv) Repair synthesis to fill the gap by Polymerase (e.g. pol δ and ε) and v) DNA ligation by Ligase. Prokaryotic NER requires 3 proteins (UvrABC endonuclease) for recognition and incision steps whereas Eukaryotic NER requires 16 proteins. NER in human cells requires 25 proteins including seven associated with the genetic disease Xeroderma Pigmentosum (XP).

Damage Tolerance: Certain biological responses to DNA damage, does not remove the damaging lesion and replace it with normal DNA constituents like the repair mechanism. These biological responses postpones repair to alleviate the then condition like arrested replication fork. Such mechanisms are called as DNA damage tolerance mechanism and they are different from the classic Repair pathways. There are three kinds of damage tolerance mechanism, they are: i) Recombinational repair, ii) Replication fork regression and iii) Tranlesion DNA synthesis.

Recombinational repair: Recombinational repair helps in the repair of arrested replication forks created by various DNA damages like bulky adducts, single and double strand DNA breaks. This process helps in reinitiating DNA synthesis after a replication fork arrest, a little downstream of the arrested fork creating a gap. This gap will be filled by strand exchanges between the altered DNA and unaltered newly synthesized DNA. The original damage is not removed but will be tolerated to be repaired later. This is an error- free mechanism as the damaged strand will not be used as template.

Replication fork Regression: The arrested replication fork folds back allowing the newly synthesized strand to be used as template instead of the damaged DNA strand. This again is a error-free mechanism.

Tranlesion DNA Synthesis: Specialized polymerases like polymerase η catalyze the replication bypass past the DNA damaged sites in the template. These polymerases have poor fidelity making them error-prone and are associated to mutagenesis.

Having understood the mechanism of different DNA repair processes, many laboratories are conducting research to understand the integrity of these pathways in a cancer model and also researching

on how different environmental factors inclusive of dietary manipulations such as caloric restriction and folate deficiency affect these repair pathways.

Folate deficiency and Genomic instability:

Folate plays an important role in DNA metabolism (3). Folate and its intermediates forming the folate cycle are very important for the maintenance of genomic stability. Folate is involved in one carbon transfer mainly in the form of methyl group. As illustrated in the figure, folic acid intermediate 5-methyltetrahydrofolate helps in the regeneration of methionine from homocysteine.
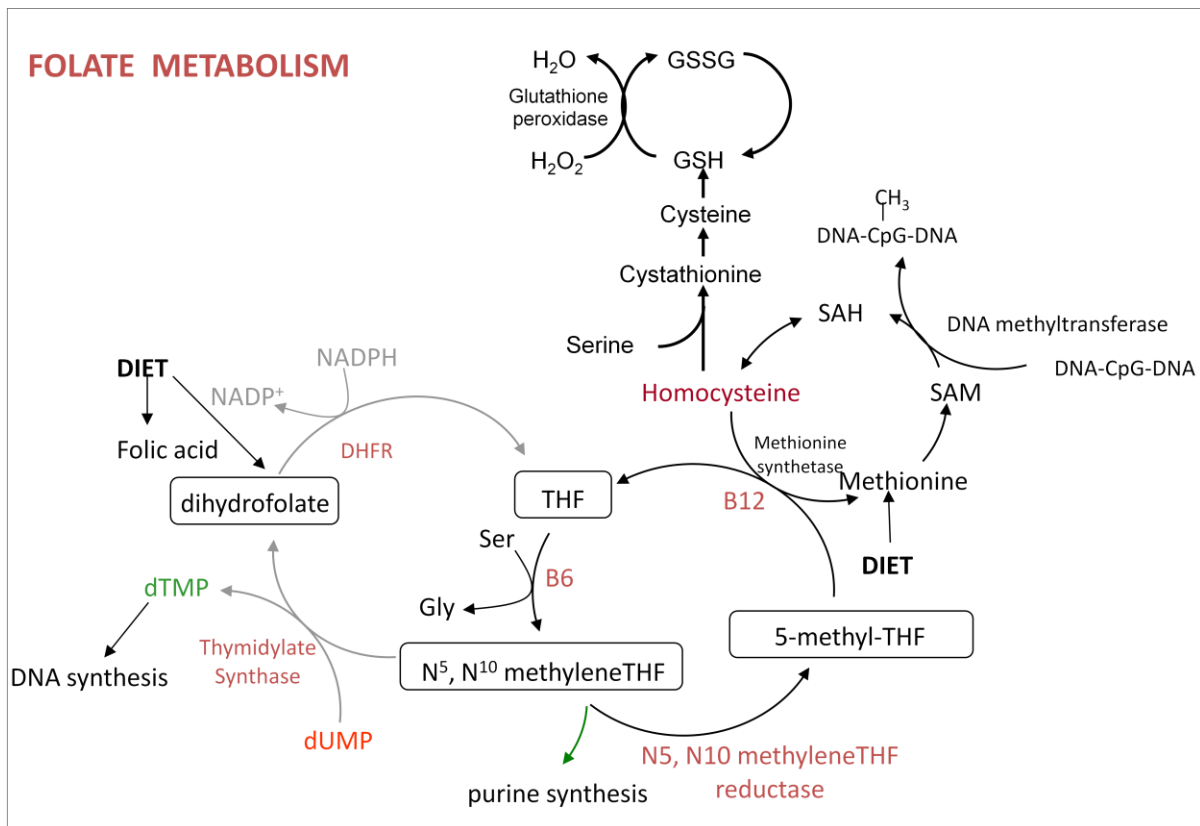
Methionine in turn helps in the formation of S-adenosylmethionine (SAM), the primary intracellular methyl donor which plays a key role in epigenetic regulation of gene expression. SAM methylates cytosine residues in the CpG sites of DNA. This cytosine methylation regulates gene transcription. During FD, SAM levels are reduced affecting DNA methylation, altering gene expression potentially leading to proto-oncogene expression (4-7). Unmethylated cytosines arising due to low levels of SAM can undergo spontaneous deamination to thymine (8). Folate also helps in the formation of thymine from

Uracil with 5, 10-methylenetetrahydrofolate acting as a methyl donor to Uracil which is crucial for DNA synthesis and repair (9). Oxidized form of 5, 10 methylene tetrahydrofolate, 10-formyltetrahydrofolate is required for the denovo synthesis of purines (10,11). When folate is depleted the nucleotide pool is affected impacting on DNA stability, synthesis and repair. Reduced synthesis of thymidylate during Folate deficiency (FD) leads to increased Uracil misincorporation into the DNA. Misincorporated Uracil in DNA and Uracil arising from deamination of cytosine would lead to U:G mispairing and finally C:G to T:A transitions if not repaired before replication (12,13). This misincorporation can cause DNA strand breaks (14), deletions, chromosomal breaks, micronucleus formation (15,16) and loss of heterozygosity, which can activate proto-oncogenes and inactivate tumor suppressor genes (17-19) all contributing to the increased risk of cancer (18,20)

Folate deficiency and cancer

The prevalence of folate deficiency remains in the US population in spite of efforts to eliminate folate deficiency through fortification of grain products (21). Folate deficiency is an important public concern because of the role folate plays in the development of many different health problems, including neural tube defects, cardiovascular disease, Alzheimer's disease and cancer. A putative role for folate in protecting from cancer is suggested by the substantial amount of epidemiologic data suggesting that a diet high in fruits and vegetables protects against the development of cancer (22,23). As these foods are rich in sources of folate, this suggests a role for dietary folate in this protective effect of fruits and vegetables. Other nutrients and phytochemicals present in fruits and vegetables may also exert this protective role.

In support of a role for folate is the growing body of data linking folate deficiency to specific types of cancer. The strongest such link exists in the connection between folate status and colon cancer. Additionally, folate deficiency is related to cancers of the lung, cervix, brain, esophagus, pancreas and breast (22,24). Also low folate diets have been found to increase premalignant cervical dysplasia (25) and to increase breast cancer risk when combined with excessive alcohol consumption (26). On the other hand

when folate intake is increased it has been found to decrease squamous metaplasia of bronchial epithelium (27). Additionally a decline in gastric cancers has been found to parallel the decline in neural tube defects (28), which is known to occur with folate supplementation. In an animal model of colon carcinogenesis, folate deficiency enhances the carcinogenic effect of dimethylhydrazine (29) while excess folate significantly reduced the number of macroscopic neoplasms in this same model of dimethylhydrazine-induced tumorigenesis (30).In the apcMin mouse, increasing dietary folate significantly reduces the number of ileal polyps and aberrant crypt foci (ACF) found at 3 months (31). Human cultured colonocytes exposed to a folate deficient medium showed accumulation of strand breaks and Uracil misincorporation, in response to oxidative and alkylation damage (61). In addition, folate supplementation in patients with recurrent adenomatous polyps of the colon showed a decrease in colonic mucosal cell proliferation (32).However, folate has also been found to increase neoplastic transformation in preneoplastic cells and a deficiency in folate has been found to be protective in preventing progression of tumors (33). Studies have shown that high levels of folate in a procarcinogenic environment promote the progression of colon cancer (30,34,35). This paradox may be explained by differences in animal models studies, differences in the severity of folate deficiencies instituted, and/or differences in the stage of cancer being assessed. In fact folate deficiency in preneoplastic cells may act in much the same way that methotrexate act, by causing genetic damage (i.e. Uracil incorporation) in rapidly dividing cells. Nonetheless, these last data provide an absolute indication that recommendations about folate supplementation and requirements must take into consideration the population under investigation.

Folate Deficiency and Oxidative stress:

Oxidative stress and Reactive oxygen species (ROS) are established factors in the genesis of cancer. Free radicals and oxidative stress induced redox imbalance have been implicated in many types of cancer (36). Oxidative stress leads to damages to the genome which acts as an initiating point in tumorigenesis. Also folate deficiency plays an important role in the pathogenesis of cancer. Uracil misincorporation, imbalance in DNA synthesis by alterations in the denovo synthesis of purines and

pyrimidines, alterations in the SAM: SAH ratio and modifications of DNA repair pathways are some of the consequences of folate deficiency implicated in development of cancer. Apart from these effects, folate deficiency can potentially lead to carcinogenesis by creating oxidative stress. Folate deficiency leads to increase in homocysteine levels, which is a pro-oxidant and has been implicated in neurological disorders, cardiovascular diseases and carcinomas (37-40). Increased homocysteine levels leads to increased hydrogen peroxide formation (41,42). Therefore folate deficiency by way of elevated homocysteine concentrations creates oxidative stress in rodents (43). Moreover, folate and its intermediates are involved directly in free radical scavenging (44). Hence depletion of the same could lead to increased ROS and oxidative stress. It would be interesting to elucidate the role of oxidative stress in folate deficiency induced cancer and the same will be addressed in this study.

Folate Deficiency and Base Excision repair   Folate has several specific functions that make it inviting to hypothesize about the mechanisms of its role in carcinogenesis. It has been proposed that the
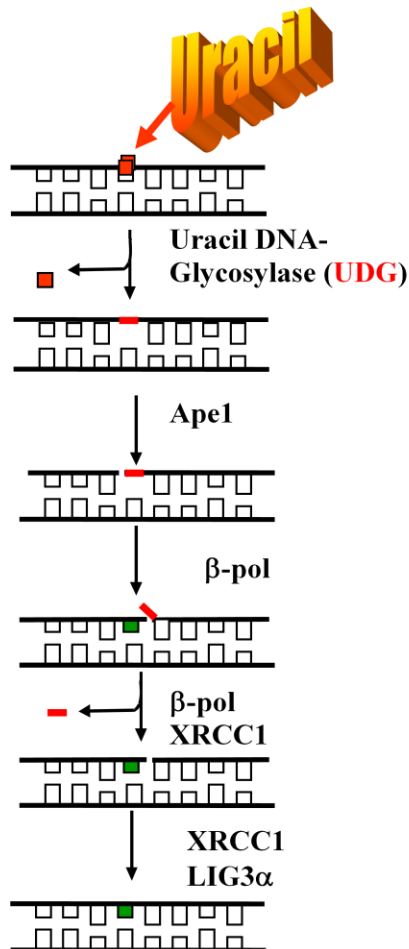
carcinogenic properties of folate deficiency may be related to a decrease in DNA methylation, perhaps as a function of reduced S-adenosylmethionine (SAM) levels, and/or to an increase in the uracil content of DNA. Both hypomethylation (45) and uracil incorporation (14,18,31,46,47) are solidly established effects of folate deficiency.   While Uracil is not a normal constituent of DNA it can arise in DNA during replication when dUMP:dTMP ratios are imbalanced. It may also arise as a result of the deaminations of cytosine. Based on a genetic reversion assay (48) it can be conservatively estimated that this occurs approximately 50 times per cell per day in the human genome. But, in the presence of low SAM levels (as occurs in folate deficiency) the rate of cytosine deaminations increases as much as 10,000-fold (8). This is

supported by data showing that SAM inhibitors have a similar effect on deaminations rates (49). The deamination of cytosine yields uracil, and even a fraction of this amount of DNA damage would likely stress or overwhelm the repair pathway for uracil in DNA.

The DNA repair pathway for removal of uracil is the base excision repair (BER) pathway as depicted in the figure. The BER pathway is believed to repair small, non-helix-distorting lesions in the DNA. It has been estimated to be responsible for the repair of as many as one million nucleotides per cell per day (50), stressing its importance in the maintenance of genomic stability. It has been suggested that BER has evolved in response to in vivo exposure of DNA to ROS and endogenous alkylation, and that this pathway suppresses spontaneous mutagenesis (51).

BER is also the main repair pathway for the repair of oxidative damages like 8-OHdG, which mispairs with Adenine. 8-OHdG is repaired by 8-oxoguanine DNA glycosylase (OGGI), a bifunctional enzyme involved in the initial step of BER.

Several lines of evidence suggest a reduced ability to process DNA damage when folate deficiency is present. Duthie and Hawdon (14) have shown that folate depletion in human lymphocytes makes the cells more sensitive to oxidative damage induced by hydrogen peroxide. Duthie et al. (31) have further shown that human colon epithelial cells grown in the absence of folate are poorly able to repair damages induced by MMS (an alkylating agent) and hydrogen peroxide (an oxidizing agent). Data from our lab show that folate deficiency reduces the efficiency of BER by inhibiting the DNA damage inducibility of DNA polymerase beta, the rate limiting enzyme of the pathway (52). With the major pathway, designated to repair oxidative damages like 8-OHdG, being compromised during folate deficiency, the oxidative stress impact of folate deficiency should be further enhanced. This effect of folate deficiency and its role in the pathogenesis of cancer will be addressed in this study.

METHIONINE RESTICTION

Methionine, an essential amino acid, is involved in the folate cycle where 5-methyl Tetrahydrofolate helps in the regeneration of methionine from homocysteine. Methionine and folate are part of the same folate metabolic cycle, alterations in which are implicated in many pathological conditions.

Folate deficiency causes uracil misincorporation, imbalance in dNTP pools, SAM: SAH ratio and potentially oxidative stress via alterations in redox balance and increase in homocysteine, a pro-oxidant. All these effects of folate deficiency could lead to tumorigenesis.

Another component of the folate metabolic cycle, methionine has been shown to have beneficial effects when restricted. Methionine restriction (MR) has been reported to reduce mitochondrial ROS production and increase life span in laboratory rodents (53,54). And methionine restriction has also been shown to inhibit colon carcinogenesis in rats when exposed to Azoxymethane (55). Tumor cells have been shown to be more sensitive than normal cells to methionine restriction. Studies have reported the induction of apoptosis by MR in cancer cell lines (56,57).However, there have been studies that show the role of free and protein bound methionine as antioxidants, required for the stability of proteins (58,59). The only protein repair system identified so far is the methionine sulfoxide repair system involved in repairing oxidative damages to methionine (Methionine sulfoxide) in a protein molecule. Two major enzymes in this pathway are Methionine sulfoxide Reductase A (MSRA) and Methionine sulfoxide Reductase B (MSRB) each for the S and R stereoisomers of methionine sulfoxide respectively. Many studies have shown the importance of the optimum activity of this repair system. Knockout mouse models (MsrA^{-/-}) show increased sensitivity to oxidative stress and decreased life span (60).With these accumulating evidences for the role played by Methionine in regulating the redox status and providing protection against cancer, it would be interesting to elucidate the effect of folate deficiency on Methionine pool.

Chapter 2

Background, Significance and Specific Aims

Folate deficiency has been implicated in the genesis of many types of cancer especially colon cancer. While the mechanism by which folate deficiency increases cancer risk is not well understood, it has been demonstrated to alter both DNA damage accumulation and DNA methylation. Some of the well established consequences of folate deficiency are modifications in DNA methylation, increase in DNA damages such as single strand breaks, micronucleus formation, and mutation frequency. Recent studies from our laboratory indicate that FD results in: (i) uracil misincorporation into DNA, a damage repaired by DNA polymerase beta dependent Base excision repair (BER); (ii) inability to induce repair activity; (iii) increased accumulation of repair intermediates; (iv) increased sensitivity to exogenous ROS and alkylation damage; (v) chromosomal instability; and (vi) inhibition of DNA damage inducibility of DNA polymerase beta creating a functional BER deficiency.

Base excision repair pathway is the pathway responsible for repairing non helix distorting damages such as oxidative damages, alkylation damages and misincorporated uracil, which occurs more frequently during folate deficiency. Base excision repair pathway is initiated by a glycosylase which removes the damaged base. Subsequently an endonuclease removes and the abasic site and the DNA polymerase add the new nucleotide. Ligase further seals the nick completing the repair. In this co-ordinated repair process different enzymes act as rate determining factors while repairing different types of damage. The endonuclease, APE1/Ref-1 has been suggested to be the rate limiting enzyme during the repair of oxidative damages in cell cultures, whereas DNA polymerase β has been shown to be rate limiting while repairing misincorporated uracil. Previous data from our lab shows, incapacitation of the base excision repair pathway during folate deficiency. We have previously demonstrated the accumulation of toxic repair intermediates such as abasic sites and single strand breaks during folate deficiency. Furthermore, apart from uracil misincorporation, folate deficiency also can potentially lead to

oxidative damages. Folate deficiency leads to the accumulation of homocysteine, a pro-oxidant and inhibits the regeneration of methionine, an antioxidant. Studies have shown that increased homocysteine leads to increased production of hydrogen peroxide, a potent oxidative stress inducing factor. These effects of folate deficiency taken together with the fact that BER is the major pathway involved in the repair of all damages associated to folate deficiency, impairment of base excision repair during FD could potentially lead to tumorigenesis. Therefore, it is important to understand the exact mechanism behind folate deficiency induced inhibition of base excision repair pathway.

Methionine, another important component of the folate cycle, interestingly, on its restriction has been shown to reduce production of mitochondrial reactive oxygen species and extend life-span in laboratory rodents. In addition methionine restriction has been shown to provide protection against colon cancer. In other words, folate and methionine, components of the same folate metabolic cycle show differential effect when depleted individually. Therefore, in this study we determined the impact of folate deficiency and methionine restriction on base excision repair pathway in response to a carcinogen. We also evaluated the development of preneoplastic lesions during folate deficiency and methionine restriction. Further, we directly tested the impact of APE1/Ref-1 haploinsufficiency during oxidative stress using an APE1/Ref-1 haploinsufficient mouse model. These studies have important health implications, as polymorphisms in genes involved in the folate cycle and base excision repair pathway within human population may render individuals functionally deficient in these nutrients and repair increase their risk for cancer development.

Study 1: To determine whether oxidative stress alters base excision repair pathway and increases apoptotic response in apurinic/apyrimidinic endonuclease 1/refox factor-1 haploinsufficient mice. Utilizing mice containing a heterozygous gene targeted deletion of APE1/Ref-1 we determined the impact of this haploinsufficiency on the processing of oxidative DNA damages induced by 2-nitropropane in the liver tissue of mice. Using this model we directly tested the hypothesis that APE1/Ref-1is rate limiting in an oxidative stress mediated base excision repair process. We also tested the impact of this APE1/Ref-1

haploinsufficiency on NF-kB DNA binding activity and the apoptotic capacity in response to oxidative stress created by 2-nitropropane.

Study 2: To determine whether folate deficiency regulates the expression of DNA polymerase b in response to oxidative stress. That is to test whether folate deficiency inhibits the upregulation of b-pol during oxidative stress. We in this study show the inhibition in the upregulation of b-pol during folate deficiency in response to a carcinogen. We further determined the mechanism behind this inhibition in b-pol expression. We evaluated the alterations in DNA methylation in b-pol promoter during folate deficiency to check whether folate deficiency mediated inhibition of b-pol is via epigenetic alterations. Furthermore, using techniques such as DNA footprinting and gel shift assays, we determined the hot spot regions in the b-pol promoter which makes the gene more susceptible during folate deficiency and oxidative stress. Through this study we hoped to dissect out the mechanism of deregulation of b-pol by folate deficiency.

Study 3: To determine the impact of folate and methionine dietary interventions on base excision repair pathway and preneoplastic lesion development in colon in response to a carcinogen. As stated previously, folate and methionine are components of the same folate cycle but show differential impact on cancer development. Here, we determined the development of preneoplastic lesions, i.e., aberrant crypt foci, during folate deficiency and methionine restriction in the colon of mice in response to 1,2-dimethylhydrazaine , a potent colon and liver carcinogen. We also studied the impact of these dietary interventions on the base excision repair pathway in the liver tissue of mice in response to 1,2-dimethylhydrazaine treatment. For this purpose we evaluated the effect of these diets on the individual enzymes in this pathway. We also determined the impact of folate deficiency and methionine restriction on the apoptotic capacity of mice in response to a carcinogen.

Chapter 3

Oxidative stress alters base excision repair pathway and increases apoptotic response in Apurinic/apyrimidinic endonuclease 1/Redox factor-1 haploinsufficient mice

Archana Unnikrishnan[1*], Julian J. Raffoul[1*], Hiral V. Patel[1], Thomas M. Prychitko[1], Njwen Anyangwe[1],

Lisiane B. Meira[3], Errol C. Friedberg[4], Diane C. Cabelof[1,2], and Ahmad R. Heydari[1,2]

[1]Department of Nutrition & Food Science, Wayne State University, Detroit, MI, 48202, USA

[2]Barbara Ann Karmanos Cancer Institute, Wayne State University School of Medicine, Detroit, MI, 48201, USA

[3]Biological Engineering Division, Massachusetts Institute of Technology, Cambridge, MA, 02139, USA

[4]Laboratory of Molecular Pathology, Department of Pathology, The University of Texas Southwestern Medical Center, Dallas, TX, 75390, USA

*The two authors Archana Unnikrishnan and Julian J. Raffoul contributed equally to this work.

Address correspondence to: Ahmad R. Heydari, Ph.D., Department of Nutrition & Food Science, Wayne

State University, Detroit, MI, 48202, Tel: 313-577-2459, Fax: 313-577-8616, E-mail:

ahmad.heydari@wayne.edu

Abstract

Apurinic/apyrimidinic endonuclease 1/redox factor-1 (APE1/Ref-1) is the redox regulator of multiple stress-inducible transcription factors, such as NF-κB, and the major 5'-endonuclease in base excision repair (BER). We utilized mice containing heterozygous gene-targeted deletion of APE1/Ref-1 ($Apex^{+/-}$) to determine the impact of APE1/Ref-1 haploinsufficiency on the processing of oxidative DNA damage induced by 2-nitropropane (2-NP) in the liver tissue of mice. APE1/Ref-1 haploinsufficiency results in a significant decline in NF-kB DNA binding activity in response to oxidative stress in liver. In addition, loss of APE1/Ref-1 increases the apoptotic response to oxidative stress where a significant increase in GADD45g expression, p53 protein stability and caspase activity are observed. Oxidative stress displays a differential impact on monofunctional (UDG) and bifunctional (OGG1) DNA glycosylase initiated BER in liver of $Apex^{+/-}$ mice. APE1/Ref-1 haploinsufficiency results in a significant decline in the repair of oxidized bases (e.g., 8-OHdG), while removal of uracil is increased in liver nuclear extracts of mice using an *in vitro* BER assay. $Apex^{+/-}$ mice exposed to 2-NP displayed a significant decline in 3'-OH-containing single-strand breaks and an increase in aldehydic lesions in their liver DNA suggesting an accumulation of repair intermediates of failed bifunctional DNA glycosylase initiated BER.

Introduction

An imbalance between pro-oxidants and anti-oxidants within the cellular milieu promotes a chronic state of oxidative stress which can damage DNA and other macromolecules within the cell [62]. The steady-state accumulation of oxidative damage is thought to be an important mechanism underlying aging and age-related diseases such as cancer [63,64]. In order to maintain DNA integrity, cells employ elaborate DNA repair mechanisms of which base excision repair (BER) is the most versatile and the pathway of choice for repairing oxidative damage, single-strand breaks, and other small, non helix-distorting DNA damage [65-67].

Apurinic/apyrimidinic (AP) endonuclease 1 (APE1) was originally characterized as an endonuclease that cleaves the backbone of double-stranded DNA containing AP sites [68,69]. Subsequently, APE1 was shown to possess 3'-phosphodiesterase, 3'-phosphatase, and $3' \rightarrow 5'$ exonuclease activities [70]. APE1 was also independently characterized as redox factor-1 (Ref-1), a redox activator of cellular transcription factors [71,72]. APE1/Ref-1 participates in cellular signaling via activation of multiple transcription factors involved in the cellular stress response, such as NF-κB [73]. Studies of NF-κB DNA binding indicate a mechanism that is redox regulated by and dependent upon APE1/Ref-1. For example, APE1/Ref-1 was shown to enhance the DNA binding activity of NF-κB *in vitro* as well as NF-κB-dependent transcriptional activation *in vivo* [74]. Furthermore, deletion of the redox-sensitive domain of APE1/Ref-1 significantly inhibited TNF-induced NF-κB activation [75]. Loss of APE1/Ref-1 also resulted in decreased NF-κB DNA binding and transcriptional activation, in addition to increased susceptibility to TNF-induced apoptosis [76,77]. These findings establish APE1/Ref-1 as an essential upstream signaling molecule regulating NF-κB.

Research focused on understanding the role of APE1/Ref-1 in the BER response to oxidative stress provides insight into its multifunctional activity. Initially, BER was believed to be a simplistic linear pathway involving damage recognition and removal, followed by base insertion and nick-sealing

activity, requiring only four enzymatic reactions [78]. However, recent studies have indicated that BER is a dynamic and environmentally responsive DNA repair pathway [79, 80], with individual BER enzymes being induced by oxidizing agents [81, 82]. Our laboratory has demonstrated that both BER activity and DNA polymerase β (β-pol) levels increase in response to the oxidative stress [83]. Research has also shown that APE1/Ref-1 expression is inducible by oxidative stress [84,85], while its down regulation increased sensitivity to DNA damaging agents [86,87] and its overexpression protected against oxidative stress-induced genotoxicity [88]. Recently, Fung and Demple [89] showed that APE1/Ref-1 repair activity is essential for cellular viability and indicate that APE1/Ref-1 redox activity may be dispensable. However, Izumi et al. [90] and Vasko et al. [91] present data supporting the notion that both functions of APE1/Ref-1, repair and redox, are essential for cell survival.

The objective of this study is to determine the functional importance of APE1/Ref-1 in the repair of oxidative damage *in vivo*. We provide evidence that in response to *in vivo* exposure to oxidative stress, an increase in BER activity, β-pol, and APE1/Ref-1 protein levels are observed. We also present data demonstrating increased activation of NF-kB in response to oxidative stress *in vivo*. To determine whether BER activity in response to oxidative stress is affected by reduced APE1/Ref-1, we utilized a mouse model of APE1/Ref-1 haploinsufficiency [*Apex*$^{+/-}$] previously characterized by our lab [92]. We find that oxidative stress displays a differential impact on monofunctional (UDG) and bifunctional (OGG1) DNA glycosylase initiated *BER* in *Apex*$^{+/-}$ mice. Oxidative stress results in a significant increase in UDG initiated BER activity, but a significant decline in the repair of oxidized bases (8-OHdG). We also observed reduced DNA binding activity of NF-kB in *Apex*$^{+/-}$ mice exposed to oxidative stress establishing a significant role for APE1/Ref-1 redox function in the activation of NF-κB in response to oxidative stress *in vivo*. Our data has relevant translational implications since APE1/Ref-1 variants have been identified in the human population [932], and variants in BER have been associated with increased cancer risk [94,954].

MATERIALS AND METHODS

Animals

The experiments were performed in young (3-6 month), wild-type and APE1/Ref-1 heterozygous heterozygous (*Apex$^{+/-}$*) male C57BL/6 specific pathogen-free mice in accordance with NIH guidelines for the use and care of laboratory animals. Mice were backcrossed to C57BL/6 background. The Wayne State University Animal Investigation Committee approved the animal protocol. Mice were maintained on a 12-hr light/dark cycle and fed standard mouse chow and water *ad libitum*. Mice were anesthetized in a CO_2 chamber and sacrificed by cervical dislocation. Harvested liver was flash frozen in liquid nitrogen and stored at -70°C for further analysis.

DNA damage induction

Experimental mice were i.p. injected with 100 mg/kg body weight 2-nitropropane (2-NP; Aldrich Chemical Company, Chem. Abstr. Serv. Reg. No. [79-46-9]) dissolved in olive oil. Control mice were injected with olive oil vehicle. Mice were sacrificed after 24-hr. The dose and exposure time were based on previous studies characterizing the effect of 2-NP on DNA damage and repair induction [83].

Gene expression profiling

The mRNA expression level of APE1/Ref-1 was quantified using a real-time PCR-based pathway focused on gene expression profiling of mouse DNA damage. Total RNA was extracted from liver tissue of control and 2-NP-treated mice using TRIzol® Reagent [GibcoBRL, Rockville, MD]. First strand cDNA was synthesized from 1 µg RNA using random primers and purified using QIAquick PCR purification kit (Qiagen, Valencia, California). Gene-profiling was analyzed using Realtime PCR array (SuperArray, Frederick, MD) according to manufacturer's instructions. Briefly, a cocktail of cDNA samples was prepared using a supplied master mix and aliquoted into each well of a 96-well plate containing primer pairs specific for 84 genes involved in the DNA damage pathway, including 5 housekeeping genes. Among the 84 genes analyzed, changes in the expression of genes related to BER pathway were confirmed using real time PCR and reported herein. Expression of β-pol, UNG, OGG1 and GADD45g

were also quantified using real time PCR with RNA extracted from liver tissue of control and 2-NP treated mice. UNG primers were designed to detect both UNG1 and UNG2 message. Primer sequences used for β-pol, GADD45g, APE-1/Ref-1, UNG, OGGI, GAPDH and β-actin transcripts are detailed in Table 1. External standards for all the genes were prepared by subcloning the amplicons, synthesized using the primers listed in Table 1, into PGEM-T easy vector. The vectors were linearized using Ecor1 to make the standard curves. All gene transcripts were normalized to both GAPDH and β-actin.

Nuclear protein isolation

Nuclear proteins were isolated as previously described [92]. Briefly, nuclear extracts were isolated using transfactor extraction kit (Clontech, Mountain View, CA). The kit uses a hypotonic buffer to lyse the cell allowing the removal of cytosolic fractions and is followed by the extraction of nuclear proteins by a high salt buffer. All samples and tubes were handled and chilled on ice, and all solutions were made fresh according to manufacturer's protocol. Low molecular weight contaminants were removed from extracts by dialysis in 1L dialysis buffer (20 mM Tris-HCl, pH 8.0; 100 mM KCl; 10 mM NaS_2O_5; 0.1 mM DTT; 0.1 mM PMSF; 1 µg/ml Pepstatin A) for 4-hr at 4°C using Slide-A-Lyzer® mini-dialysis units (Pierce Biotechnology, Rockford, IL) with a molecular weight cut off of 3.5kDa. Dialyzed extracts were aliquoted and flash frozen in liquid nitrogen and stored at -70°C for subsequent analyses. Protein concentrations were determined according to Bradford using Protein Assay Kit I (Bio-Rad, Hercules, CA).

Protein expression analysis

Western blot analysis was performed using 200 µg nuclear protein as previously described [92]. Upon completion of SDS-PAGE, the region containing the protein(s) of interest was excised and prepared for western blot analysis while the remaining portion of the gel was stained with GelCode®Blue Stain Reagent (Pierce Biotechnology, Rockford, IL) to ensure equal protein loading. Manufacturer recommended dilutions of anti-sera developed against APE1/Ref-1 (Clone 13B8E5C2, Novus

Biologicals, Littleton, CO), β-pol (Ab-1 Clone 18S, NeoMarkers, Fremont, CA) and p53(Pab 240, Santa Cruz Biotechnology, Delaware, CA) were used to detect proteins of interest followed by incubation with HRP-conjugated secondary antibody (Santa Cruz Biotechnology, Santa Cruz, CA). As an internal control to ensure equal protein transfer, membranes were reprobed with anti-Lamin B antibody (Santa Cruz Biotechnology, Santa Cruz, CA) The bands were visualized and quantified using a ChemiImager™ System (AlphaInnotech, San Leandro, CA) after incubation in SuperSignal® West Pico Chemiluminescent Substrate (Pierce Biotechnology, Rockford, IL). Data are expressed as the integrated density value (I.D.V.) of the band per μg of protein loaded.

Electrophoretic mobility shift assay (EMSA)

A non-radioisotopic EMSA was used to determine the NF-κB and CREB DNA binding activity of nuclear extracts isolated from liver tissue of control and 2-NP-treated *Apex*$^{+/+}$ and *Apex*$^{+/-}$ mice according to the manufacturer's protocol (LightShift® Chemiluminescent EMSA kit, Pierce Biotechnology, Rockford, IL). Briefly, 40 fmol biotin-end-labeled DNA containing an NF-κB consensus sequence (5' AGTTGAGGGGACTTTCCCAGG 3'BTN from Panomics, Redwood City, CA) and CRE sequence with β-pol flanking region (-36..AGCCTGG**CGCGTGACGTCAC CGCG**CTGCGC..-7) was incubated with 10 μg nuclear extract in a 20 μl reaction mixture containing 1X binding buffer (100 mM Tris, 500 mM KCl, 10 mM DTT; pH 7.5), 2.5% glycerol, 5 mM MgCl$_2$, 50 ng/μl poly (dI-dC), and 0.05% NP-40. Negative controls (all components except nuclear extract) were included in all experiments. In competitive assays, 100X molar excess of unlabeled oligonucleotide was added to the reaction mixture. Samples were incubated for 20 min at room temperature then resolved on a 6% non-denaturing polyacrylamide gel in 0.5X TBE buffer. After electrophoresis, samples were transferred from the gel to a positively charged nylon membrane and cross-linked. Biotin-labeled protein/DNA complexes were detected by chemiluminescence and quantified using a ChemiImager™ System (AlphaInnotech, San Leandro, CA). Data are expressed as the integrated density value (I.D.V.) of the band per μg of protein loaded.

DNA base excision repair activity assay

The G:U mismatch repair assay is developed to measure monofunctional glycosylase-initiated base excision repair (BER) activity. Purified radio-end-labeled 30-bp oligonucleotides (upper strand: 5'-ATATACCGCGGUCGGCCGATCAAGCTTATTdd-3'; lower strand: 3' ddTATATGGCGCCG GCCGGCTAGTTCGAATAA-5') containing a G:U mismatch and a *Hpa II* restriction site (CCGG) were incubated in a BER reaction mixture containing 50 μg nuclear protein as previously described [90]. This repair assay uses a 30bp long oligonucleotide with G:U mismatch as no significant difference was seen in the catalytic efficiency of the in vitro assay when a plasmid or oligonucleotide was used as a substrate [96]. Repair of the G:U mismatch to a correct G:C base pair was determined via treatment of the duplex oligonucleotide with 20U of *HpaII* (Promega, Madison, WI) for 1-hr at 37°C and analysis by electrophoresis on a 20% denaturing 19:1 acrylamide/bis-acrylamide gel (SequaGel® Sequencing System, National Diagnostics, Atlanta, GA). Repair activity (presence of a 16-mer band) was visualized and quantified using a Molecular Imager® System (Bio-Rad, Hercules, CA) by calculating the ratio of the 16-mer product with the 30-mer substrate (product/substrate). Data are expressed as machine counts per μg of protein.

The *8-OH G:C* repair assay is utilized to measure bifunctional glycosylase- initiated BER activity. Fluorescein-end-labeled 30-bp oligonucleotides (upper strand: 5'-ATATACCGC GGGCG*GCCGATCAAGCTTATTdd-3'; lower strand:3' ddTATATGGCGCCGGCCGGCTAGTT CGAATAA-5',* G=8-hydroxydeoxyguanine) containing a Hpa *II* restriction site (CCGG) were incubated in a BER reaction mixture containing 50 μg nuclear protein as described previously [92]. The repair activity was determined as described above.

DNA damage analysis: Random oligonucleotide primed synthesis [ROPS] Assay

The relative number of single-strand breaks containing a 3'-OH group was quantified using a Klenow (exo⁻) incorporation ROPS assay as previously described [92,97]. This assay is based on the

ability of Klenow to initiate DNA synthesis from 3'-OH ends of single-strand DNA. Incorporation of α

(^{32}P) dCTP was quantified using a Packard scintillation counter. DNA for the ROPS assay was isolated

using Qiagen (Valencia, CA) gravity tip columns as described in the manufacturer's protocol. This

method generates large fragments of DNA (up to 150-kb) while minimizing shearing.

ASB Assay

Detection of aldehydic DNA lesions (ADLs) was carried out by ASB as described previously [98]

with slight modifications. DNA [8ug] from liver tissue was incubated in 30ul of phosphate-buffered

saline with 2 mM aldehyde reactive probe (Dojindo Laboratories, Kumamoto, Japan) at 37 °C for 10 min.

DNA was precipitated by the cold ethanol method and resuspended in 1X TE buffer overnight at 4 °C.

DNA was heat-denatured at 100 °C for 10 min, quickly chilled on ice, and mixed with an equal volume of

2 M ammonium acetate. The nitrocellulose membrane (Schleicher & Schuell) was prewet in deionized

water and washed for 10 min in 1 mM ammonium acetate. DNA was immobilized on the pretreated

nitrocellulose membrane using an Invitrogen filtration manifold system. The membrane was washed in

5X SSC for 15 min at 37 °C and then baked under vacuum at 80 °C for 30 min. The dried membrane was

incubated in a hybridization buffer (20 mM Tris, pH 7.5, 0.1 M NaCl, 1 mM EDTA, 0.5% (w/v) casein,

0.25% (w/v) bovine serum albumin, 0.1% (v/v) Tween 20) for 30 min at room temperature. The

membrane was then incubated in fresh hybridization buffer containing 100 ul of streptavidin-conjugated

horseradish peroxidase (BioGenex, San Ramon, CA) at room temperature for 45 min. Following

incubation in horseradish peroxidase, the membrane was washed three times for 5 min each at 37 °C in

TBS, pH 7.5 (0.26 M NaCl, 1 mM EDTA, 20 mM Tris, pH 7.5, 0.1% Tween 20). Membrane was

incubated in ECL (Pierce) for 5 min at room temperature and visualized using a ChemiImager™ system

(AlphaInnotech, San Leandro, CA).

Caspase Activity

Caspase-3 activity was measured using Enzchek Caspase-3 Assay kit No.1 (Molecular probes Eugene, OR). Briefly, Liver tissues were homogenized, and cytosolic extracts were isolated using transfactor extraction kit (Clonetech, Mountain View, CA). The extracts (250 $\square$g protein) were incubated for 2hr at room temperature in the working solution (25mM PIPES, pH 7.4, 5mM EDTA and 0.25% CHAPS) containing synthetic Caspase-3 substrate, Z-DEVD-AMC. Caspase mediated proteolytic cleavage of the substrate yields a bright blue-fluorescent product. An additional control assay was performed using reversible aldehyde inhibitor Ac-DEVD-CHO to confirm that the fluorescence observed in the sample assay was due to caspase activity. The fluorescence was measured using a fluorescence microplate reader (Genios plus, Tecan) at excitation:342nm, emission:441nm. The caspase activity was determined using an AMC (7-amino-4-methylcoumarin) standard curve (0-100uM), and reported as fluorescence per microgram of protein.

Statistical analysis

Statistical significance between means was determined using ANOVA followed by the Fisher's least significant difference test where appropriate [99]. P-values less than 0.05 were considered statistically significant.

RESULTS

Analysis of the liver tissue for APE1/Ref-1 expression and redox activity in response to 2-Nitropropane

Using the hepatocarcinogen 2-nitropropane (2-NP), we analyzed the impact of oxidative stress on the expression and redox activity of APE1/Ref-1 *in vivo*. Metabolism of 2-NP in liver generates reactive oxygen species (ROS) and promotes oxidative DNA damage, e.g., 8-oxo-7,8-dihydro-2'-deoxyguanosine (8-OHdG), both of which are believed to be one of the causative factors behind 2-NP-induced carcinogenesis [100]. 2-NP has also been shown to be genotoxic *in vitro*, inducing mutations in bacteria and unscheduled DNA synthesis in hepatocytes [101]. Our laboratory has demonstrated that 2-NP (100mg/kg body weight) induces levels of 8-OHdG [by 4-5 fold, p< 0.01], followed by a concomitant

increase in BER activity and β-pol protein levels [50%, p< 0.01] in liver tissues of mice and rats [83]. In addition, 2-NP is also shown to increase mutation frequency in liver tissues of these animals [83]. Using RT-PCR and Western blot analyses, we analyzed the expression of APE1/Ref-1 in response to 2-NP treatment. Our data show that 2-NP induces APE1/Ref-1 mRNA (Fig. 3.1A) and protein levels significantly (Fig. 3.1B) in the liver. Thus, we confirmed previous reports from cultured cells e.g. HeLa S3 tumor cells and WI 38 primary fibroblast [85] where expression of APE1/Ref-1 was shown to be inducible by oxidative stress and extended this observation to *in vivo* study establishing APE1 as a stress response gene,. Consequently, we examined the impact of 2-NP on DNA binding activity of NF-κB (Fig.3.1C). As expected, NF-kB DNA binding activity was significantly increased in response to oxidative stress in liver nuclear extracts. Furthermore, increase in NF-kB DNA binding activity was correlated with an increase in expression/activity of APE1/Ref-1, the redox activator of NF-kB. To determine the role of APE1/Ref-1 and its redox function in this process, we evaluated the activation of NF-kB DNA binding activity in response to 2-NP in mice heterozygous for the APE1/Ref-1 gene, i.e., *Apex*$^{+/-}$ mice.

Analysis of APE1/Ref-1 expression and redox activity in response to oxidative DNA damage in liver nuclear extracts of Apex$^{+/-}$ *mice.*

We determined whether reduced level of the APE1/Ref-1 gene in *Apex*$^{+/-}$ mice would impact the activation of NF-kB in response to oxidative damage generated by 2-NP treatment. APE1/Ref-1 protein level was significantly reduced in *Apex*$^{+/-}$ mice (Fig. 3.2), in addition, NF-κB DNA binding activity was reduced in *Apex*$^{+/-}$ mice suggesting that the redox activation of NF-κB and its consequent DNA binding activity is significantly reduced when the expression of APE1/Ref-1 is compromised (Fig. 3.3). The specificity of the NF-kB DNA binding activity in our assay is established as the shifted band is completely abolished using an oligonucleotide containing the NF-κB unlabeled consensus sequence (Fig. 3.3, Lane A). In agreement with our previous data [92], we confirmed that APE1/Ref-1 heterozygosity

promoted haploinsufficiency with respect to APE1/Ref-1 gene expression. In this study we established that wild-type mice exposed to 2-NP showed a significant increase in APE1/Ref-1 protein and redox activation of NF-kB *in vivo*, while mice haploinsufficient for APE1/Ref-1 showed similar response to oxidative stress via their intact allele, the ultimate level of induction was significantly lower in heterozygous mice reducing its redox capacity (Figs. 3.2 and 3.3). This suggests that the induction in APE1/Ref-1 expression and increased NF-kB activation in response to oxidative stress are dependent on APE1/Ref-1 genotype. Based on these data, it appears that the level of APE1/Ref-1 protein is instrumental in redox activation of NF-kB and its DNA binding activity *in vivo*.

Analysis of DNA damage intermediates in the liver tissue of Apex$^{+/-}$ mice

Data from our laboratory and other labs indicate that down regulation of APE1/Ref-1 promotes a damage hypersensitive phenotype [87, 92]. Thus, it was essential to determine the impact of APE1/Ref-1 haploinsufficiency on the level of DNA damage. We have previously reported the levels of AP sites, single-strand breaks and Aldehydic lesions in DNA isolated from liver of young *Apex$^{+/-}$* mice under normal condition. Interestingly, no significant difference in DNA damage in *Apex$^{+/-}$* mice as compared to wildtype counterparts was observed [97]. In this study, wild-type mice exposed to oxidative stress displayed a 2-fold induction in the level of 3'-OH-containing single-strand breaks (Fig. 3.4A) and no significant increase in the level of Aldehydic lesions (Fig. 3.4B). Interestingly, the level of 3'-OH-containing single-strand breaks was significantly lower in Apex$^{+/-}$ mice exposed to similar treatment as compared to their wildtype counterparts (Fig. 3.4A). However, the level of aldehydic lesions was significantly higher in Apex$^{+/-}$ mice exposed to oxidative stress as compared to wildtype animals (Fig 3.4B). We suggest that the processing of oxidized bases by a bi-functional DNA glycosylase such as OGG1 (8-oxoguanine DNA glycosylase) could result in generation of aldehydic blocking lesions at 3' end. Inability to process these 3' blocking groups in the absence of the 3'-phophoesterase activity of Apex in *Apex$^{+/-}$* mice [102], could result in lower detection of endonuclease-mediated single-strand breaks in the heterozygous animal.

Nevertheless, the decrease in the detection of 3'-OH-containing single-strand breaks in $Apex^{+/-}$ mice could also arise from an increase in β-pol-dependent BER capacity and rapid removal of oxidized bases and their repair-intermediates. Based on the findings that APE1 is not the rate limiting enzyme in Uracil initiated BER pathway [92,102] and emergence of AP endonuclease-independent BER pathway for repair of oxidized bases [103], upregulation in BER pathway could be the plausible mechanism for decline in 3'-OH-containing single strand breaks in $Apex^{+/-}$ mice exposed to oxidative stress. Accordingly, it has become important to evaluate BER capacity using a BER assay and determine the expression of its rate limiting enzyme, β-pol, in $Apex^{+/-}$ mice in response to oxidative stress. Understanding this mechanism is important as these data potentially sheds light on the means by which APE1/Ref-1 haploinsufficiency alters the DNA damage signal in $Apex^{+/-}$ mice.

Analysis of the BER response to oxidative DNA damage in the liver nuclear extracts of Apex$^{+/-}$ mice

We examined whether loss of APE1/Ref-1 affects the BER activity in liver in response to 2-NP-induced oxidative DNA damage *in vivo*. Using a G:U mismatch repair assay where APE1 endonuclease activity is essential, we analyzed the *in vitro* BER activity in $Apex^{+/-}$ mice and their wild-type counterparts in response to 2-NP treatment. For this assay we utilized a 30bp long oligonucleotide as no significant difference has been observed in the catalytic efficiency of the G:U mismatch assay when a plasmid or small oligonucleotide were used as substrate [96]. As expected, BER activity was significantly increased in response to oxidative stress in wildtype mice (Fig. 3.5A) with a concomitant increase in β-pol protein (Fig. 3.5B). We confirmed previous reports that mice haploinsufficient for APE1/Ref-1 display reduced *in vitro* BER activity (Fig. 3.5A) and β-pol expression (Fig. 3.5B). However, while the BER activity significantly declined in $Apex^{+/-}$ mice, much to our surprise this activity was significantly higher in $Apex^{+/-}$ mice treated with 2-NP as compared to its wildtype littermates. In other words, APE1/Ref-1 haploinsufficiency resulted in a significant increase in BER activity in response to oxidative stress. In

addition, we provide evidence that 2-NP treatment resulted in a significantly higher induction in β-pol expression/protein stability as compared to wildtype animals (Fig. 3.5B).

Regulation of eukaryotic gene expression is controlled, in part, though interaction of cis-elements within promoters of the genes with their associated DNA-binding factors. One of the candidates responsible for triggering induction of a specific gene by oxidative stress is the cAMP responsive element (CRE). The CRE sequence is present within the promoter of both the APE1/Ref-1 as well as the β-pol genes. Interestingly, mutational inactivation of CRE sequence in the APE1/Ref-1 promoter completely eliminates APE promoter activity in response to oxidative stress in cells [104]. In addition, the CRE sequence in human β-pol promoter has been shown to play a key role in the basal expression as well as induction of β-pol in response to DNA-alkylating agents [105,106]. Based on these findings, we propose that attenuation in the redox function of APE1/Ref-1 in *Apex*^{+/-} mice impacts the handling of oxidative stress perhaps via alterations in activation of factors such as NF-kB and consequently results in increased CREB binding activity that impacts the expression of the β-pol gene. In support of this notion, we determined whether APE1/Ref-1 haploinsufficiency alters ATF/CREB binding activity to CRE sequence within the β-pol promoter. In gel retardation experiments, the protein binding capacity of the CRE element was significantly increased in *Apex*^{+/-} mice in response to oxidative stress as compared to their wildtype littermates (Fig. 3.5C). The shifted band is completely abolished using an oligonucleotide containing the consensus CRE sequence as competitor (Fig 3.5C, Lane B) while using an oligonucleotide with mutational inactivation of the CRE site does not compete with the shifted band (Fig 3.5C, Lane A). Interestingly, the increase in CREB/CRE binding activity within the β-pol promoter in *Apex*^{+/-} mice corresponds to an increase in β-pol mRNA levels in heterozygous animals (Fig 3.5C). Based on these results, it appears that alteration in the redox function of APE1/Ref-1 enzyme impacts the handling of oxidative stress and consequently results in an oxidative DNA damage repair response, e.g., increased expression of β-pol gene.

Further, to directly determine the role of APE1/Ref-1 in the repair of oxidized bases, we used a 8-OHdG:C repair assay where APE1 3'-phosphoesterase activity are reported to be rate limiting [102]. As expected, the wildtype animals displayed an increase in 8-OHdG:C repair activity when exposed to 2-NP (Fig. 3.6A). However, while the *Apex*$^{+/-}$ mice showed similar response to 2-NP, the overall repair activity remained considerably lower for *Apex*$^{+/-}$ mice when compared to their wildtype counterparts (Fig. 3.6A). Additionally, to confirm the role of APE1/Ref-1 in repairing the oxidized base, the 8-OHdG:C BER assay was performed in the presence of APE1/Ref-1 purified protein. When purified APE1/Ref-1 (Novus biologicals, Littleton, CO) was added to the reaction mixture, the reduced BER activity was restored in control and 2-NP treated *Apex*$^{+/-}$ mice, while the wildtype mice displayed no noticeable differences (Fig. 3.6B). Taken together, these results confirm that APE1/Ref-1 plays an important role in the repair of oxidized bases (e.g., 8-OHdG) and that APE1/Ref-1 haploinsufficiency results in a significant decline in this repair activity, while monofunctional DNA glycosylase dependent BER activity is increased in these mice.

Analysis of Glycosylases in the liver of Apex$^{+/-}$ mice in response to oxidative DNA damage

To further confirm the impact of APE1/Ref-1 heterozygosity on the BER pathway, we determined the expression of two glycosylases responsible for initiating the repair of oxidative damage. Using Real time PCR we determined the expression of OGGI, a bi-functional glycosylase and UNG (Uracil DNA glycosylase), a monofunctional glycosylase. Both these glycosylases are involved in the removal of oxidized bases from DNA. There are two types of 8-Oxoguanine DNA glycosylase; OGG1 and OGG2 [107]. Hazra et al, [107] have demonstrated that both these enzymes are involved in processing oxidized bases, with OGG1 being involved in the removal of 8-OHdG paired with cytosine, thymine and guanine and OGG2 in responsible for the removal of 8-OHdG paired with Adenine. UNG has two isoforms arising from alternative splicing; UNG1 and UNG2 [108,109]. UNG 1 is a mitochondrial enzyme whereas UNG2 is found in the nucleus [108,109]. In addition to initiating uracil removal from DNA, UNG is also involved in the repair of Uracil derivatives like isodialuric acid, 5-hydroxyuracil and alloxan, derived

from oxidative damage to cytosine residues in the DNA [110], thus playing an important role in repair of oxidative damage. Interestingly, UNG expression follows the profile of β-pol and the G:U mismatch BER activity. In other words, mice treated with 2-NP showed significant increase in UNG expression with maximum induction seen in *Apex*$^{+/-}$ mice (Fig. 3.7A). Using a UDG activity assay as described by our laboratory [97], we determined the impact of oxidative stress on UNG activity in liver tissue of mice treated with 2-NP. Interestingly, oxidative stress resulted in a significant increase in UNG activity following the expression of UNG gene and BER activity (data not shown). However, OGG1 mRNA levels did not change significantly among the control and experimental groups (Fig. 3.7B). Interestingly, addition of purified human OGG1 (Novus biologicals, Littleton, CO) protein to BER reaction mixture did not increase OGG1 initiated BER activity in 2-NP treated *Apex*$^{+/-}$ mice (data not shown) suggesting that APE1/Ref-1 activity is essential for bifunctional DNA glycosylase initiated BER. Thus, upregulation in UNG expression and simultaneous increase in β-pol protein explain the increase in G:U mismatch BER activity in 2-NP treated *Apex*$^{+/-}$ mice (Fig. 3.5A). Conversely, lack of induction of OGG1 initiated BER in the liver tissue of *Apex*$^{+/-}$ mice exposed to 2-NP (Fig. 3.6A) are expected to increase oxidative DNA damage that drives apoptosis.

Analysis of Apoptosis in the liver of Apex$^{+/-}$ *mice in response to oxidative stress*

To characterize the effect of Ape1/Ref-1 heterozygosity on cell cycle arrest and apoptosis during oxidative stress, we analyzed three factors associated with apoptosis; GADD45g (Growth Arrest and DNA-damage-inducible, gamma), p53 and Caspase-3. GADD45g, a genotoxic stress inducible gene associated with cell cycle arrest and apoptosis was analyzed by real time PCR. The mRNA level of GADD45g was significantly increased in *Apex*$^{+/+}$ mice in response to 2-NP (Fig. 3.8A). Under control conditions, there was no effect of genotype on GADD45g expression (Fig. 3.8A), while in response to oxidative stress, expression of GADD45g was significantly greater in *Apex*$^{+/-}$ mice as compared to their wildtype counterparts. As a p53 responsive gene, we wanted to evaluate the role of p53 in GADD45g gene response. Using western blot assay, we determined the effect of Ape1/Ref-1 heterozygosity on p53

stability in response to oxidative stress in the liver nuclear extracts. p53, a tumor suppressor protein is a well established determinant of cell cycle arrest and apoptosis. p53 protein stability followed the same trend as GADD45g expression, with 2-NP treated $Apex^{+/-}$ mice displaying the highest level of p53 protein stability (Fig. 3.8B). We further analyzed the activity of caspase-3, one of the final effectors in the apoptotic pathway under the same conditions using liver cytosolic extracts. Caspase-3 activity was significantly induced in the 2-NP treated $Apex^{+/-}$ mice compared to its untreated counterpart (Fig. 3.8C). Thus, loss of APE1/Ref-1 increases the apoptotic response to oxidative stress.

DISCUSSION

APE1/Ref-1 is a multifunctional protein involved in the maintenance of genomic integrity and in the regulation of gene expression. In addition to its role in BER as the major 5'-endonuclease and 3'phosphoesterase, APE1/Ref-1 was independently characterized as a redox activator of cellular transcription factors. Although research has demonstrated that APE1/Ref-1 is involved in the cellular response to oxidative DNA damage, it is currently unclear whether this response is strictly due to APE1/Ref-1 repair activity, APE1/Ref-1 redox regulatory activity, or both. A study by Fritz et al. [111] suggests that APE1/Ref-1 repair activity is constitutively expressed, while APE1/Ref-1 redox activity is subject to regulation under various stimuli. Furthermore, Hsieh et al. [112] present data indicating that APE1/Ref-1 redox activity is mediated by phosphorylation in response to oxidative stress.

Reports to date have shown that APE1/Ref-1 expression is inducible by various forms of oxidative stress *in vitro* [84-91]. For example, HeLa cells exposed to damaging agents like hypochlorite or methyl methane sulfonate show an increase in both the APE1/Ref-1 expression and activity [112]. Additionally, Ramana et al. [85] have shown induction of APE1/Ref-1 mRNA and protein levels with increased translocation of the protein into the nucleus when HeLa S3 tumor cells and WI 38 primary fibroblasts were exposed to ROS generators. Ape1/Ref-1 protein has also been shown to be translocated from the cytoplasm to the nucleus during H_2O_2 and ATP stimulation [113]. In order to determine the effect of oxidative stress on APE1/Ref-1 *in vivo*, we used mice containing a heterozygous gene-targeted

deletion of APE (*Apex*^{+/-}). Homozygous deletion of the APE1/Ref-1 gene (*Apex*^{-/-}) is embryonic lethal, but heterozygous mice survive and are fertile [87, 114,115]. These APE1/Ref-1 haploinsufficient (*Apex*^{+/-}) mice show tissue specific differences in BER capacity characterized using an in vitro G:U mismatch repair assay. In addition Huamani et al. [116] have demonstrated that *Apex*^{+/-} mice show a significant increase in spontaneous mutagenesis in *lacI* transgenes in liver and spleen. Furthermore, MEF's and brain cells obtained from *Apex*^{+/-} mice have been shown to be more susceptible to oxidizing agents [87,117]. In this study we used 2-nitropropane (2-NP), a well known hepatocarcinogen [100,118] to induce oxidative stress *in vivo*. 2-NP, an industrial solvent, is found in paints, varnishes and cigarette smoke [100,118]. 2-NP promotes formation of 8-oxo-7,8-dihydro-2'-deoxyguanosine (8-OHdG) and 8-aminoguanine through its metabolites N-isopropylhydroxylamine and hydroxylamine-O-sulfonic acid, which are believed to be the causative factors behind 2-NP-induced carcinogenesis [100]. In addition, 2-NP occurs as Propane 2-nitronate (P2N) at physiological pH and promotes genotoxicity through production of NO species [118]. NO is shown to induce genotoxicity by deaminating DNA and increasing uracil to cytosine ratio [109, 119]. 2-NP has also been shown to be genotoxic *in vitro*, inducing mutations in bacteria and increasing unscheduled DNA synthesis in cultured hepatocytes [101]. Additionally, our laboratory has previously demonstrated that 2-NP-treatment results in an increase in the levels of 8-OHdG *in vivo* in the liver of mice and rats, followed by a concomitant increase in β-pol expression and BER activity [83]. Here we verify that APE1/Ref-1 is indeed an inducible protein (Fig. 3.1B). While fold increase is the same in response to oxidative stress across the genotypes, the total accumulative level of APE1/Ref-1 protein is lower in the liver of *Apex*^{+/-} mice, i.e., even though the intact allele is induced in response to 2-NP, it does not compensate for the lost allele.

APE1/Ref-1 has been shown to be an essential component of transcription complexes by directly interacting with other transcription factors such as HIF-1 and p300 [120,121]. Research has shown that APE1/Ref-1 enhances the DNA binding activity of NF-κB *in vitro* as well as NF-κB-dependent transcriptional activation *in vivo* [74,75]. Deletion of the redox-sensitive domain of APE1/Ref-1 has been shown to inhibit TNF-induced NF-κB activation, while loss of APE1/Ref-1 is shown to result in a

significant decline in NF-κB activity and increased susceptibility to TNF-induced apoptosis [76,77]. Furthermore, down-regulation of APE1/Ref-1 by soy isoflavones *in vitro* and *in vivo* resulted in concomitant reduction of NF-κB activity, while a 2-fold increase in APE1/Ref-1 expression, obtained by cDNA transfection, resulted in a concomitant 2-fold increase in NF-κB activity, confirming the cross-talk between these molecules [122]. In line with these findings the *Apex*^{+/+} mice showed a significant increase in APE1/Ref-1 redox activation of NF-κB when exposed to 2-NP, while increase in NF-kb activation is the same in response to oxidative stress across the genotypes, the total NF-kb DNA binding activity is lower in the liver of *Apex*^{+/-} mice, i.e., the ultimate level of NF-kB activation was significantly attenuated in the heterozygous animals. It is well established that NF-κB is a mediator of inflammatory responses promoting cell proliferation and survival by inhibiting cell cycle arrest & apoptosis [123,124], thus reduced activation of NF-κB and other redox-regulated transcription factors in response to oxidative stress in *Apex*^{+/-} mice may prove detrimental due to alterations in the signaling mechanisms necessary to differentiate between repair and apoptosis.

We have previously reported tissue-specific differences in BER capacity in APE1/Ref-1 haploinsufficient mice [92]. Moreover, previous studies have indicated that down-regulation of APE1/Ref-1 may promote a damage hypersensitive phenotype [87-89]. Therefore, it was essential to analyze the effect of reduced APE1/Ref-1 on the level of DNA damage production and BER. In this study, we demonstrate that the liver tissue of *Apex*^{+/-} mice expresses a BER phenotype that is more susceptible to accumulation of DNA damage in response to oxidative stress as a result of reduced APE1/Ref-1 3'-phoshoesterase activity *in vivo*. Here we show the differential impact of APE1/ref-1 heterozygosity on monofunctional and bifunctional glycosylase initiated *BER*. The traditional BER response to certain DNA base damages like uracil and alkylated bases, involves a monofunctional glycosylase-mediated removal of the damaged base resulting in the generation of an abasic site (AP site) that serves as a substrate for APE1/Ref-1 endonuclease activity. APE1/Ref-1 subsequently promotes formation of a transient single-strand break that serves as a substrate for β-pol-mediated nucleotide

insertion and is followed by DNA ligase-mediated BER completion. β-pol, dRP lyase activity serves as the rate limiting step in this pathway [125]. On the other hand, other damages like oxidized bases (e.g. 8-hydroxyguanosine and thymine glycol) requires a bi-functional glycosylase mediated removal of the damage. These glycosylases have associated AP lyase activity resulting in 3'blocking ends. DNA polymerase requires a 3'OH group as its substrate for repair synthesis. Therefore 3'-blocking end trimming requires the 3'-phosphoesterase activity of APE1/Ref-1. β-pol and DNA ligase subsequently complete the repair process. The 3'-phoshoesterase activity of APE1/Ref-1 is a crucial step in this bi-functional glycosylase mediated BER [102]. In this study, we show the difference in the requirement of Ape1/Ref-1 in BER pathway in vivo. Our $Apex^{+/-}$ mice exposed to 2-NP show significant upregulation in the UNG message with concomittant increase in the β-pol protein and G:U mismatch BER capacity in the liver tissue. We suggest that 2-NP, via its NO generation leads to increased uracil levels in the DNA resulting in the upregulation of UNG, a monofunctional glycosylase which is also associated in the processing of oxidized cytosine derivatives [110]. Since β-pol is the rate limiting enzyme in this pathway, the liver extracts of $Apex^{+/-}$ mice treated with 2-NP show significant induction in the G:U mismatch repair. $Apex^{+/-}$ mice treated with 2-NP showed increased CREB binding activity, a stress response transcriptional activator of β-pol promoter, potentially explaining the induction of β-pol expression [105]. It is widely accepted that β-pol protein expression and activity strongly correlate with BER activity in response to a variety of stressors [83, 126-128]. Moreover, the endonuclease activity of APE1/Ref-1 is 100 fold more efficient than the 3' phosphoesterase activity [129], thus we suggest that the available APE1/Ref-1 protein in apex$^{+/-}$ mice is adequate to sustain the monofunctional glycosylase initiated BER. In addition, increased p53 level can stabilize the APE1/Ref-1 and β-pol protein complex on the DNA abasic site which would enhance BER activity [130,131].

Alternatively, the liver tissues of the 2-NP treated $Apex^{+/-}$ mice displayed significantly lower 8-OH G:C BER activity compared to the wildtype animals. OGG1 is a bifunctional glycosylase known to be involved in the removal of 8-OHdG. While, OGG1 mRNA and protein levels are shown to be

unaffected during oxidative stress, the activity of this enzyme is enhanced by the increased APE1/Ref-1 protein [132]. In line with these findings, our 2-NP treated *Apex*$^{+/-}$ mice did not show any significant difference in the OGG1 mRNA levels. Furthermore, addition of purified human OGG1 protein to BER reaction mixture did not increase OGG1 initiated BER activity in 2-NP treated *Apex*$^{+/-}$ mice. However, addition of purified APE1/Ref-1 protein to BER reaction mix resulted in a significant increase in the 8-OH G: C BER activity in these mice confirming the significant role played by APE1/Ref-1 in the removal of 3'blocking groups. These data indicate that APE1/Ref-1 3' phosphoesterase activity is critical in removing the 3'blocking lesion created by a bifunctional glycosylase, e.g., OGG1. Therefore, APE1/Ref-1 heterozygosity compromises this function resulting in reduced detectable single strand break, increased aldehydic lesions and reduced bifunctional DNA glycosylase initiated BER activity.

Previously, we have measured the presence of AP sites, single-strand breaks and aldehydic lesions in isolated liver DNA from APE1/Ref-1 haploinsufficient mice and observed no significant difference in DNA damage accumulation as a result of reduced APE1/Ref-1 [92]. The lack of damage accumulation in untreated *Apex*$^{+/-}$ mice suggested that APE1/Ref-1 haploinsufficiency in liver does not cause an accumulation of genotoxic DNA repair intermediate products under baseline conditions. In line with previous studies from our laboratory [83] and others [133], we have demonstrated a significant increase in 3'-OH-containing single-strand breaks in response to oxidative stress. However the level of detectable single strand breaks (SSB's) in the liver tissue of 2-NP treated *Apex*$^{+/-}$ mice was found to be significantly lower than its wildtype counterpart while the level of aldehydic lesion was significantly higher. We suggest that the processing of oxidized bases by a bi-functional DNA glycosylase such as OGG1 (8-oxoguanine DNA glycosylase) could result in generation of aldehydic blocking lesions at 3' end. Inability to process these 3' blocking groups in the absence of the 3'-phophoesterase activity of Apex in *Apex*$^{+/-}$ mice [102], could result in lower detection of endonuclease-mediated single-strand breaks in the heterozygous animal.
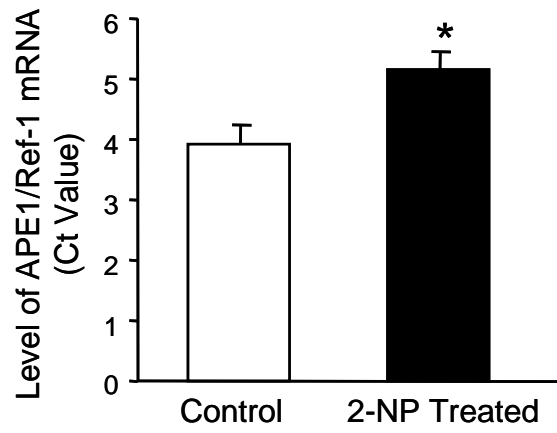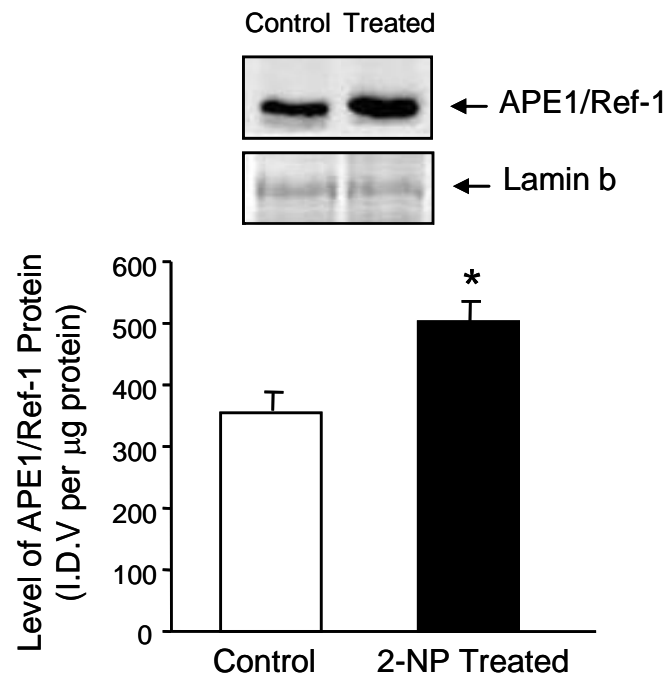
Herein, we demonstrate that Ape1/Ref-1 haploinsufficiency does not promote a concomitant decline in G:U mismatch BER activity in the liver in response to oxidative stress, it rather displays a significant increase in this activity. While, the high efficiency of APE1/Ref-1 endonuclease activity, upregulation in UNG and β-pol expression appear to be the reason behind the significant increase in G:U mismatch repair activity, alternatively, recent studies report an APE1/Ref-1-independent BER pathway in human cells [103]. While mono-functional DNA glycosylases such as SMUG1 and TDG and bi-functional DNA glycosylases/lyases such as OGG1 and NTH require APE1/Ref-1 to process AP sites and the 3'-OH aldehydic groups, respectively, APE1/Ref-1 backup enzymes have been identified for the repair of oxidative damage *in vivo* [134]. The recently discovered mammalian DNA glycosylase/AP lyases NEIL1 and NEIL2 recognize oxidative damage and generate DNA strand breaks with 3'-phosphate termini. Removal of the 3'-phosphate termini was shown to be dependent upon polynucleotide kinase (PNK) activity, not APE1/Ref-1, with NEIL1 serving as a backup enzyme. Additionally, a study by Das *et al.* [135] has demonstrated that NEIL1 is induced by oxidative stress. Therefore, it is likely that the observed increase in BER may be due to increased processing of DNA damage by an APE-independent β-pol regulated BER pathway, however, this alternative pathway does not rescue the observed decline in 8OHdG:C BER capacity in APE1/REF-1 haploinsufficient mice.

In conclusion, we suggest that the optimal balance between the stress response transcription factors, notably NF-κB, and the DNA repair pathway required for cell survival is attenuated in APE1/Ref-1 haploinsufficient mice exposed to oxidative stress. Reduced redox activity of APE1/Ref-1 leads to reduced activation of NF-κB potentially leading to cell cycle arrest and apoptosis. This notion is supported by the augmentation of GADD45g expression, a cell cycle arrest gene, observed in the liver of 2-NP treated *Apex*^{+/-} mice. GADD45g has also been implicated in the promotion of apoptosis under environmental stress via the p38K-Jun NH$_2$-terminal Kinase pathway [136,137]. Furthermore, *Apex*^{+/-} mice exposed to 2-NP show significant induction in the p53 protein levels and Caspase-3 activity in the liver, both being markers of apoptosis. Therefore, when APE1/Ref-1 is compromised the cells are more

susceptible to oxidative stress mainly due to reduced redox and 3'phosphodiestrase activity impacting cell survival, pushing it towards apoptosis. This finding has therapeutic importance as increased APE1/Ref-1 levels in tumor cells have been shown to confer resistance to chemotherapeutic drugs perhaps via decrease in apoptosis [138]. In line with previous findings, inhibition of DNA repair or redox or both activities of APE1/Ref-1 using inhibitors could potentially sensitize the tumor cells to the therapeutic agents [138] making APE1/Ref-1 an attractive molecular target in the treatment of cancer.

FIGURE LEGENDS

Fig. 3.1. Expression and activity of APE1/Ref-1 in response to 2-NP *in vivo*. (A) APE1/Ref-1 mRNA expression was quantified using a real-time PCR and the data were normalized using GAPDH. Values represent an average (± S.E.M.) for data obtained from 5 mice in each group (**B**) The level of the 37-kDa APE1/Ref-1 protein in 200 μg of liver nuclear extract as determined by western blot analysis. Values represent an average (± S.E.M.) for data obtained from 5 mice in each group (**C**) The level of APE1/Ref-1 redox-activation of NF-κB in 10 μg of live nuclear extract as determined using EMSA. Values represent an average (± S.E.M.) for data obtained from 5 mice in each group and are representative of separate independent experiments. (I.D.V.): integrated density value corresponding to the level of APE1/Ref-1 protein as quantified by an AlphaInnotech ChemiImager™; Lane A: nuclear extracts incubated in the presence of 100X molar excess of unlabeled NF-kB consensus DNA to confirm binding specificity; (*): value significantly different from control, wild-type mice at *P* < 0.05; (**): value significantly different from control, *Apex*$^{+/-}$ mice at *P* < 0.05. Lamin B protein level served as nuclear protein loading control. The picture depicts the representative sample from each group.

A

Level of APE1/Ref-1 mRNA
(Ct Value)

*

Control   2-NP Treated

B

Control Treated

← APE1/Ref-1

← Lamin b

Level of APE1/Ref-1 Protein
(I.D.V per μg protein)

*

Control   2-NP Treated

C

Fig. 3.2. Effect of 2-NP on APE1/Ref-1 expression levels in *Apex*$^{+/-}$ mice. The level of the 37-kDa APE1/Ref-1 protein in 200 μg of liver nuclear extract was determined by western blot analysis. Values represent an average (± S.E.M.) for data obtained from 5 mice in each group and are representative of separate independent experiments. (SDS-PAGE]: the level of APE1/Ref-1 protein was normalized based on the amount of protein loaded on each gel. (I.D.V.): integrated density value corresponding to the level of APE1/Ref-1 protein as quantified by an AlphaInnotech ChemiImager™; Values with different letter superscripts indicate significant differences at P < 0.05. Lamin B protein level served as nuclear protein loading control. The picture depicts the representative sample from each group.
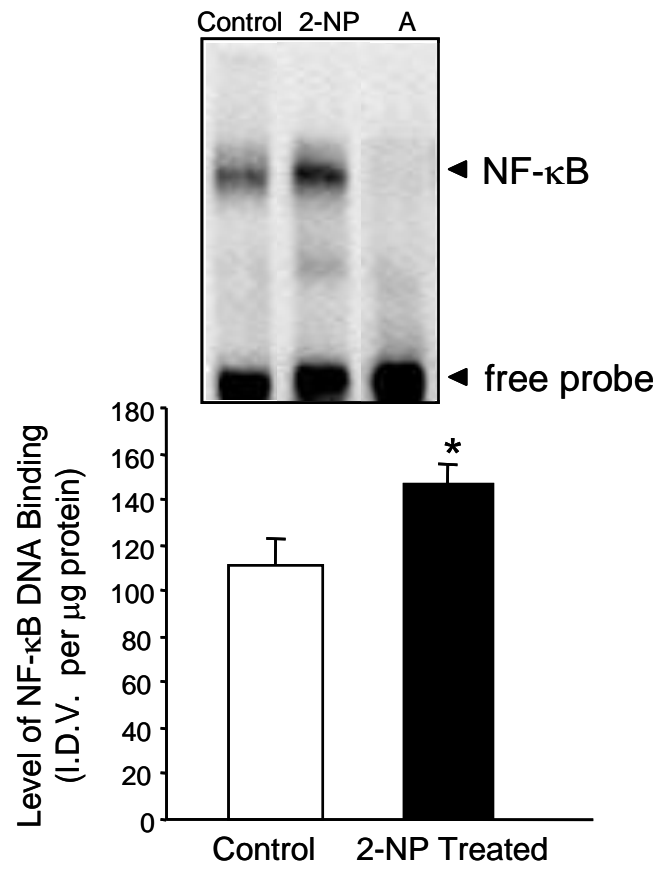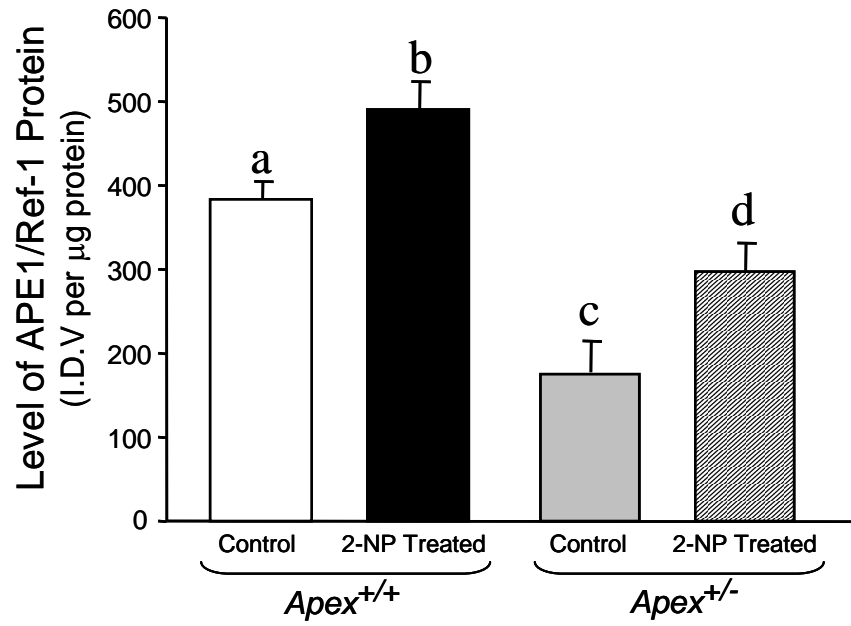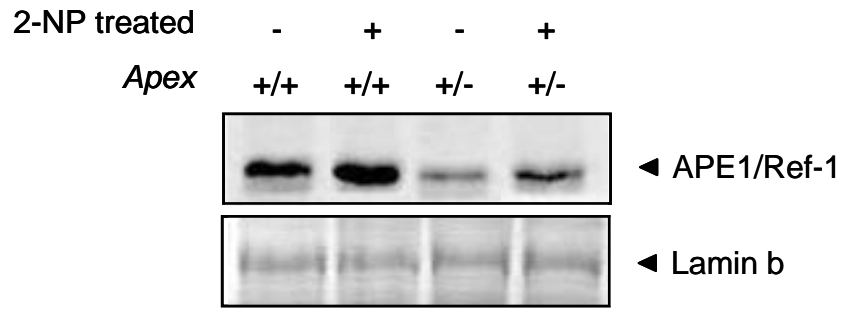
Fig. 3.3. Effect of 2-NP on APE1/Ref-1 redox activation of NF-κB in *Apex*$^{+/-}$ mice. The level of NF-κB

DNA binding in 10 μg of liver nuclear extract was determined using EMSA. Values represent an average

(± S.E.M.) for data obtained from 5 mice in each group and are representative of separate independent

experiments. (I.D.V.): integrated density value corresponding to the level of NF-κB DNA binding as

quantified by an AlphaInnotech ChemiImager™; Lane A: nuclear extracts incubated in the presence of

100X molar excess of unlabeled NF-κB consensus DNA to confirm binding specificity; Values with

different letter superscripts indicate significant differences at P < 0.05. The picture depicts the

representative sample from each group.
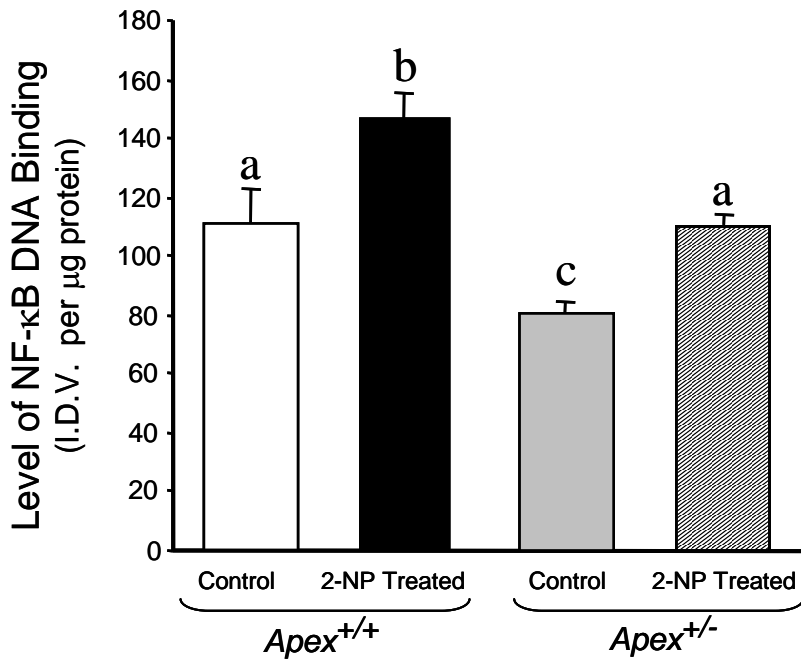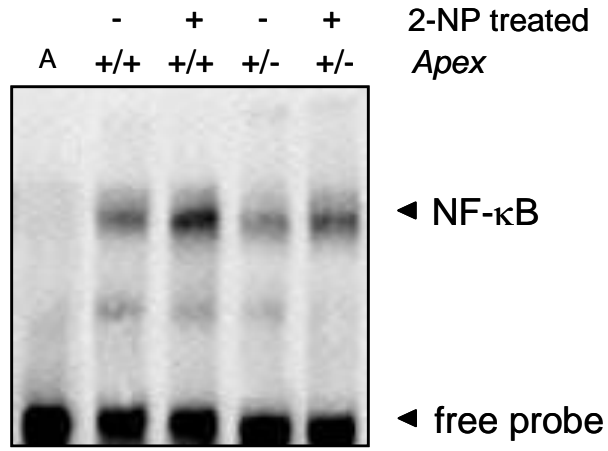
Fig. 3.4. DNA Damage analysis in liver DNA of *Apex*$^{+/-}$ mice injected with 2-NP. (A) The level of 3'-OH single-strand breaks as determined by the ROPS assay in liver of wild-type (*Apex*$^{+/+}$) and *Apex*$^{+/-}$ mice treated with 100 mg/kg body weight 2-NP. (B) The level of Aldehydic lesions as determined by the ASB assay in liver of wild-type (*Apex*$^{+/+}$) and *Apex*$^{+/-}$ mice treated with 100 mg/kg body weight 2-NP. Values represent an average ($\pm$ S.E.M.) for data obtained from 5 mice in each group and are representative of separate identical experiments. (C.P.M.): machine counts per minute corresponding to the level of α-[^{32}P]dCTP incorporation as quantified by a Packard scintillation counter; (I.D.V.): integrated density value corresponding to the level of DNA as quantified by an AlphaInnotech ChemiImager™; Values with different letter superscripts indicate significant differences at $P < 0.05$.
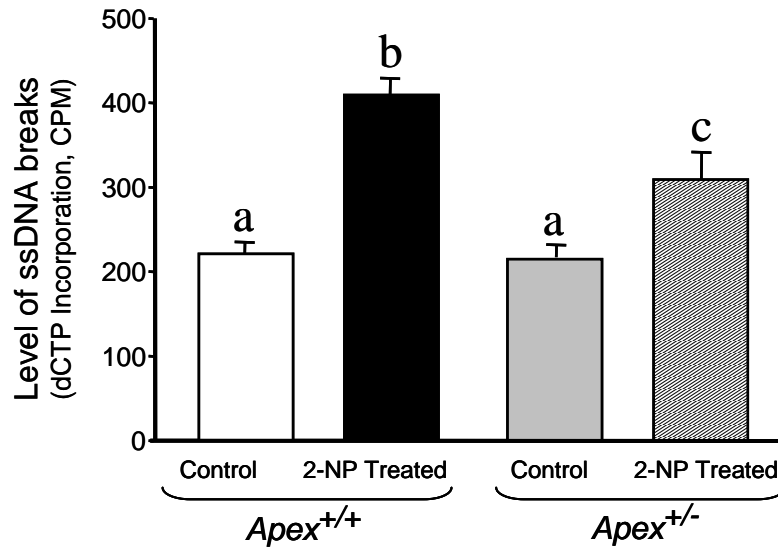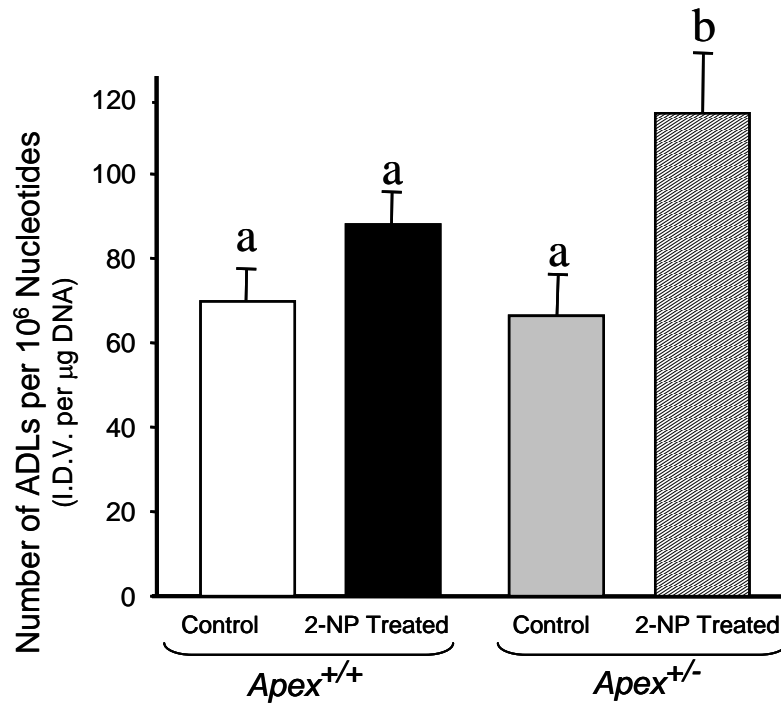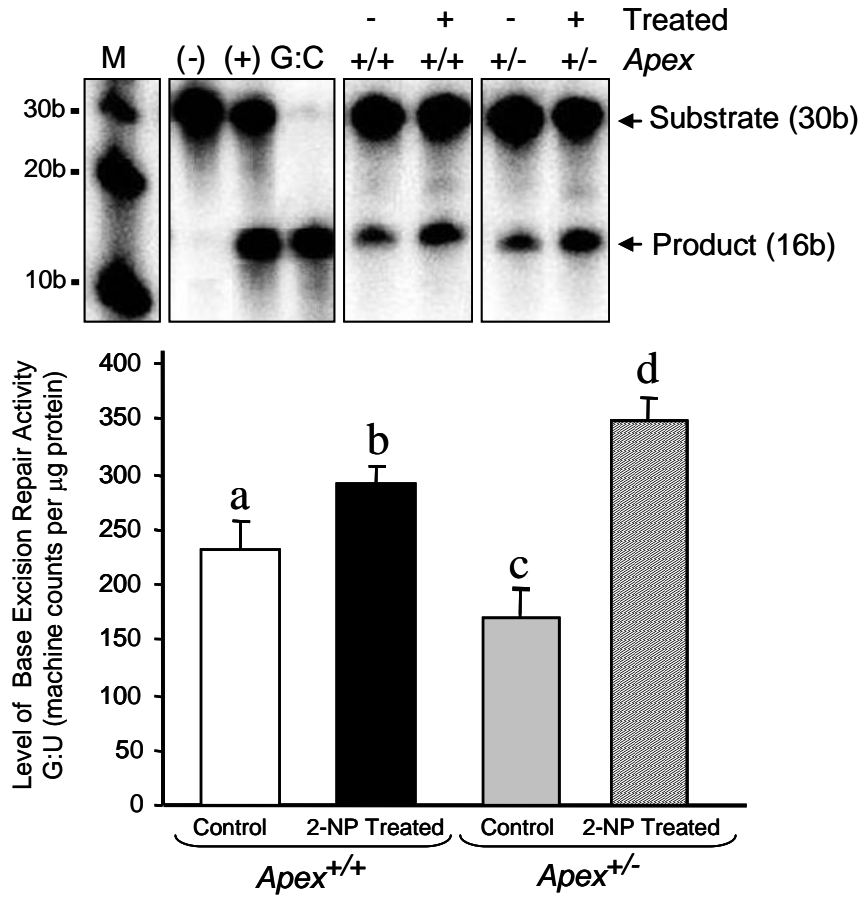
A

B

Fig. 3.5. Effect of APE1/Ref-1 haploinsufficiency and 2-NP on G:U mismatch BER, DNA polymerase β expression and CREB DNA binding activity. (A) The *in vitro* G:U mismatch BER was conducted using nuclear extracts from liver of control and 2-NP treated *Apex*$^{+/+}$ and *Apex*$^{+/-}$ mice. Base excision repair (BER) reaction products were resolved on a sequencing gel and visualized by autoradiography. Repair activity is visualized by the appearance of a 16b fragment. The relative level of BER was quantified using a Bio-Rad Molecular Imager® System. The data were normalized based on the amount of protein used in each reaction and expressed as machine counts per μg of protein. (B) The level of the 39-kDa β-pol protein in 200 μg of liver nuclear extract was determined by western blot analysis. (SDS-PAGE): the level of β-pol protein was normalized based on the amount of protein loaded on each gel. (C) The level of CREB DNA binding in 10 μg of liver nuclear extract was determined using EMSA and β-pol mRNA expression level as quantified using a real-time PCR and normalized with GAPDH Values represent an average (± S.E.M.) for data obtained from 5 mice in each group and are representative of separate identical experiments. (M): molecular weight standard; (-): negative control, G:U mismatch oligonucleotide incubated in the absence of nuclear extract and treated with *HpaII* restriction endonuclease; (+): positive control, G:U mismatch oligonucleotide incubated with recombinant β-pol and treated with *HpaII* restriction endonuclease; (G:C): positive control, G:C oligonucleotide incubated with nuclear extract and treated with *HpaII* restriction endonuclease; (I.D.V.): integrated density value corresponding to the level of β-pol protein and the level of CREB DNA binding as quantified by an AlphaInnotech ChemiImager™; Lane A & B: nuclear extracts incubated in the presence of 100X molar excess of mutated and unlabeled CRE sequence with β-pol flanking region respectively to confirm binding specificity; Lamin B protein level served as nuclear protein loading control. 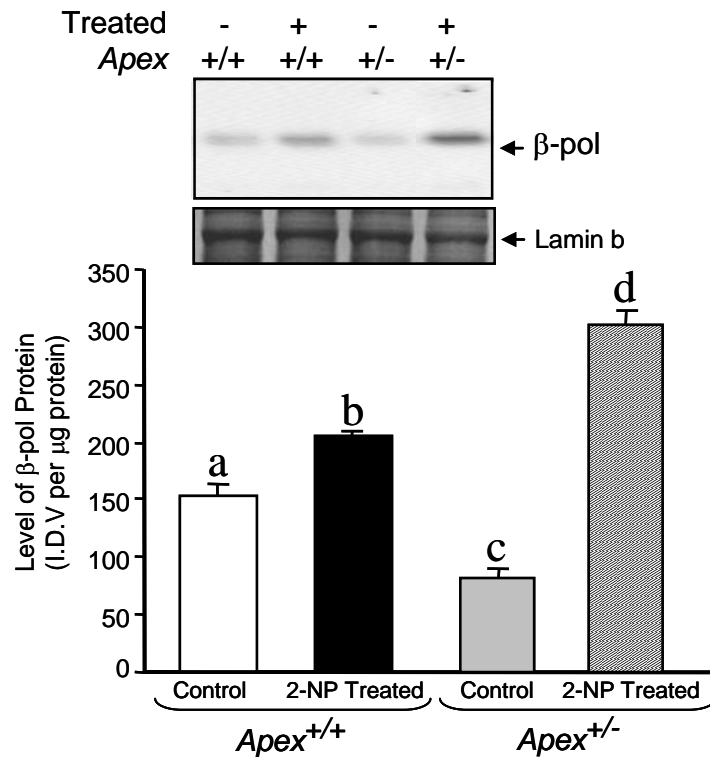Values with different letter superscripts indicate significant differences at P < 0.05. (*): value significantly different from wild-type (*Apex*$^{+/+}$) mice treated with 2-NP at *P* < 0.05. The picture depicts the representative sample from each group.

A

B

C

Treated   +   +
Apex   +/+ +/-   *A*   *B*

CREB →

Level of CREB DNA Binding
(I.D.V. per µg protein)

$Apex^{+/+}$ $Apex^{+/-}$
2-NP Treated

β-pol mRNA Levels
(normalized / GAPDH)

$Apex^{+/+}$ $Apex^{+/-}$
2-NP Treated
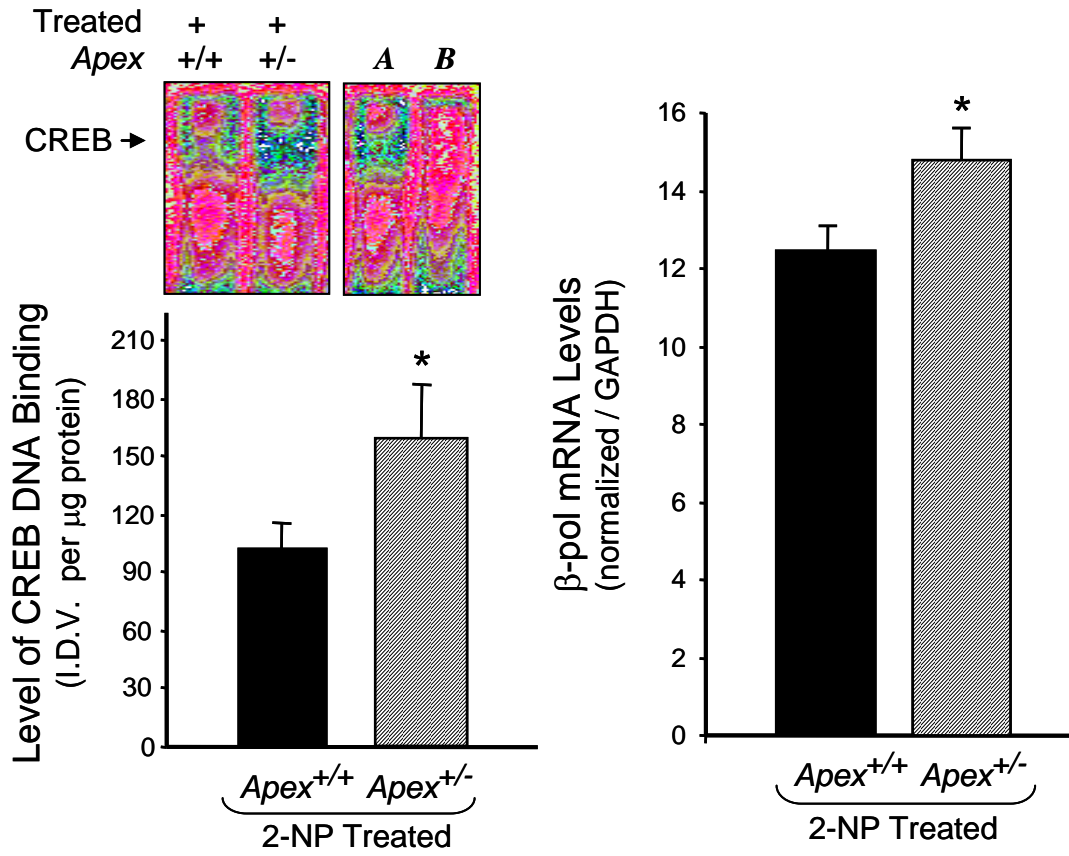
Fig. 3.6. Effect of APE1/Ref-1 haploinsufficiency and 2-NP on 8 OH G:C BER and the consequence of hApe1 enrichment on the repair capacity. (A) The *in vitro* 8-OH G:C BER was conducted using nuclear extracts from liver of control and 2-NP treated *Apex*$^{+/+}$ and *Apex*$^{+/-}$ mice in the presence of 1.6 U of *ogg1* enzyme (New England Biolab, MA). Base excision repair (BER) reaction products were resolved on a sequencing gel. Repair activity is visualized by the appearance of a 16b fragment. The relative level of BER was quantified using an Bio-rad ChemiImager™. The data were normalized based on the amount of protein used in each reaction and expressed as machine counts per μg of protein. (B) The *in vitro* 8-OH G:C BER was conducted with human Ape1/Ref-1 (hApe1) enrichment. Values represent an average (± S.E.M.) for data obtained from 5 mice in each group and are representative of separate identical experiments. (M): molecular weight standard; (-): negative control, G:U mismatch oligonucleotide incubated in the absence of nuclear extract and treated with *HpaII* restriction endonuclease; Values with different letter superscripts indicate significant differences at P < 0.05. The picture depicts the representative sample from each group.
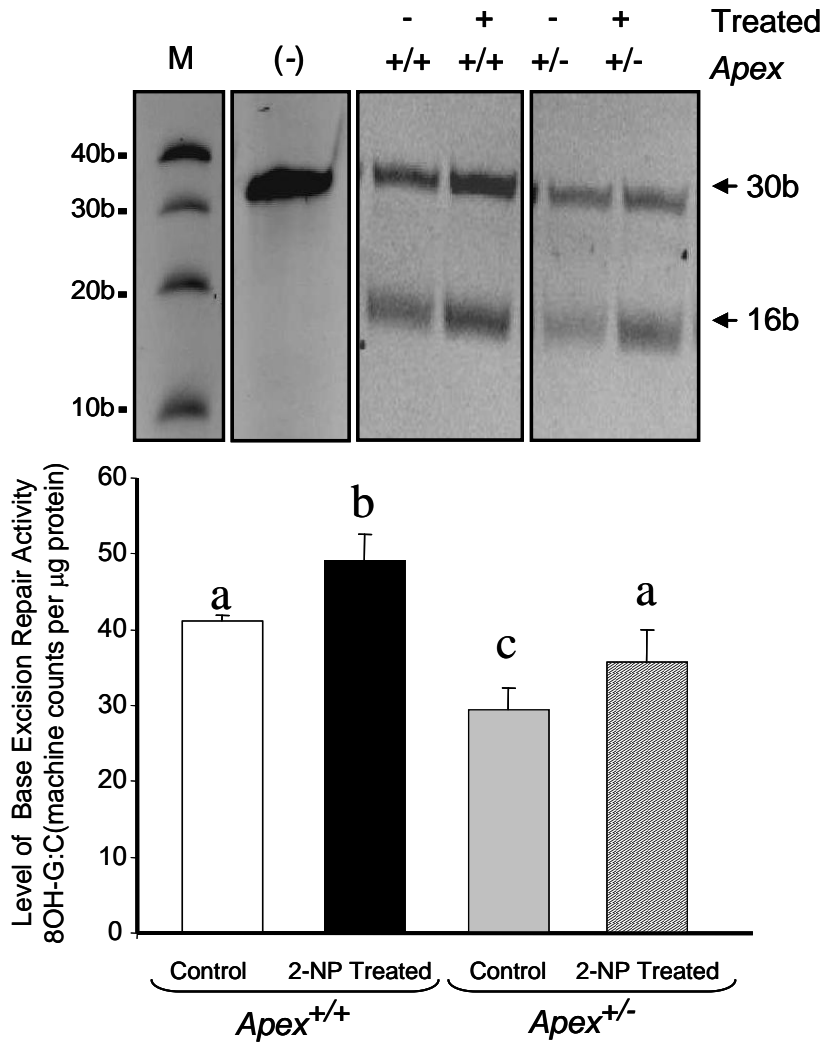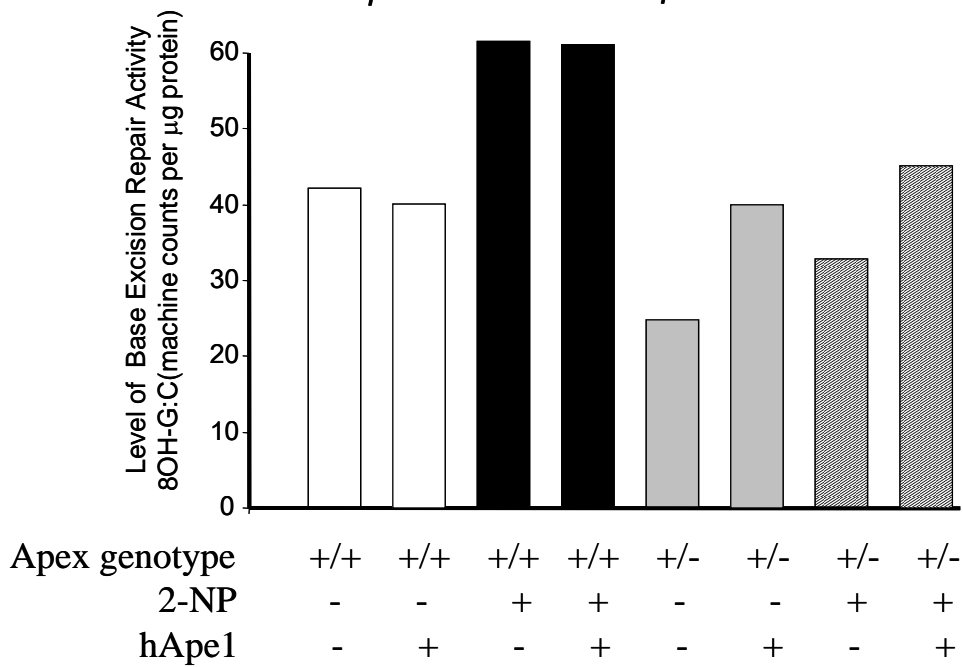
Fig. 3.7. Effect of 2-NP on UNG and OGG1 expression in $Apex^{+/-}$ mice. (A) UNG mRNA expression level in control and 2-NP treated $Apex^{+/+}$ and $Apex^{+/-}$ mice as quantified using real-time PCR and normalized against GAPDH. (B) OGG1 mRNA expression level in control and 2-NP treated $Apex^{+/+}$ and $Apex^{+/-}$ mice as quantified using real-time PCR and normalized against GAPDH. Values represent an average ($\pm$ S.E.M.) for data obtained from 5 mice in each group and are representative of separate identical experiments; Values with different letter superscripts indicate significant differences at $P < 0.05$.

A

B
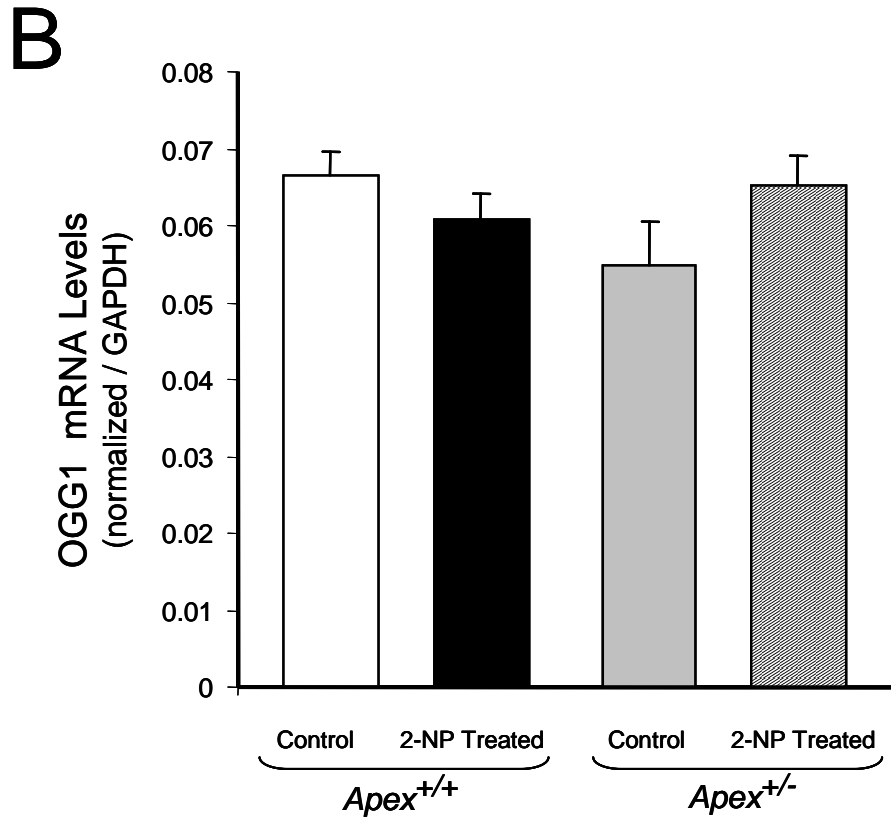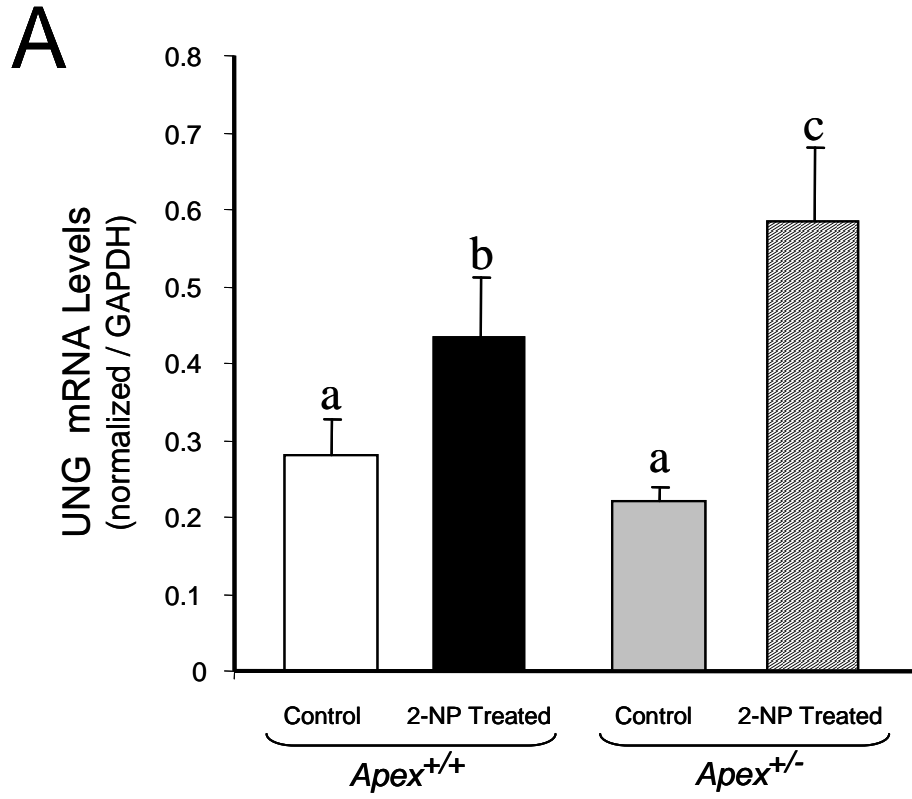
Fig. 3.8. Effect of 2-NP on apoptosis in *Apex*$^{+/-}$ mice. (A) GADD45g mRNA expression level was quantified using real-time PCR and normalized with GAPDH. (B) The level of the p53 protein in 200 μg of liver nuclear extract was determined by western blot analysis. (SDS-PAGE): the level of p53 protein was normalized based on the amount of protein loaded on each gel. (C) The level of Caspase-3 activity in liver cytosolic extract as determined by Caspase-3 enzyme assay. Values represent an average (± S.E.M.) for data obtained from 5 mice in each group and are representative of separate identical experiments; Values with different letter superscripts indicate significant differences at P < 0.05. Lamin B protein level served as nuclear protein loading control. The picture depicts the representative sample from each group.
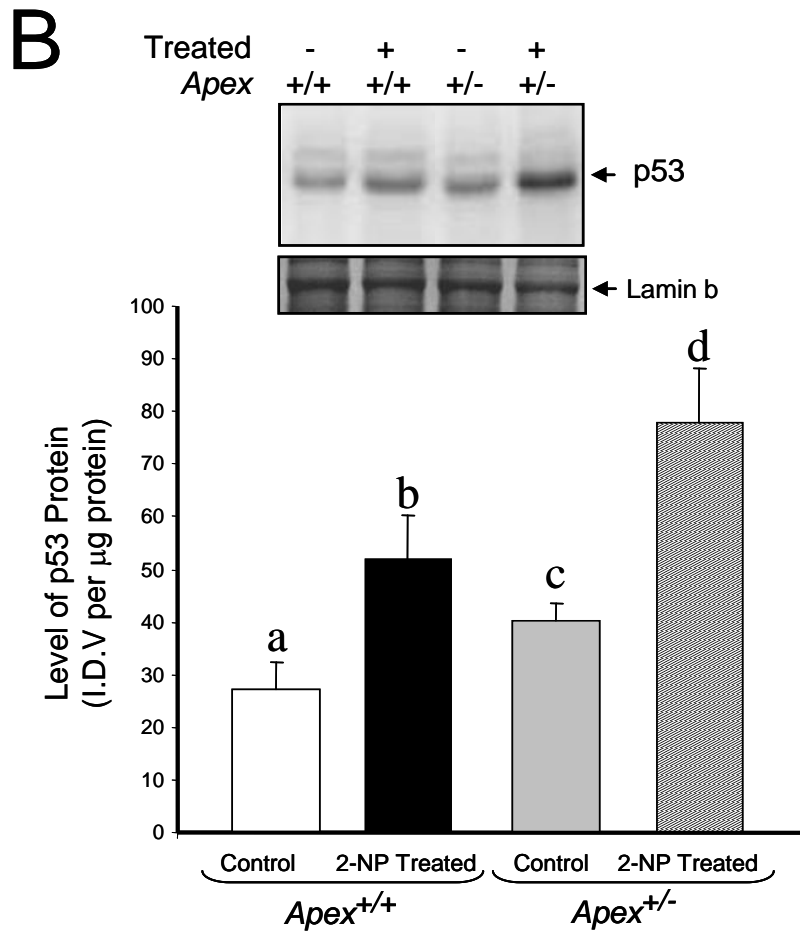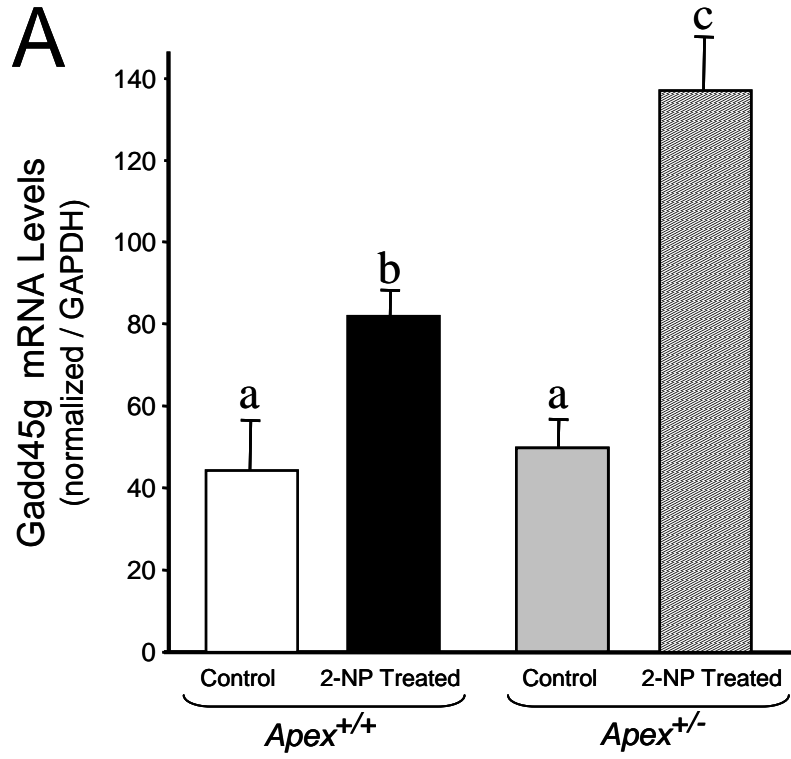
C
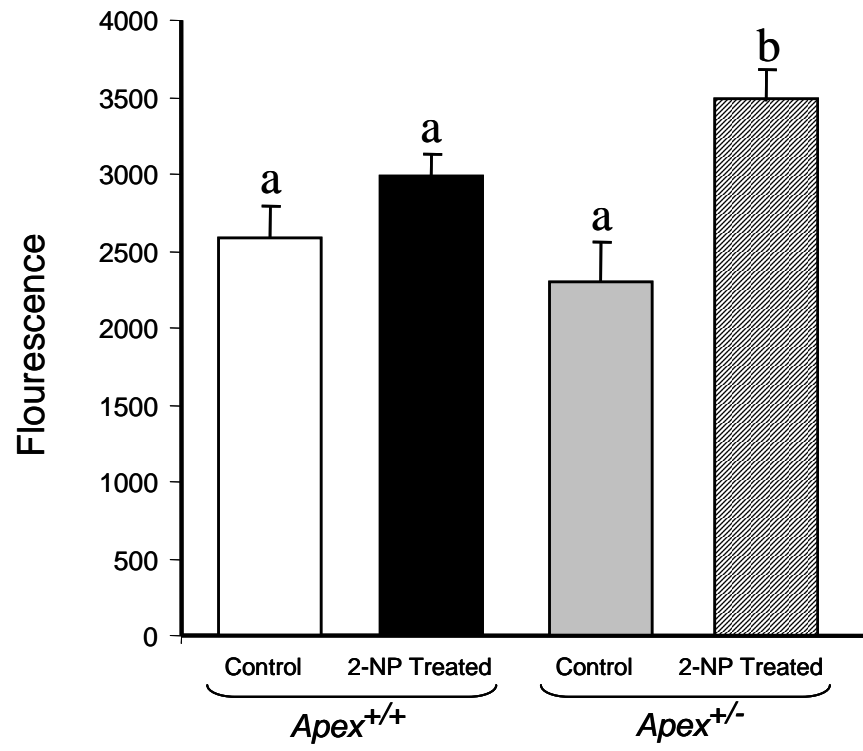
Table 1: Primer Sequences for Real-Time PCR

Gene	Sense Primer Sequence	Antisense Primer Sequence
Ape1/Ref-1	5'-ATGAAGAAATTGACCTCCGTAACC-3'	5'-GTGTAAGCGTAAGCAGTGTTG-3'
β-actin	5'-ACCAACTGGGACGACATGGAGAAG-3'	5'-TACGACCAGAGGCATACAGGGACT-3'
β-pol	5'-CTGGAAAAGGGCTTCACAATCAATG-3'	5'-GCGCCACTGGATGTAATCAAAAATG-3'
GADD45g	5'-AGTTCCGGAAAGCACAGCCAGGATG-3'	5'-GCCAGCACGCAAAAGGTCACATTGT-3'
GAPDH	5'-GCACAGTCAAGGCCGAGA-3'	5'-TACGACCAGAGGCATACAGGGACT-3'
OGG1	5'- CGGCTGGCATCCTAAGACATC-3'	5'-AACAGGCTTGGTTGGCGAAGG-3'
UNG	5'-AAGAGCTGTCTACAGACATCGA- 3'	5'- ATAAGAGCCCCAGAGGAGGAA-3'

Chapter 4

Folate deficiency regulates expression of DNA polymerase β in response to oxidative stress

Archana Unnikrishnan[1], Tom M. Prychitko[1], Hiral V. Patel[1], Mahbuba E. Chowdhury[1],

Amanda B. Pilling[1], Lisa F. Ventrella-Lucente[1], Erin V. Papakonstantinou[1], Diane C. Cabelof [1,2],

Ahmad R. Heydari[1,2]

[1]Department of Nutrition and Food science, Science College of Liberal Arts and Sciences and [2]Barbara

Ann Karmanos Cancer Institute, School of Medicine, Wayne State University, Detroit, Michigan 48202.

Running Head: Folate deficiency, *β-pol* and Oxidative stress

Address Correspondence to: Ahmad R. Heydari, 3009 Science Hall, department of Nutrition and Food

Science, Wayne State University, Detroit, Michigan 48202.

Tel: 313-577-2459, Fax: 313-577-8616. E-mail: ahmad.heydari@wayne.edu.

ABSTRACT

Folate deficiency has been shown to influence carcinogenesis by creating an imbalance in the base excision repair (BER) pathway impacting BER homeostasis. The inability to mount a BER response to oxidative stress in a folate deficient environment results in the accumulation of DNA repair intermediates, i.e., DNA strand breaks. Our data indicate that upregulation in β-*pol* expression in response to oxidative stress is inhibited by folate deficiency at the level of gene expression. Alteration in expression of β-*pol* in a folate deficient environment is not due to epigenetic changes in the core promoter of the β-*pol* gene, i.e., the CpG islands within the β-*pol* promoter remain unmethylated in the presence and/or absence of folate. However, the promoter analysis studies show a differential binding of regulatory factor(s) to the -36 to -7 region (the folic acid response region, FARR) within the core promoter of β-pol. Moreover, we observe a tight correlation between the level of binding of regulatory factor(s) with the FARR and inhibition of β-*pol* expression. Based on these findings, we propose that folate deficiency results in an upregulation/stability of negative regulatory factor(s) interacting with FARR, repressing the upregulation of the β-*pol* gene in response to oxidative stress.

KEYWORDS: Oxidative stress; *DNA polymerase-* β; Base excision repair; cAMP response element; DNA methylation; transcriptional regulation; folate deficiency

INTRODUCTION

Bioactive food components found in normal diets have been determined to confer protection against many diseases by impacting the onset, progression and severity of the disease [139]. Studies on nutritional genomics, nutritional transcriptomics, nutritional epigenomics and proteomics provide evidence of the effect of these bioactive food components on individual biomolecules and their overall effect on health and disease. Through their effect on biomolecules, bioactive food components can regulate many different pathways such as cell growth, differentiation, DNA repair, apoptosis and carcinogenesis [140]. These essential and/or non-essential factors of the diet have been shown to be capable of regulating gene expression [139]. Folic acid, an essential water soluble vitamin and a cofactor in one-carbon metabolism, has been associated with the etiology of many chronic diseases such as cardiovascular disease, neurological degeneration and cancer. Folate deficiency has been shown to enhance the potency of carcinogenic agents [141] and increase the accumulation of preneoplastic changes in the colon and liver of animal models [141,142]. Although the underlying mechanism of folate deficiency induced tumorigenesis is largely unknown, many different factors have been suggested as being responsible for its carcinogenic effect. Among those are epigenetic alterations, e.g., DNA methylation possibly via the reduction of S-adenosylmethionine [143,144], uracil misincorporation into the DNA [144,145] and deoxynucleotide imbalance [145,146]. However, data from human and animal studies reject the possibility of global DNA methylation as a potential mechanism behind folate deficiency induced tumorigenesis [147].

Data from our laboratory and others suggest that apoptotic and DNA repair pathways might be potential targets of folate deficiency [146,148]. In other words, increased accumulation of DNA damages such as DNA strand breaks, increased somatic mutations and chromosomal aberrations observed during folate deficiency can be attributed to defective DNA repair. Moreover, folate deficiency has been shown to act synergistically with DNA damaging agents to increase mutation frequency and DNA strand breaks, suggesting potential compromises in DNA repair capacity as has been discussed previously[144,146,149].

Base Excision Repair [BER] is a sequential pathway involved in the repair of endogenous DNA damage and damages that arise from alkylation and oxidative stress, along with misincorporated uracil [150]. Data from our laboratory and others have provided strong evidence to indicate that BER is a stress response pathway [151,152]. In addition, we have previously demonstrated deregulation of BER in response to folate deficiency [149]. We have shown that folate deficiency impacts initiation of the BER pathway, i.e., *uracil DNA glycosylase* activity is upregulated, while no upregulation in the *DNA polymerase* β(β-*pol*) protein level and/or activity is observed. The inability to mount a BER response to stress in a folate deficient environment resulted in accumulation of DNA repair intermediates, i.e., DNA strand breaks which could potentially result in double strand breaks and chromosomal aberrations. The objective of this study was to elucidate the molecular mechanism by which folate status impacts the regulation of DNA polymerase- β expression.

EXPERIMENTAL PROCEDURES

Animals -The experiments were performed in young (3-4 month), wild-type male C57BL/6 specific pathogen-free mice in accordance with NIH guidelines for the use and care of laboratory animals. The Wayne State University Animal Investigation Committee approved the animal protocol. The mice were maintained on a 12-hr light/dark cycle and fed standard mouse chow and water ad libitum. At 3-4 months of age, the mice were randomly assigned to two dietary groups and were fed AIN93G-purified isoenergetic diets (Dyets, Inc., Lehigh Valley, PA). Diets were stored at –20°C. 1% succinyl sulfathiazole was added to all diets. The control group received a folate adequate diet containing 2 mg/kg folic acid. The experimental group received a folate-deficient diet containing 0 mg/kg folic acid. The animals' food intake and body weights were monitored twice weekly to monitor for signs of toxicity (*e.g.,* weight loss), and the experimental diets were continued for 8 weeks. Mice were anesthetized in a CO_2 chamber and sacrificed by cervical dislocation. Harvested liver was flash frozen and stored in liquid nitrogen.

DNA damage induction- Experimental mice were intraperitonealy injected with 100 mg/kg body weight 2-nitropropane [2-NP; Aldrich Chemical Company, Chem. Abstr. Serv. Reg. No. (79-46-9)] dissolved in olive oil. Control mice were injected with olive oil vehicle intraperitonealy. Mice were sacrificed after 12hrs, 24hrs and 48hrs. The dose and exposure time were based on previous studies characterizing the effect of 2-NP on DNA damage and repair induction [153].

Analysis of 8-OHdG levels- Genomic DNA isolation was done using the NaI DNA extractor kit (Wako chemicals, Inc.,Richmond, VA) as described previously [154]. DNA oxidation that occurs during DNA isolation was minimized by the usage of NaI instead of phenol. Nuclease P1 and calf alkaline phosphatase were used to hydrolyze 30ug of DNA. The levels of both 8-OHdG and 2dG in the DNA hydrolysates were quantified using a HPLC-EC detection system with a polar mobile phase. The level of DNA oxidation is expressed as the ratio of 8-OHdG to 2dG.

Gene expression profiling-The mRNA expression level of *β-pol* was quantified using real-time PCR as described previously [155]. Briefly, total RNA was extracted from liver tissue of folate adequate and folate deficient control and 2-NP treated mice using the RNeasy Kit (Qiagen, Valencia, CA). First strand cDNA was synthesized from 1 μg RNA using random primers (Promega, Madison, Wisconsin) and purified using the QIAquick PCR purification kit (Qiagen, Valencia, California). Expression of *β-pol* was quantified using real time PCR with specific primers for the gene. The gene transcript was normalized to both *Gapdh* and *β-actin* [155]. External standards for all the genes were prepared by subcloning the amplicons, synthesized using the specific primers into PGEM-T easy vector.

Nuclear protein isolation- Nuclear extracts were isolated using a transfactor extraction kit (Clontech, Mountain View, CA) as described previously [155]. The kit uses a hypotonic buffer to lyse the cell allowing the removal of cytosolic fractions and is followed by the extraction of nuclear proteins by a high salt buffer. All samples and tubes were handled and chilled on ice, and all solutions were made fresh according to the manufacturer's protocol. Low molecular weight contaminants were removed from extracts by dialysis in 1L of dialysis buffer (20mM Tris-HCl, pH 8.0; 100mM KCl; 10mM NaS_2O_5; 0.1mM DTT; 0.1mM PMSF; 1mg/ml PepstatinA) for 3 hours at 4°C using Slide-A-Lyzer® mini-dialysis units (Pierce Biotechnology, Rockford, IL) with a molecular weight cut off of 3.5kDa. Dialyzed extracts were aliquoted and flash frozen in liquid nitrogen and stored at -70°C for subsequent analyses. Protein concentrations were determined according to Bradford using Protein Assay Kit I (Bio-Rad, Hercules, CA).

Protein expression analysis- Western blot analysis was performed using 200 μg of nuclear protein as described previously [155]. Upon completion of SDS-PAGE, the region containing the protein[s] of interest was excised and prepared for western blot analysis while the remaining portion of the gel was stained with GelCode®Blue Stain Reagent (Pierce Biotechnology, Rockford, IL) to ensure equal protein loading. Anti-sera developed against β–pol were used to detect the proteins of interest

followed by incubation with HRP-conjugated secondary antibody (Santa Cruz Biotechnology, Santa Cruz, CA). As an internal control to ensure equal protein transfer, membranes were reprobed with PCNA antibody. The bands were visualized and quantified using a ChemiImager® System (Bio-Rad, Hercules, CA) after incubation in SuperSignal® West Pico Chemiluminescent Substrate (Pierce Biotechnology, Rockford, IL). Data are expressed as the integrated density value (I.D.V.) of the band per mg of protein loaded.

DNA Base Excision Repair Assay- The G:U mismatch repair assay is developed to measure monofunctional glycosylase-initiated base excision repair (BER) activity. Radio-end labeled 30-bp oligonucleotides (upper strand: 5'-ATACCGCGGUCGGCCGATCAAGCTTATT dd-3'; lower strand: 3'-ddTATATGGCGCCG GCCGGCTAGTTCGAATAA-5') containing a G:U mismatch and a *Hpa II* restriction site (CCGG) were incubated in a BER reaction mixture containing 50 μg of the nuclear protein as previously described [156]. Repair of the G:U mismatch to a correct G:C base pair was determined via treatment of the duplex oligonucleotide with 20U of HpaII (Promega, Madison, WI) for 1hour at 37°C and analysis by electrophoresis on a 20% denaturing 19:1 acrylamide/bis-acrylamide gel (SequaGel® Sequencing System, National Diagnostics, Atlanta, GA). Repair activity (presence of a 16-mer band) was visualized and quantified using a Molecular Imager® System (Bio-Rad, Hercules, CA) by calculating the ratio of the 16-mer product with the 30-mer substrate (product/substrate). Data are expressed as machine counts per microgram of protein.

Methylation Assay- Methylation status of *β-pol* promoter region: -643 to +44 was determined using the bisulfite genomic sequencing method to generate a methylation map with single base resolution. In brief, genomic DNA was isolated (Qiagen, Valencia, CA) from liver tissue obtained from folate adequate/deficient animals treated with/without 2-NP. DNA samples were treated with a bisulfite conversion reagent converting unmethylated cytosine residues to uracil according to the manufacturer's protocol (Zymo Research, Orange, CA). Then, bisulfite treated DNA was PCR amplified using primers

designed around CpG islands: -105 to +44 and -322 to -123 (Methprimers, San Francisco, CA) present in the *β -pol* promoter. The resulting amplicons were cloned into pGEM-T Easy Vector (Promega, Madison, Wisconsin). Plasmids from 7 colonies of each subclone were sequenced and the presence of preserved methylated cytosine residues representing methylation status was determined.

Cell Culture and promoter Analysis- Mouse hepatoma (hepa 1-6) cells of epithelial origin were obtained from American Type Culture Collection (ATCC). The cells were cultured in monolayer condition in a standard DMEM medium (GIBCO BRL, Grand Island, NY) containing 4.5g/L glucose, 4mg/L folic acid, or in a customized DMEM medium (GIBCO BRL, Grand Island, NY) free of folic acid and supplemented with 10% dialyzed fetal bovine serum (Thermo Scientific Hyclone, West Palm Beach, FL). Each of the growth mediums were supplemented with 1% penicillin streptomycin and maintained at 37ºC in 10% CO_2 and 95% relative humidity.

For the promoter analysis a number of promoter-reporter constructs were created using fragments of the β-pol promoter. The fragments   -924 to +38, -602 to +38, -360 to + 38, -173 to +38, and -104 to +38 of the 5'-flanking region of the mouse β-pol gene encompassing the basal promoter and 5' untranslated region were inserted into a pGL3 vector creating an array of promoter-reporter constructs: p924Luc, p602Luc, p360Luc, p173Luc and p104Luc, respectively. The hepa 1-6 cells maintained in a folate adequate medium were transfected with these promoter-reporter constructs using the effectene transfection reagent according to the manufacturer's protocol [Qiagen, Valencia, CA].   After 24 hours of transfection, the cells were treated with 100μM of H_2O_2 for two hours. 24 hours later the cell lysates were quantified for the luciferase activity using the Luciferase assay kit (Promega, Madison, WI) utilizing a 20/20 luminometer (Turner Biosystems).   β-galactosidase was used as an internal control for transfection.   For determining the β-pol promoter activity during folate deficiency,   hepa 1-6 cells maintained in folate adequate and folate deficient medium for 48hrs were transfected with p924Luc using the effectene transfection reagent following the manufacturer's protocol (Qiagen, Valencia, CA).   After 24 hours of transfection, the cells were treated with 100μM of H_2O_2 for two hours. 24 hours later, the cell

lysates from each of the conditions were quantified for the luciferase activity using the Luciferase assay kit (Promega, Madison, WI) utilizing a 20/20 luminometer (Turner Biosystems, Promega, Madison, Wisconsin). β-galactosidase was used as an internal control for transfection.

DNA Foot printing- For DNA foot printing analysis fragments contained by the -924 to +311 region of the *β-pol* gene was amplified that included a 6-FAM labeled oligonucleotide for the forward primer. The 6-FAM labeled fragment consisted of a region of the β-*pol* promoter, exon 1 and a portion of intron 1. We used this fragment for DNA footprinting. Each reaction required 8μg of nuclear extract, and 50μg of template DNA. Nuclear extract, buffer and DNA template were added in this order to each tube while being kept on ice. Reactions were then transferred to a room temperature water bath and incubated for 20 minutes. Following the 20 min incubation at room temperature, 10 μl of a 1:50 dilution of DNase 1 (10 U/μl) was added to each reaction and reaction mixtures were incubated at room temperature for 1 minute. After 1 minute incubation with DNase 1, 50 μl of cold EDTA was added to each reaction, and the reactions were placed on ice. A control without nuclear extracts was also treated with DNase 1 along with the other samples. The completed reactions were then purified using the Qiaquick nucleotide removal kit (Qiagen, Valencia, CA). Fragments were separated on an ABI Prism 310 DNA genetic analyzer (Life Technologies, Carlsbad, CA) and processed by software using the Gene Scan application

Electrophoretic mobility shift assay (EMSA)- A non-radioisotopic EMSA was used to determine the protein-DNA binding activity of nuclear extracts isolated from liver tissue of folate adequate and folate deficient mice treated with and without 2-NP, according to the manufacturer's protocol (LightShift® Chemiluminescent EMSA kit, Pierce Biotechnology, Rockford, IL). Briefly, 40 fmol of biotin-end-labeled DNA -36 to -7 upstream *β-pol* promoter was incubated with 10 μg of nuclear extract in a 20 μl reaction mixture containing 1X binding buffer (100 mM Tris, 500 mM KCl, 10 mM DTT; pH 7.5), 2.5% glycerol, 5 mM $MgCl_2$, 50 ng/μl poly (dI-dC), and 0.05% NP-40. Negative controls (all components except nuclear extract) were included in all experiments. In competitive assays, 100X molar excess of unlabeled -36 to -7 oligonucleotide, mutant -36 to -7 oligonucleotide or consensus CRE/CREB

sequence were added to the reaction mixture. Samples were incubated for 20 min at room temperature and then resolved on a 6% non-denaturing polyacrylamide gel in 0.5X TBE buffer. After electrophoresis, samples were transferred from the gel to a positively charged nylon membrane and cross-linked. Biotin-labeled protein/DNA complexes were detected by chemiluminescence and quantified using a ChemiImager™ System (AlphaInnotech, San Leandro, CA). Data are expressed as the integrated density value (I.D.V.) of the band/mg of protein loaded.

Statistical analysis- Statistical significance between means was determined using ANOVA as described previously [155]. P-values less than 0.05 were considered statistically significant.

RESULTS

Analysis of formation of 8-OHdG, expression of DNA polymerase β and G:U mismatch BER during folate deficiency and 2-NP treatment in the liver of mice-

Folate deficiency has been shown to influence carcinogenesis by creating an imbalance in the base excision repair pathway [149]. In this study we have characterized the effect of folate deficiency on BER in response to oxidative stress *in vivo*. We used 2-Nitropropane (2-NP, a hepatocarcinogen) to induce oxidative stress in the liver of C57BL/6 mice. 2-NP has been shown to increase mutation frequency in rodents and has been suggested to induce cancer through the formation of DNA damages such as 8-OHdG and 8-aminoguanine in liver [153,155]. As reported previously by our laboratory [153,154], 2-NP treatment (i.p. injection of 100 mg/kg body weight) resulted in a significant increase in DNA oxidation, 8-OHdG, and an upregulation in expression of *β–pol* in a time dependent manner. We observed a six-fold increase ($p < 0.001$) in 8-OHdG levels 12 hr post treatment (Fig. 4.1A), while the *β-pol* mRNA level reached its maximum at 12 hr and remained high at 24 hr post 2-NP treatment (Fig. 4.1B). Moreover, we show a steady increase in the level of β-pol protein in response to 2-NP (Fig. 4.1C). Previously, it has been shown that β-pol is a critical enzyme in BER [154,157]. As such, we observed a concurrent increase in BER activity (40%, $p < 0.01$) in response to 2-NP in liver tissues of the mice (Fig. 4.1D).

To further study the effect of folate deficiency on BER in response to oxidative stress, we analyzed BER activity in 2-NP treated animals fed a folate deficient diet. We performed an eight-week feeding study where the C57BL/6 mice were fed a folate deprived diet. As reported previously [148], this regimen resulted in a 90% decrease in plasma folate level and a 40% decrease in tissue folate levels with no significant change in the food intake and weight of these animals (data not shown). As such, we expected to see an increase in BER activity in these animals. However, BER activity failed to be upregulated in response to folate deficiency. Moreover, we expected to see a further increase in BER activity in folate deficient mice in response to 2-NP. Surprisingly, we observed no increase in BER activity in response to 2-NP in mice fed a folate deficient diet (Fig. 4.1D). In agreement, we show that the lack of inducibility of BER in response to 2-NP in a folate deficient environment is preceded by a lack of induction in *β-pol* expression, i.e., *β-pol* mRNA and protein levels (Figs. 4.2A and 4.2B). Interestingly, 2-NP treatment of folate deficient mice resulted in a significant up-regulation in the expression of two key enzymes in the BER pathway, *Ung* and *Ape1/Ref*-1 (data not shown), while, upregulation of the *β-pol* gene was inhibited by folate deficiency. These findings signify that the effect of folate on gene expression is tightly regulated, i.e., the impact of folate deficiency is gene dependent. Thus, the inability to induce BER in response to oxidative stress in a folate deficient environment appears to be due to attenuation in the ability of the *β-pol* gene to mount a response to oxidative stress. Based on these findings, it is inviting to suggest that the mechanism by which folate deficiency induces carcinogenesis in response to DNA damaging agents is due in part to the inability to induce a BER response at the level of *β-pol* expression, an important observation in the realm of nutrient gene interaction.

Analysis of the promoter of DNA polymerase β for the methylation of CpG islands in the liver of mice-

Folate deficiency has been shown to alter S-adenosylmethionine/S-adenosyl homocysteine ratio, thus impacting the levels of the universal methyl donor. As such, folate deficiency has been suggested to impact gene expression through epigenetic modulation by modifying the methylation pattern of the

genome. DNA methylation generally occurs in the cytosine of CpG dinucleotides, converting the cytosine to 5-methyl cytosine. In order to dissect out the epigenetic effect of folate deficiency on *β-pol* expression, we analyzed the methylation status of the CpG islands found in the promoter of the *β-pol* gene, using the bisulfite genomic sequencing method. Using MethPrimer software [158], we identified two CpG islands within the first 687bp region of the *β-pol* promoter, and part of exon 1(Island 1: -105 to +44 and Island 2: -322 to -123). Subsequently, primers were designed to amplify both islands, and the methylation status of the CpG sites within these regions was determined. Herein, we demonstrate that folate deficiency does not alter the methylation pattern of the CpG islands in the promoter region of β-pol. Interestingly, no CpG sites were methylated in DNA samples obtained from liver of mice fed a folate deficient and/or adequate diet and treated with 2-NP (Fig.4.3). We were concerned whether the lack of methylation at the CpG sites within these two islands is due to an artifact of the assay conditions. Thus, we examined the methylation pattern of exon 8 of the *p53* gene as control. Exons 5-8 of *p53* has been shown to be a 'hot spot' involved in neoplastic transformations, and this region has been shown to undergo alteration in its methylation patterns during folate deficiency [143,159]. Interestingly, all the CpG sites within exon 8 of the *p53* gene were methylated. Our findings with respect to the methylation patterns of the *β-pol* promoter are consistent with the notion that promoter regions of housekeeping genes remain unmethylated. Therefore, our data illustrate that deregulation of *β-po*l expression by folate deficiency is not through epigenetic alteration of the core region of its promoter. It is inviting to suggest therefore that folate deficiency might be impacting *β-pol* expression transcriptionally by way of regulatory factors.

Analysis of the DNA polymerase β promoter using DNA footprinting and gel retardation assays-

To further investigate the mechanism of altered transcription of *DNA polymerase β* gene in response to oxidative stress in folate deficient mice, the *cis* acting region that is involved in this regulation was analyzed. We initially determined the promoter region required for the upregulation of *β-pol* gene in response to oxidative stress in cultured liver cell lines, hepa 1-6. First, the effect of H_2O_2 on *β-pol* mRNA in the mouse hepa 1-6 was examined. In hepatoma cells, *β-pol* mRNA increased 2-fold by 100μM H_2O_2

treatment for 2 hr, where no sign of cellular toxicity was observed (Fig.4.4A). Consequently, we used a similar treatment to determine the promoter activity of the *β-pol* gene in cultured cells to identify the region of the promoter responsible for upregulation in response to oxidative stress. Using a promoter analysis assay, we examined the regulation of β-*pol* promoter activity in response to H_2O_2 and folate deprivation. The fragments -924 to +38, -602 to +38, -360 to + 38, -173 to +38, and -104 to +38 of the 5'-flanking region of the mouse *β-pol* gene were inserted into pGL3 vector creating an array of promoter-reporter constructs: p924Luc, p602Luc, p360Luc, p173Luc and p104Luc, respectively. After transfection, the luciferase activity for each construct was quantified and normalized against β-galactosidase activity. The luciferase activity in the cells transfected with p924Luc, p602Luc, p360Luc, p173Luc and p104Luc were stimulated 2 to 3.5-fold following a 2 hr treatment with 100μM H_2O_2. This suggests that the core promoter encumbers the necessary elements required for response to oxidative stress (Fig.4.4B). Interestingly, while folate deprivation resulted in a slight increase in *β-pol* promoter activity in cell culture, the robust upregulation in luciferase activity in response to oxidative stress was lost when the cells were cultured in the medium without folic acid (Fig. 4.4C). These results suggest that the sequence -924 to +38 contains the *cis*-element which responds to oxidative stress as well as the elements harboring the regulatory factor(s) responding to folate deprivation. This is the first report demonstrating that the folate responsive region of the *β-pol* gene promoter is located within the basal promoter encumbering the CRE region.

To determine the differential protein-DNA binding pattern within the *β-pol* promoter, we performed a footprinting assay using DNA fragments contained by the -924 to +311 region of the *β-pol* promoter. To elucidate the protein/DNA interactions in a physiologically relevant model, liver nuclear extracts from mice were utilized for this assay. As depicted in Fig. 4.5, a significant difference in protection pattern in a region previously shown to hold the core promoter activity of human *β-POL* [160,161] was detected. In other words, the DNA footprinting profiles generated using this fragment showed differential protein-DNA binding patterns in the -36 to -7 upstream *β-pol* promoter region.

Interestingly extracts from 2-NP treated animals fed a folate adequate diet displayed maximum DNase I sensitivity suggesting the absence /reduced protein binding in this region (Fig. 4.5).

The above findings provide evidence that region -36 to -7 upstream of the mouse *β-pol* promoter shows a differential DNA protein binding pattern in response to folate deprivation and oxidative stress. This region which we refer to as the Folic Acid Response Region (FARR) contains a binding site for CRE. CREB is a stress induced transcription factor shown to be responsible for activating gene expression when bound to the CRE region. The CRE site of the human *β-POL* promoter has been demonstrated to be involved in its expression both under basal conditions and when exposed to DNA alkylating agent [162-164]. Herein we attempted to identify transcription factor(s) that mediate the up-regulation of the β-*pol* in response to oxidative stress and potential factors that appear to have negative regulatory impact on the expression of *β-pol* in response to folate deficiency. We performed electrophoresis mobility shift assays (EMSA) to measure the ability of nuclear extracts isolated from the liver of mice to bind to the FARR (-36 to -7). For these experiments, nuclear extracts from the liver of mice fed a folate adequate and a folate deficient diet, were subjected to gel shift assays using the FARR probe. As shown in Fig. 4.6A, we observed a shifted band, complex 1. The intensity of this band was consistently stronger in extracts obtained from liver tissues of folate deficient mice as compared to mice fed a folate adequate diet and/or mice exposed to oxidative stress, 2-NP. In other words, the protein composing this shifted band appeared to be the factor that responds to oxidative stress and folate deficiency by altering its binding capability to the FARR. For example, the 2-NP treated folate adequate animals showed protein binding ~50% lower than the controls (Fig. 4.6A, lane 3), whereas the folate deficient animals exposed to oxidative stress showed ~50% increase in binding activity (Fig. 4.6A, lane 3). Interestingly, these data show an inverse correlation between the level of DNA binding activity to the *β-pol* promoter, FARR, and the β-pol mRNA expression (Fig. 4.1 D), i.e., the least binding activity in folate adequate 2-NP corresponds to maximal *β-pol* expression, and higher binding activity in folate deficient 2-NP corresponds to the lowest *β-pol* expression.

To address the specificity of the protein/DNA binding activity observed above, we performed competition assays, using cold, mutated FARR and CRE/CREB consensus oligonucleotides. Fig. 4.6C shows the results of a competition assay using 100X molar excess of the unlabelled probe. This competitor eradicated the shifted band indicating the binding activity to be specific. Moreover, the shifted band was also eliminated with 100X molar excess of an unlabelled mutated -36 to -7 probe (FARR with mutation in the CRE site: 5'-TG**AC**GTCA-3' mutated to 5'-TG**TGG**TCA-3') suggesting that the binding activities seen in these conditions are not specific to the consensus CRE site (Fig. 4.6C lane 3). Furthermore, Fig. 4.6C also shows the result of a competition assay using a consensus CRE/CREB (5'-TGACGTCA-3') probe as competitor. This competitor did not affect the formation of the shifted band, indicating that the factor involved is less likely to belong to the CREB/ATF family. We cannot, however, exclude the possibility that CREB/ATF is one of the components of this complex, given that the affinity of CREB/ATF to the CRE site of the mouse β-*pol* promoter is not known. Additionally, a gel shift assay performed with the labeled CRE mutated FARR showed significant DNA binding activity, confirming that the binding is not specific to CRE, while the shifted band did not show any super shifts when antibodies to ATF and AP-1 complex were added to the nuclear extracts (Data not shown). These findings indicate that the factors which show differential binding activity to the FARR segment of the *β-pol* promoter do not belong to the ATF or AP-1 families. Therefore, it is inviting to suggest that the proteins binding to the elements within the FARR region in nuclear extracts obtained from 2-NP treated mice fed a folate deficient diet are negative regulatory factors independent of CREB/ATF, and inhibit induction of β-*pol* expression in response to oxidative stress.

DISCUSSION

Folate deficiency has been associated with many types of cancer, but the underlying molecular mechanism of its tumorigenic effect has not yet been elucidated. Inconsistencies observed in studies conducted on folate deficiency and supplementation suggest that association between cancer and folate status is dependent on the timing of dietary treatment and the exposure to stress inducing agents and

carcinogens [165-169]. Low plasma folate levels have been associated with increased risk of colorectal cancer development in individuals with single nucleotide polymorphism in the *methylene tetrahydrofolate reductase* gene [139,170]. Folate deficiency has also been shown to incapacitate the DNA repair pathways, a potential mechanism behind the accumulation of DNA damage during this deficiency [144,146,149,171]. Moreover, agents such as methotrexate, an inhibitor of dihydrofolate reductase, have been shown to reduce the efficiency of excision repair in CHO cells [172]. Furthermore, BER, a DNA damage inducible pathway [151-153,164,173,174] has been shown to lose its ability to respond to damage during folate deficiency, leading to the accumulation of toxic intermediates [149].

Although folate deficiency has been implicated in inducing cellular stress and impacting DNA repair potential in cells and animal models, the exact mechanism is still not understood. Using microarray analysis and a proteomics approach, recent studies demonstrate the differential effect of folate deficiency on pathways associated with cancer development, DNA repair and apoptosis. A study done on colon cancer cells shows that folate deficiency alters the expression of vital genes involved in many pathways, such as DNA repair, apoptosis, angiogenesis and cell cycle control [175]. Data from our lab shows that folate deficiency in BER compromised mice suppresses DNA repair and promotes apoptosis by altering the expression of key genes involved in these pathways [148]. Furthermore, proteomic analyses, done on folate deficient rat livers, show differential expression of certain proteins involved in oxidative stress and cancer pathways [176]. Thus folate deficiency seems to affect these pathways by targeting specific genes involved in them. In line with these studies, earlier data from our lab demonstrate that folate deficiency negatively regulates BER by affecting the expression of its key enzyme *DNA polymerase β*, and that folate deficiency and *β-pol* haploinsufficiency interact to increase the accumulation of DNA damage [149]. In this study, we provide further data that sheds light on the mechanism by which folate deficiency impacts *β-pol* expression at the level of transcription and prevents its upregulation even under the influence of oxidative stress.

DNA polymerase β plays a very important role in embryogenesis, gap-filling repair synthesis and recombination repair [161-163]. *β-pol* is considered to be a housekeeping gene and is constitutively expressed in all cell cycle stages with differential expression based on the tissue type [161-163]. *β-pol* exhibits dual function in short patch BER, namely polymerase and dRP lyase activity, and has also been demonstrated to play a critical role in Long-Patch BER [157,177,178]. Homozygous deletion of *β-pol* is embryonic lethal, whereas the heterozygous knockouts survive and are fertile [179]. *β-pol* haploinsufficient mice display ~ 50% reduced β-pol protein levels and significant reduction in their β-pol dependant G:U mismatch BER efficiency [153,154]. This reduction in *β-pol* and BER efficiency is thought to be responsible for the increase in mutation frequency seen in these animals when exposed to alkylating agents [154]. In addition, studies conducted on *β-pol* null cells show the accumulation of DNA damage in response to stress inducing agents [180,181].

DNA polymerase β has been demonstrated to be a DNA damage inducible gene i.e., *β-pol* expression has been shown to be upregulated in response to alkylating and oxidizing agents [153,155,164]. In this study, folate deficiency is shown to inhibit the upregulation of *β-pol* mRNA and protein levels in response to 2-NP, an oxidizing agent, whereas, upregulation of other key enzymes in the BER pathway, namely *Ung* and *Ape1/Ref*-1, are unaffected. Thus, the impact of folate deficiency on gene expression seems to be gene specific. Folate deficiency is well known for its effect on DNA methylation via the reduction of the universal methyl donor, SAM. Alterations in DNA methylation in general have been strongly associated with cancer formation, and these alterations are believed to occur early in cancer development [182]. Due to the strong association between genomic hypomethylation and tumor formation especially in colon, stomach, thyroid, breast, uterine and prostate cancers [166,182-185], folate deficiency is suggested to cause cancer via this epigenetic effect. Here in this study, we observed no alterations in the methylation pattern of the CpG rich regions within *β-pol* promoter during folate adequacy and deficiency. No methylated CpG sites were found in the CpG islands identified within this region of *β-pol* promoter. This data suggests that epigenetic alterations, at least in the core promoter region of *β-pol,* are not the

mechanism behind the loss of induction of *β-pol* during folate deficiency. This observation is in line with the notion that the promoter regions of the housekeeping genes are usually not methylated to maintain basal expression [186].

Expression of a gene can be tightly regulated at different points during its conversion from DNA to protein. Gene expression in part is controlled by the interaction of cis-elements within the promoter of the gene with their associated protein factors. Our study shows that the elements within the -104 to +38 region of a *β-pol* promoter are sufficient for the induction of the *β-pol* gene in hepa 1-6 cells exposed to oxidative stress. This finding is in agreement with previous work from other labs which showed that the first 100 nucleotides 5' of exon 1 of human *β-POL* had the core promoter activity [160,161]. Wilson et al further identified SP1 and CRE sites within this region [161]. Sp1 sites in the human core *β-POL* promoter have been shown to be involved in the transcriptional activation of the TATA less promoter [187]. The CRE site, the general binding site for ATF-1, CREB-1, CREM-1 and AP-1, has been shown to be involved in the expression of human *β-POL* during basal conditions and during stress [162-164,188]. Mouse *β-pol* has also been shown to have this consensus palindromic sequence for CREB, and was shown to be required for transcriptional activation of *β-pol* by adenovirus type 12 E1A proteins [189]. DNA alkylating agents like MNNG require the CRE region for inducing *β-pol* [162]. MNNG treatment increases CREB-1 levels by 10-fold in CHO cells which in turn is responsible for *β-pol* induction [162]. In addition, Lamph et al. have demonstrated that CREB, the CRE binding protein, can act as an activator when phosphorylated, and can also act as a repressor in the dephosphorylated state [190]. Further, the CRE consensus sequence has similarities to the AP-1 binding site (TGACTCA) [190,191] and the AP-1 complex can act both as an activator and repressor [192-194]. It has also been shown that AP-1 can bind to the CRE site and act as a repressor in the expression of MyoD1 involved in muscle cell differentiation [195]. Additionally, Wilson et al, have identified a 60Kda novel ATF protein called ATF2d in human testis with incomplete N-terminus [163]. This ATF-2d protein has been demonstrated to have the capacity to bind to a *β-pol* promoter and negatively regulate it [163]. Our data from hepa1-6 cells show that the

promoter activity of *β-pol* is attenuated during folate deficiency even under oxidative stress. This correlates closely with the attenuation of *β-pol* expression observed in mouse liver during folate deficiency. Our footprinting analysis and gel shift assays done on mouse liver extracts show the involvement of the FARR site of *β-pol* promoter encompassing the CRE in the regulation of *β-pol* expression during folate deficiency and oxidative stress. The footprinting and gel shift assays provide evidence that the elements within the FARR site behaves as a negative regulatory site, and the factors binding to these elements act as potential repressors of *β-pol* expression, keeping the *β-pol* expression at the basal level. Furthermore, our data show that the factors binding to the FARR are not specific to the consensus CRE sequence. This observation indicates that the negative regulatory factor binding to the FARR site during folate deficiency might be independent of the CREB/ATF family.

In conclusion, folate deficiency impacts the BER capacity by regulating *β-pol* expression at the level of transcription. This regulation possibly goes beyond folate deficiency's general impact on DNA methylation and controls the *β-pol* expression through the interplay of *cis* and *trans* acting regulatory factors. Our data provides evidence that folate deficiency potentially inhibits *β-pol* induction through negative regulatory factors and keeps its expression at the basal level. However, further characterization is required to identify the inhibitory factors as well as other potential regions of repression.

FIGURE LEGENDS

Fig. 4.1. *Effect of 2-NP on β-pol expression and level of 8-OHdG in liver of* C57BL/6 mice. [A] The 8-OHdG levels in liver tissues of control and 2-NP treated mice were measured by HPLC and EC detector. The data are expressed as values relative to the amount of 2dG detected by UV absorbance at 290nm. [B] *DNA polymerase β* mRNA levels in the liver tissues of control and 2-NP treated mice were quantified using real-time PCR and normalized against *Gapdh*. [C] The levels of β-pol protein in 100 μg of liver nuclear extract obtained from control and 2-NP treated mice were determined by western blot analysis. The level of *β-pol* protein was normalized based on the amount of protein loaded on each gel. PCNA served as the nuclear protein loading control. [I.D.V.]: integrated density value corresponding to the level of β-pol protein as quantified by a Bio-Rad ChemiImager® System. *Effect of folate deficiency and 2-NP on Base Excision Repair activity.* [D] The *in vitro* G:U mismatch BER assay was conducted using nuclear extracts obtained from liver of control and 2-NP treated mice fed a folate adequate and/or folate deficient diet. The reaction products were resolved on a sequencing gel. Repair activity was visualized by the appearance of a 16b fragment. The relative level of BER was quantified using a Bio-Rad Molecular Imager® System. The data were normalized based on the amount of protein used in each reaction and expressed as machine counts per μg of protein. Values represent an average [± S.E.M.] for data obtained from 5 mice in each group and are representative of separate identical experiments. Values with different letter superscripts indicate significant differences at P < 0.05. FA: Folate adequate; FD: Folate deficient.

Fig. 4.2. *Effect of folate deficiency and 2-NP on the expression of β-pol.* [A] *DNA polymerase β* mRNA expression level in the liver tissues of control and 2-NP treated mice fed a folate adequate and/or folate deficient diet were quantified using real-time PCR and normalized against *Gapdh*. [B] The levels of β-pol protein in 100 μg of liver nuclear extract obtained from control and 2-NP treated mice fed a folate adequate and/or folate deficient diet were determined by western blot analysis. The levels of β-pol protein were normalized based on the amount of protein loaded on each gel. [I.D.V.]: integrated density value corresponding to the level of β-pol protein as quantified by a Bio-Rad ChemiImager® System. Values represent an average [± S.E.M.] for data obtained from 5 mice in each group and are representative of separate identical experiments. Values with different letter superscripts indicate significant differences at $P < 0.05$. FA: Folate adequate; FD: Folate deficient.
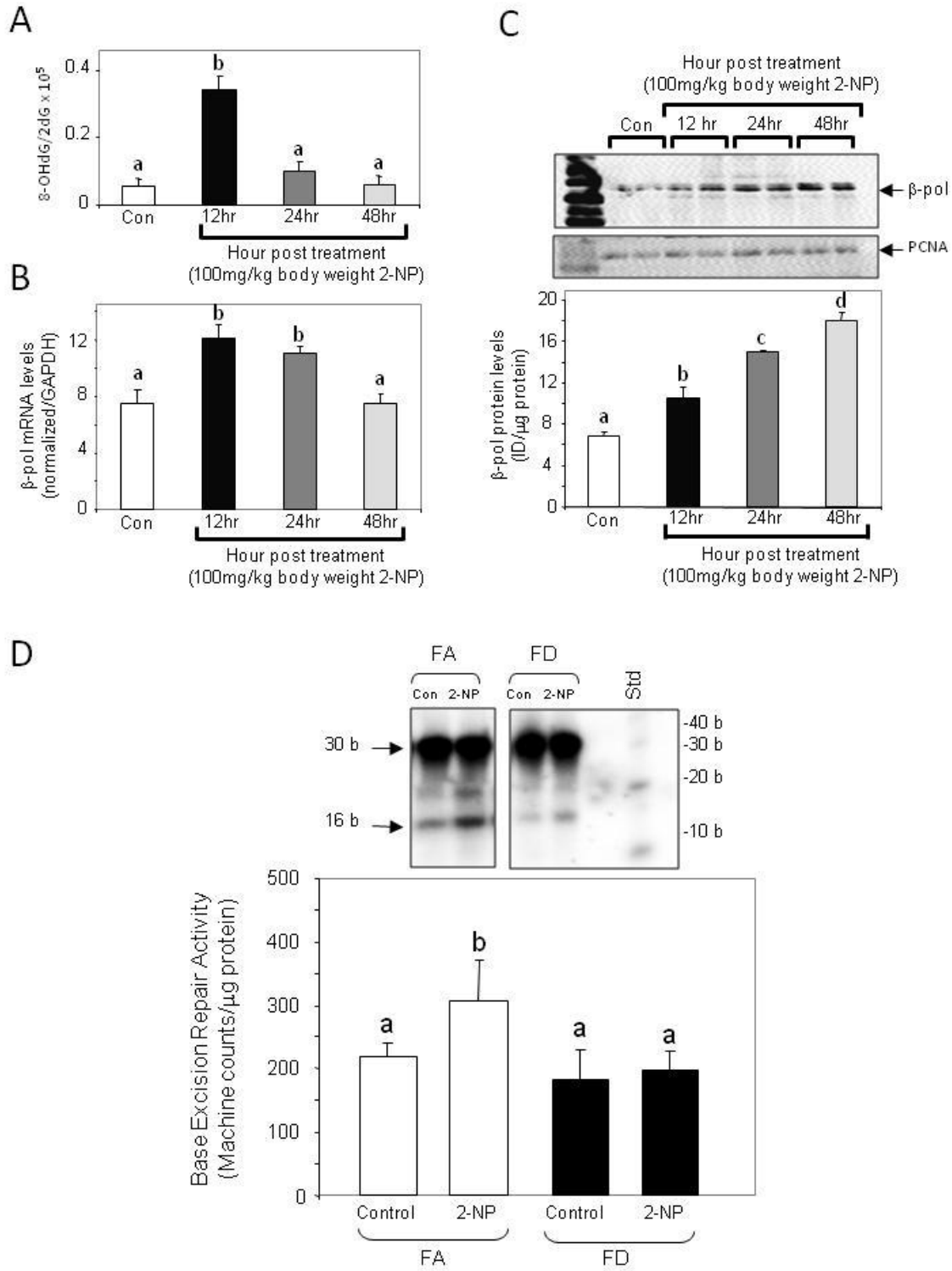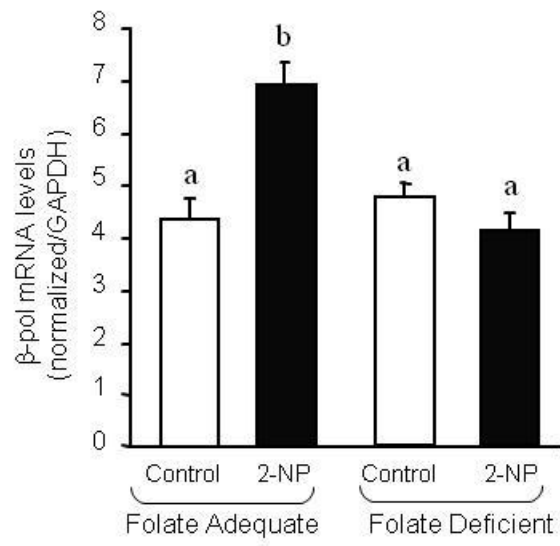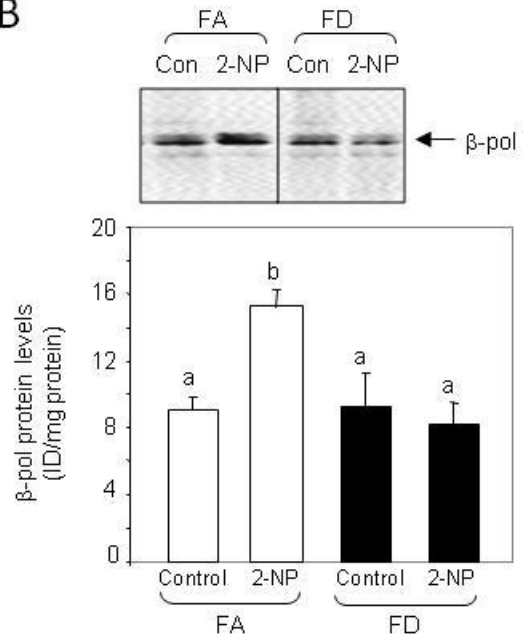
Fig. 4.3. *Effect of folate deficiency and 2-NP on methylation of β-pol promoter.* Methylation of promoter/Exon1 of the *β-pol* gene was determined by bisulfite sequencing assay with single base resolution. The bisulfite treated DNA was PCR amplified using primers designed around CpG islands. The resulting amplicons were cloned into pGEM-T Easy Vector. Plasmids from 7 colonies of each subclone were sequenced and the presence of preserved methylated cytosine residues representing methylation status was determined. [A] Sequence of the two CpG islands [Island 1: -105 to +44 and Island 2: -322 to -123] present in the *β-pol* promoter/Exon1 has been illustrated. [B] Methylation patterns of the CpG sites present within the CpG islands of the *β-pol* promoter/Exon1 has been depicted. Open circle: unmethylated CpG site; Solid circle: methylated CpG site. FA: Folate adequate; FD: Folate deficient.

A

Island 1

-105

taaacctgacctcctagctcccctc**cg**cccagagattcccc**cg**cacc**cg**ca

cc**cg**ctagcccc**cg**cccc**cg**tagcctgg**cgcg**tgac**g**tcacc**cgcg**ctg**cg**cc

ctgtcagg**cg**c**cg**ccattgttccac**cg**gtaagacccaggtgtgggtccc +44

Island 2

-322

ttccatgttttacatggtgtccagaagcacagagcagctcttggattctg

acagcagaacc**cgcg**c**cg**gca**cg**cctcacaaacagtacaggc**cg**tgtgtt

ccatagctactgtccacagcagccaa**cg**tccacctc**cg**tctgcatct**cg**g

gctctaaatcagactattctcagaccaggagagcagatttgatctctcag -123

B

Fig.4.4. *Effect folate deficiency and hydrogen peroxide on β-pol expression and promoter activity in hepa 1-6 cell line.* [A] *DNA polymerase β* mRNA levels in hepa 1-6 cells treated with H_2O_2 [0, 100, 200, 300, 500μM] were determined. Hepa 1-6 cells were treated for 2 and 4 hrs with H_2O_2 and the levels of □-*pol* mRNA were quantified using real-time PCR 24hrs post treatment. The data were normalized against *Gapdh*. [B] Relative promoter activity of sequential deletions of -924 to +38 upstream region of *β-pol* promoter transfected into hepa 1-6 cell line was determined. The transfected hepa 1-6 cells were treated with H_2O_2 [100μM] for 2hrs. Luciferase activity was determined 24hrs post treatment and normalized by β-galactosidase activity. [C] Effect of folate deficiency and H_2O_2 treatment on the relative promoter activity of -924 to +38 upstream region of *β-pol* promoter transfected into hepa 1-6 cell line were determined. The transfected cells were treated with H_2O_2 [100□M] for 2 hrs as described in Methodology. Luciferase activity was determined 24hrs post treatment and normalized by β-galactosidase activity. Values represent an average [± S.E.M.]. FA: Folate adequate; FD: Folate deficient.

A

B

β-pol promoter
Plasmid Construct

C
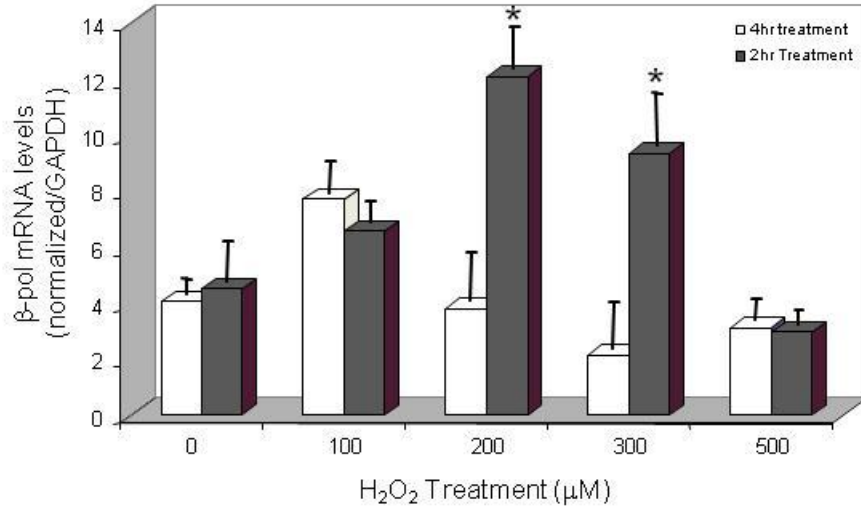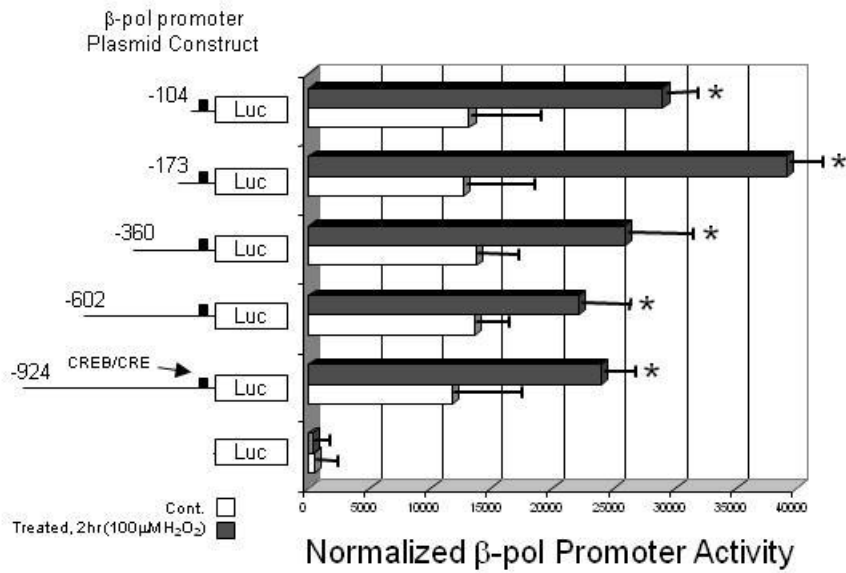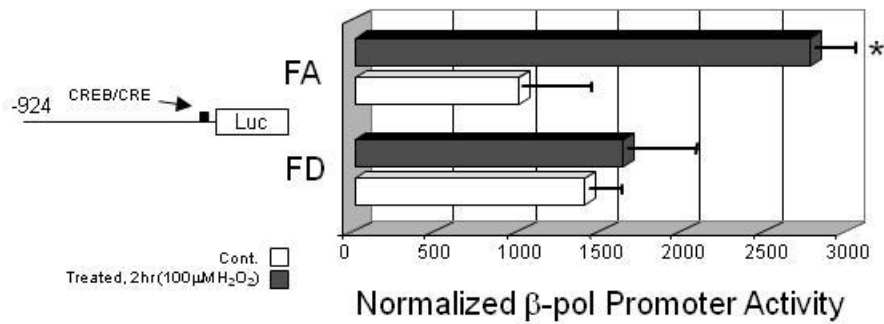
Fig.4.5. *β-pol promoter DNase I footprinting analysis.* DNase I footprinting assay was performed using the −360 to +97 fragment of *β-pol* promoter and nuclear extracts obtained from liver tissues of mice fed a folate deficient and/or folate adequate diet. DNA fragments were analyzed using ABI Prism 310 Genetic Analyzer [Life Technologies, Carlsbad, CA]. Numbers at the top of the panel represent fragment length in nucleotides. The specific protected fragment encompassing the CRE/CREB binding site is shown in an expanded view. The DNA sequence of the region is displayed above with the CRE/CREB consensus site highlighted. FA: Folate adequate; FD: Folate deficient.

Promoter Region   5'utr   Exon 1

CREB/CRE

CCCCGTAGCCTGGCGCGTGACGTCACCGCGCTGCGCC

FA-2NP

FD-2NP

FA

FD

Control

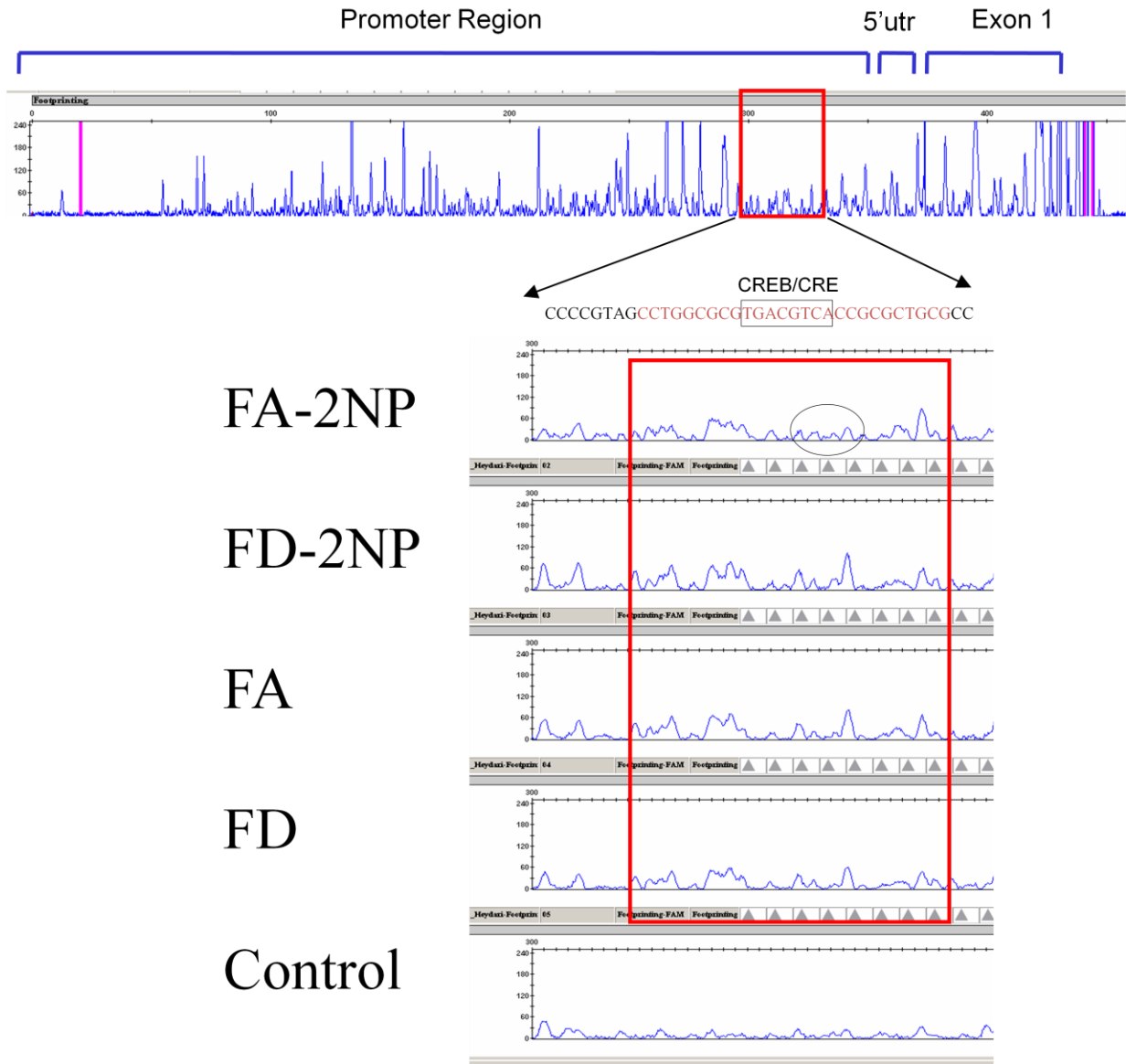**Fig.4.6.** *Effect of folate deficiency and 2-NP on DNA binding activity in nuclear extracts obtained from liver tissues of C57BL/6 mice.* [A] Binding of liver nuclear extracts to the -36 to -7 region [FARR, 5'–AGCCTGGCGCGTGACGTCACCGCGCTGCGC-3'] of the *β-pol* promoter. Nuclear extracts were obtained from liver tissues of mice fed a folate deficient and a folate adequate diet and were analyzed [10 □g of nuclear extracts per assay] by the mobility shift assay, using biotin-end-labeled FARR oligonucleotide as described in Methodology. [B] The shifted bands observed in the Panel A [Complex 1] were quantified using a Bio-Rad ChemiImager[®] System. Values represent an average [± S.E.M.] for data obtained from 5 mice in each group and are representative of separate independent experiments. [C] The specificity of protein-DNA binding activity was determined by competition assays. Mobility shift assays were performed in the presence of 100x molar excess of cold FARR [Lane b, 5'–AGCCTGGCGCGTGACGTCACCGCGCTGCGC-3'], mutated FARR [Lane c, 5'-AGCCTGGCGCG**TG**TGGTCACCGCGCTGCGC-3'], and CRE/CREB Consensus [lanes d-f, 5'-AGAGATTGCCTGACGTCAGAGAGCTAG-3'] oligonucleotides. Lane a is a positive control and does not contain any competitor. I.D.V., integrated density value. Values with different letter superscripts indicate significant differences at P < 0.05. FA: Folate adequate; FD: Folate deficiency.

A
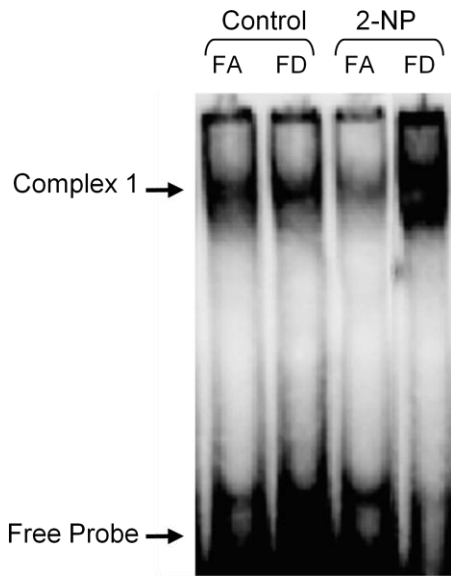
B
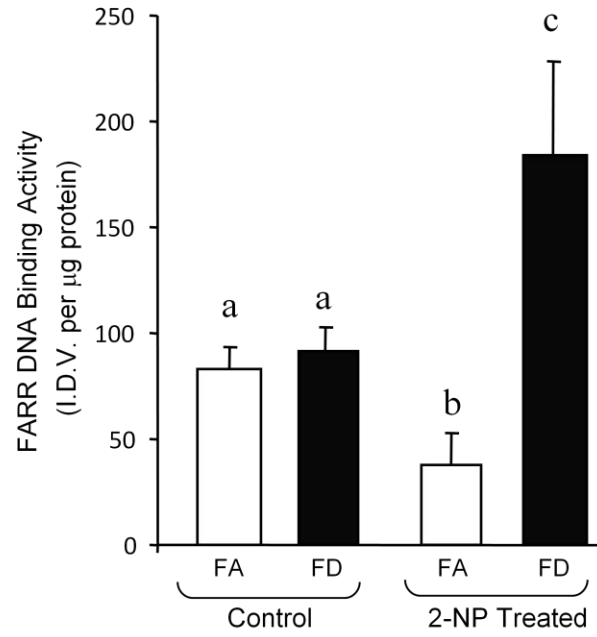
C
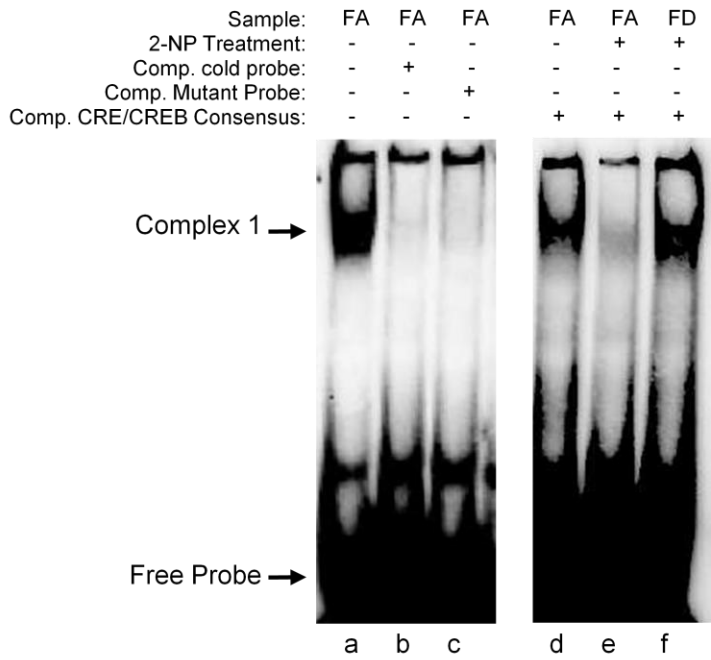
Chapter 5

The impact of folate and methionine dietary interventions on base excision repair pathway and colon cancer in response to a carcinogen

[1]Department of Nutrition and Food science, Science College of Liberal Arts and Sciences, Wayne State

University, Detroit, Michigan 48202.

Address Correspondence to: Ahmad R. Heydari, 3009 Science Hall, department of Nutrition and Food

Science, Wayne State University, Detroit, Michigan 48202.

Tel: 313-577-2459, Fax: 313-577-8616. E-mail: ahmad.heydari@wayne.edu

Introduction

Base excision repair (BER) is one of the major excision repair pathways capable of processing upto 1,000,000 nucleotides/cell/day. Base excision repair is a dynamic repair pathway responsible for repairing endogenous damages. This DNA repair pathway is a stress inducible pathway capable of repairing non helix distorting damages such as oxidative and alkylation damages (196-201). Base excision repair is a linear pathway consisting of a series of enzymes which functions in a co-ordinated manner. The traditional BER pathway involves the removal of a single damaged base such as an alkylated base or misincorporated uracil from the DNA. Briefly, the repair begins with a monofunctional glycosylase which removes the damaged base and leaves behind an abasic site. This abasic site acts as the substrate for the next enzyme in the pathway, apurinic/apyrimidinic endonuclease 1/redox factor-1 (APE1/Ref-1), an endonuclease which also functions as a 3'-phosphodiesterase, 3'-phosphatase and 3'-5'-exonuclease activities (202). APE1/Ref-1, has also been characterized as a redox factor involved in many redox signaling pathways (203,204). The single strand break with 3'-OH end left behind by the endonucleolytic action of APE1/Ref-1 becomes the substrate for the next enzyme DNA polymerase β (β-pol). β-pol, functions as a dRPlyase initially removing the dRP flap. This dRPlyase activity has been found to the rate determining step in this monofunctional glycosylase initiated pathway (205). After the removal of the dRP flap, β-pol inserts a new nucleotide to the 3'-OH end. Subsequently, DNA ligase seals the nick completing base excision repair. On the other hand, certain other damages such as 8-hydroxyguanosine and thymine glycol require a bifunctional glycosylase for its removal. These bifunctional glycosylase's have Ap lyase activity which blocks the 3'end. This blocked end requires trimming by the 3'-phosphoesterase activity of APE1/Ref-1, thus generating 3'-OH end and subsequently β-pol inserts a new nucleotide and ligase seals the nick. The base excision repair pathway and specifically the enzymes involved in this pathway are critical during embryonic development. Deletion of both alleles of APE1/Ref-1 has been shown to be embryonically lethal, but the heterozygous knockout mice survive and are fertile (206-208). In our previous study we have reported the loss of bifunctional DNA glycosylase-

initiated BER and increased induction of aldehydic lesions during APE1/Ref-1 haploinsufficiency in response to oxidative stress (208). Likewise, homozygous deletion of β-pol in mice has been shown to be embryonically lethal, but again the heterozygous knockout mice survive (209). Cabelof et al, have shown the impairment of the BER pathway and the consequent increase in single strand break accumulation during β-pol haploinsufficiency (210). Furthermore, dietary manipulations like folate deficiency have been reported to deregulate the base excision repair pathway and this impairment was shown to be accelerated by β-pol haploinsufficiency (211).

Folic acid, a water soluble vitamin is essential for one-carbon transfer reactions and plays a vital role in all metabolic reactions. The folate cycle consists of three major segments. The first segment involves the conversion of dietary folate into tetrahydrofolate and dihydrofolate and the regeneration of tetrahydrofolate. During this cycling of folate intermediates one carbon transfers take place for purine and pyrimidine especially thymidine biosynthesis. The second segment of the folate cycle is the trans-methylation pathway, whereby the universal methyl donor s-adenosyl methionine is formed. Methionine, an essential amino acid enters the folate cycle at this point from the diet and helps in the formation of s-adenosyl methionine and homocysteine. Finally, methionine is regenerated with the help of a folate intermediate. The third segment of the folate cycle consists of the trans-sulfuration pathway, which results in the conversion of homocysteine into cystathionine. Cystathionine further forms cysteine which in turn gets converted to glutathione, a major cellular antioxidant. Therefore, a low folate status because of its multivariate role could impair DNA synthesis, DNA methylation and redox status of the cell.

Intrauterine folate deficiency has been very definitively shown to result in neural tube defects in newborns and this has lead to the scheme of the current folate fortifications. Folate deficiency has also been associated with many other diseases such as anemia, cardiovascular diseases, neurological degeneration and cancer, in particular colorectal cancer. Although the exact mechanism behind folate deficiency induced tumorigenesis is largely unknown, many studies on folate deficiency have shown abnormal epigenetic alterations and accumulation of DNA damages such as single strand breaks and

mutations, leading to genomic instability, micronuclei formation, chromosomal aberrations and eventually cancer. Further, folate deficiency has been suggested to impair DNA repair pathways which provide a plausible explanation for the accumulation of the aforementioned damage. In support of this, folate deficiency has been shown to increase the potency of DNA- damaging agents and increase mutation frequency and DNA strand breaks (211-213). On the other hand, the second essential component of the folate cycle, methionine, when restricted has been shown to extend mean and maximum life-span in laboratory rodents (214-216). Methionine restriction has also been shown to reduce free radical leak and oxidative stress in laboratory rodents (214-216). Depletion in methionine has also been shown to reduce proliferation of cancer cells and promote apoptosis making methionine restriction a potent anti-cancer strategy. It is intriguing that these two integral factors of the same cyclic pathway display very different effects when they are depleted. Therefore, the objective of this study is to evaluate the differential effect of folate deficiency and methionine restriction on the BER pathway and cancer incidence.

Experimental Procedures

Animals- All the experiments were performed in male C57BL/6 specific pathogen–free young wildtype mice in accordance with NIH guidelines for the use and care of laboratory animals. The Animal protocol was approved by the Wayne State University Animal Investigation Committee. The animals were fed the standard mouse chow and water ad libitum and were maintained on a 12-hr light/dark cycle.

Diets and Carcinogen treatment- At 3-4 months of age, the mice were randomly assigned to four dietary groups and were fed AIN93G-purified isoenergetic diets (Dyets, Inc.,Lehigh Valley,PA) as described previously (211). Diets were stored at -20°C. The control group received a folate adequate/ methionine adequate diet (2mg/kg folic acid and8.2 mg/kg methionine: FA/MA). The experimental groups received folate deficient diet (0 mg/kg folic acid: FD), methionine restricted diet (1.64mg/kg methionine: MR) and folate deficient/methionine restricted diet (0mg/kg folic acid/1.64mg/kg methionine: FD/MR). All diets were supplemented with 1% succinyl sulfathiazole. The animals were monitored for signs of toxicity. One

week into the respective diets, mice were treated with 1,2-dimethylhydrazine HCl (DMH, 30 mg/kg body weight) in 10 mmol/litre of $NaHCO_3$ (Fisher Scientific)intraperitoneously once a week for 6 weeks (Fig. 1A) as previously described (lisa's,JBC). The animals were monitored for signs of toxicity and the experimental diets were continued for 12 weeks. Mice were anesthetized in a CO_2 chamber and the abdominal cavity was opened up for excising the colon and harvesting the liver tissue. The harvested liver was flash frozen and stored in liquid nitrogen.

Aberrant crypt foci (ACF) analysis- The excised colons were rinsed with cold phosphate-buffered saline, cut longitudinally, and fixed flat overnight in 10% neutral buffered formalin as described previously (217). The fixed colons were stained with 2g/litre of methylene blue in phosphate-buffered saline for 5 mins. The number of ACF and aberrant crypts per foci were determined by light microscopy at 10X magnification in a blinded manner as described previously (217).

Tumor Analysis- Randomly selected animals from the folate adequate control and folate deficient groups were continued on the experimental diets for 40 weeks after the last dosage of DMH. After 40 weeks these animals were anesthetized under CO_2 and sacrificed for tumor analysis as described previously (217). Briefly, all organs and tissues were examined for grossly visible lesions. Liver and colon tissues, including gross abnormalities, were fixed in 10% neutral buffered formalin, trimmed, embedded in paraffin, sectioned to a thickness of 5-6uM, stained with H&E, and examined microscopically. Preparation of slides for histopathology evaluation was performed by pathologists at the Department of pathology, Wayne State University.

Uracil-Aldehyde-Reactive Slot blot Assay- Liver DNA for the Uracil and aldehyde reactive probe slot blot (ASB) assay was extracted using DNeasy Kit (Qiagen, Maryland, USA) as described in the manufacturer's protocol.

*ASB assay-*Aldehydic lesions in the DNA was quantified using the ASB assay as described previously (211,218). Briefly, about 8ug of extracted DNA in 1X Tris-EDTA buffer (TE) was treated

with aldehyde reactive probe (ARP; Dojindo Laboratories, Kumamoto, Japan) at 37°C for 15 mins. Further the DNA was precipitated using NaCl/Glycogen/Isopropanol precipitation and resuspended in 1X TE buffer. The probed DNA was heat denatured at 100°C for 10 min, quickly chilled on ice, and mixed with an equal volume of 2M ammonium acetate. The nitrocellulose membrane (Schleicher and Schuell) was prewet in deionized water and washed for 10 min in 1mM ammonium acetate. DNA was immobilized on the pretreated nitrocellulose membrane using an Invitrogen filtration manifold system. The membrane was washed in 5X SSC for 15 min at 37°C and then baked under vacuum at 80°C for 30mins. The dried membrane was incubated in a hybridization buffer (20mM Tris, pH7.5, 0.1 M NaCl, 1mM EDTA, 0.5% (w/v) casein, 0.25% (w/v) bovine serum albumin, 0.1% (v/v) Tween 20) for 30 min at room temperature. The membrane was then incubated in fresh hybridization buffer containing 100ul of strptavidin-conjuagated horseradish peroxidase (BioGenex, San Ramon, CA) at room temperature for 45 min. Following incubation in horseradish peroxidase, the membrane was washed three times for 5min each at 37° C in TBS, pH 7.5, (0.26 M NaCl, 1mM EDTA, 20mM Tris, pH 7.5, 0.1% Tween 20). Membrane was incubated in Super signal West Pico Chemiluminescent Substrate (ThermoScientific, Rockford, IL) for 5 min at room temperature and visualized using Molecular Imager [R] system (Bio-Rad, Hercules, CA).

Uracil-ASB assay-About 4ug of the DNA in TE buffer was treated with Tris-Methoxyamine (Sigma-Aldrich) and incubated at 37°C for 2 hrs. DNA was precipitated using NaCl/Glycogen/Isopropanol precipitation and resuspended in 1X TE (pH 8.0). The resuspended DNA was treated with Uracil DNA glycosylase (UDG; 1:10 dilution, New England Biolab) for 15 mins at 37°C. The UDG treated DNA was further precipitated using NaCl/Glycogen/Isopropanol precipitation and again resuspended in 1X TE buffer (pH 8.0). Further, the DNA was probed with 2mM ARP (Dojindo Laboratories, Kumamoto, Japan) for 15 mins at 37°C. The probed DNA was further precipitated as previously using NaCl/Glycogen/Isopropanol precipitation and resuspended in 1X TE. From here, the procedure is similar to the ASB assay.

Isolation of Crude Nuclear extract- Nuclear extracts were isolated using a transfactor extraction kit (Clontech, Mountain View, CA) as previously described (208). Briefly, a hypotonic buffer is used to lyse the cell allowing for the removal of cytosolic fractions, followed by a hypertonic buffer which helps in the extraction of nuclear proteins. All solutions were made fresh and all samples and tubes were maintained on ice. Low molecular weight contaminants were removed from extracts by dialysis using Slide-A-Lyzer^R mini-dialysis units (Pierce Biotechnology, Rockford, IL) with a molecular weight cut off of 3.5 KD for 3 hours at 4°C. The dialysis buffer has 20mM Tris-HCl, pH 8.0, 100mM NaS2O5, 0.1mM PMSF, and 1mg/ml PepstatinA. Dialyzed extracts were aliquoted and stored at -80°C for subsequent analysis. Protein concentrations were determined using to Bradford protein assay kit I (Bio-Rad, Hercules, CA).

Isolation of Whole cell extract- Whole cell extracts were isolated using hypotonic and hypertonic salt solutions from transfactor extraction kit (Clontech, Mountain View, CA). Briefly, 100mg of liver tissue was homogenized with the hypotonic salt solution to lyse the cell and further treated with the hypertonic salt solution to release the nuclear contents without any fractionations. The whole cell extract thus obtained was used for various assays.

Uracil Excision assay- Uracil excising activity was determined as described previously (211) with minor modifications. Briefly, the assay reaction mixture contained 70mM Hepes (pH7.5), 1mM EDTA, 1mM NaCl, 0.5% bovine serum albumin, 90 fmol of 5' fluorescein-end-labeled single stranded uracil-containing 30-mer oligonucleotide (5' – ATATACCGCGGUCGGCCGATCAAGCTTATT-3', Sigma-Aldrich, St.Louis) and 5ug of whole cell extract from liver tissue. The reaction mixture was incubated at 37°C for 1hr. After 1hr the reaction was terminated using 5μg of proteinase K and 1 μl of 10% SDS and incubated at 55°C for 30min. The reaction mixture was further suspended in a loading buffer containing 80% formamide, 10mM EDTA, 1μg/ml of bromophenol blue and 1μg/ml of xylene cyanol. The substrate and reaction products were separated on a 20% denaturing sequencing gel (SequaGel Sequencing System, National Diagnostics, Atlanta, GA). Glycosylase activity (presence of an 11-mer band) was visualized and quantified using a Molecular Imager System (Bio-Rad, Hercules, CA) by calculating the ratio of the

11-mer product with the unreacted 30-mer substrate (product/product +substrate). The data are expressed as machine counts per µg of protein.

DNA base excision repair activity assay- The G:U mismatch repair assay is developed to measure monofunctional glycosylase-initiated base excision repair activity and the assay was performed as describe previously (208). Briefly, purified fluorescein-end-labeled 30bp oligonucleotides (upper strand: 5'– ATATACCGCGGUCGGCCGATCAAGCTTATTdd-3'; Lower strand: 3'-ddTATATGGCGCCGGCCGGCTAGTTCGAATAA-5') containing a G:U mismatch and a *Hpa II* restriction site (CCGG) were incubated in a BER reaction mixture containing 50 µg nuclear protein. This assay uses a 30bp long oligonucleotide with G:U mismatch as no significant difference was seen in the catalytic efficiency of the in vitro assay when a plasmid or oligonucleotide was used as a substrate (219). Repair of the G:U mismatch to a correct G:C base pair was determined via treatment of the duplex oligonucleotide with 20U of *Hpa II* (Promega, Madison, WI) for 1hr at 37°C and analysis by electrophoresis on a 20% denaturing sequencing gel, 19:1 acrylamide/bis-acrylamide (SequaGel Sequencing System, National Diagnostics, Atlanta, GA). Repair activity i.e., the presence of a 16-mer band, was visualized and quantified using a Molecular Imager System (Bio-Rad, Hercules, CA) by calculating the ratio of the 16-mer product with the unreacted 30-mer substrate (product/product+substrate). The data are expressed as machine counts per µg of protein.

Western Blot Analysis- Protein expression analysis was performed using western blot technique as previously described (208). 100 µg nuclear protein was used to run the SDS-PAGE. Upon completion of SDS-PAGE, the region containing the proteins of interest was excised and prepared for western blot analysis while the remaining portion of the gel was stained with Gel Code Blue Stain Reagent (Pierce Biotechnology, Rockford, IL) to ensure equal protein loading. Manufacturer recommended dilutions of anti-sera developed against UDG (Santa Cruz Biotechnology, Santa Cruz, CA), APE1/Ref-1 (Novus Biologicals, Littleton, CO), β-pol (Abcam, Cambridge, MA), and Thioredoxin 1 (Millipore, Billerica,

MA) were used to detect proteins of interest followed by incubation with HRP-conjugated secondary antibody (Santa Cruz Biotechnology, Santa Cruz, CA). The bands were visualized and quantified using a Molecular Imager System (Bio-Rad, Hercules, CA) after incubation in SuperSignal West Pico Chemiluminescent Substrate (Pierce Biotechnology, Rockford, IL). Data are expressed as the integrated density value (I.D.V.) of the band normalized to β-actin.

Gene expression profiling- The mRNA expression level of Gadd45g was quantified using a real-time PCR-based pathway focused on gene expression profiling of mouse DNA damage. Total RNA was extracted from liver tissue using RNeasy extraction kit (Qiagen, Valencia, CA). First strand cDNA was synthesized from 1μg RNA using random primers and purified using QIAquick PCR purification Kit (Qiagen, Valencia, CA). Expression of Gadd45g was quantified using real time PCR with specific primers for the gene (FP: 5'-AGTTCCGGAAAGCACAGCCAGGATG3' and RP: 5'-GCCAGCACGCAAAAGGTCACATTGT-3'). The gene transcript was normalized to RPLO. External standards for all the genes were prepared by subcloning the amplicons, synthesized using the specific primers into PGEM-T easy vector.

Caspase Assay- Caspase-3 activity was measured using Enzchek Caspase-3 Assay Kit No.1 (Molecular probes, Eugene, OR) as described previously (208). Briefly, Liver tissues were homogenized, and cytosolic extracts were isolated using Transfactor Extraction Kit (Clonetech, Mountain View, CA). The extracts (250 μg protein) were incubated for 2hr at room temperature in the working solution (25mM PIPES, pH 7.4, 5mM EDTA and 2.25% CHAPS) containing synthetic caspase-3 substrate, Z-DEVD-AMC. Caspase mediated proteolytic cleavage of the substrate yields a bright blue-fluorescent product. An additional control assay was performed using reversible aldehyde inhibitor Ac-DEVD-CHO to confirm that the fluorescence observed in the sample assay was due to caspase activity. The fluorescence was measured using a fluorescence microplate reader (Genios plus, Tecan) at excitation: 342nm, emission: 441nm. The caspase activity was determined using an AMC (7-amino-4-methylcoumarin) standard curve (0-100μM), and reported as fluorescence per μg of protein.

Glutathione Peroxidase Assay- Glutathione peroxidase assay was performed using the assay kit from Cayman Chemical Company, Ann Arbor, MI, according to the manufacturer's protocol. The principle of the assay makes use of a coupled reaction between Glutathione peroxidase and Glutathione reductase. The oxidized glutathione released during the reduction of hydroperoxide by glutathione peroxidase acts as the substrate for glutathione reductase. The conversion of NADPH to NADP+ during the gluatathione reaction creates a decrease in absorbance at 340nm. Briefly, about 200mg of the liver tissue was homogenized in 1ml of cold phosphate buffer (50mM phosphate, pH6.7, containing 1mM EDTA) and centrifuged at 10,000 X g for 15 minutes at 4°C. The supernatant was used for the enzyme assay. The supernatant was mixed with the assay buffer (50 mM Tris-HCl, pH 7.6, containing 5mM EDTA), co-substrate mixture, containing NADPH, glutathione and glutathione reductase, and subsequently treated with cumene hydroperoxide to initiate the reaction. The decrease in absorbance was measured at 340nm using a microplate reader (Genios plus, Tecan) to 5 time points. Bovine erythrocyte Gpx was used as the positive control.

Thioredoxin Reductase Assay- Thioredoxin reductase assay was performed using the assay kit from Cayman Chemical Company, Ann Arbor, MI, according to the manufacturer's protocol. The principle of the assay is the reduction of Ellman's reagent-DTNB [5,5'-dithio-bis(2-dinitrobenzoic acid)] with NADPH to TNB (5-thio-2-nitrobenzoic acid) producing a yellow product with an absorbance range of 405-414nm. Briefly, liver tissues were homogenized, and cytosolic extracts were isolated using Transfactor Extraction Kit (Clontech, Mountain View, CA). The cytosolic extracts were treated with the assay buffer (50 mM potassium phosphate, pH 7.0, containing 50mM KCl, 1mM EDTA, and 0.2 mg/ml BSA) and subsequently treated with NADPH and DTNB to initiate the reaction. The absorbance was measured at 405-414nm using a microplate reader (Genios plus, Tecan). Reactions were conducted with and without sodium aurothiomalate to measure reduction of DTNB specifically by Thioredoxin Reductase. Rat liver Thioredoxin reductase was used as the positive control.

Single Strand Break Assay- Assessment of single-strand breaks was done using the Fast Micromethod DNA Single Strand Break assay as described by Henderson, DNA repair protocols. 100 mg of liver tissue was homogenized and whole cellular content was further untilized for this assay. This method is based on the ability of the specific fluorochrome Picogreen (Molecular Probes, Eugene OR) to make a stable complex with double-stranded DNA, from whole cell content, in alkaline conditions. The preferential binding of Picogreen to double-strand DNA over single-strand DNA or proteins allows detection of single-strand breaks in the DNA by following the fluorometric signal intensity. The decreasing signal intensity during denaturation is measured at Excitation/Emission of 485/538 using a fluorescence microplate reader (Genios Plus, Tecan) and is proportional to increasing single-strand break content. Results were calculation after 10 minutes in denaturing solution (1M NaOH, 20mM EDTA, 1% DMSO) and normalized to reference control sample and expressed as fluorescence units at 538 nm.

Statistical Analysis- Statistical significance between means was determined using t-test and analysis of variance followed by post tukey test wherever appropriate. P-values less than 0.05 were considered statistically significant.

Results

Analysis of Aberrant crypt foci formation during folate deficiency in the colon of C57Bl/6 mice-

Folate deficiency has been associated to the development and progression of different types of cancer, more notably colon cancer. In this study, we have investigated the effect of folate deficiency on the development of cancer in C57BL/6 mice. In the first series of experiments we determined the impact of folate deficiency on the development of Aberrant Crypt foci, an early indicator of colon cancer (220-222). At the commencement of the study, as illustrated in Fig.5.1A., we randomly assigned c57BL/6 mice into the folate adequate and folate deficient groups. These animals were started on a folate adequate (2mg/kg of folic acid) and folate deficient (0mg/kg of folic acid) diet at 6 weeks of age. To attain severe folate deficiency, the folate deficient diet was supplemented with 1% succinyl sulfathiazole, an

antibacterial drug that inhibits folic acid biosynthesis by the colon bacteria. The dietary regimens were continued for twelve weeks. And at the end of the 12th week the animals were sacrificed and tissues were harvested for analysis. Periodically, the amount of food consumed and body weight measurements were taken during the entire study. In line with our previous findings, the amount of food consumed and body weight measurements did not significantly differ between the folate adequate and folate deficient groups (data not shown). Serum folate levels measured as a competitive assay using SimulTRAC-SNB radioassay kit for vitamin B$_{12}$ (^{57}CO) and folate (^{125}I), was found reduced by 90% whereas the colon folate levels were reduced by 40% in these animals. These results were very similar to results obtained in other studies conducted on folate deficiency (data not shown). For measuring the development of preneoplastic lesions, i.e. aberrant crypt foci (ACF), the excised colons were opened and flat fixed in 10 % neutral buffered formalin for 24 hours, stained with methylene blue and scored under a light microscope. As shown in fig. 1B, the colons from both folate adequate and deficient group appeared morphologically normal and no aberrant crypts were found in them, emphasizing the need for a carcinogen to induce these lesions in the laboratory animals. The liver tissue from the same set of animals did not show any gross/ visible abnormalities. This study only show that short term i.e., 12 weeks of folate deficiency by itself does not generate preneoplastic lesions; therefore it becomes important to determine the development of the aberrant crypts during prolonged feeding.

Analysis of damages to DNA during folate deficiency in the liver of c57BL/6 mice-

Methyl donor deficiency has been shown to accumulate preneoplastic lesions in the liver of rats (223). Although our liver tissue from our folate deficient animals did not show any gross/ visible abnormalities, many studies have shown liver to be a major site affected by folate deficiency. Folate deficiency has been reported to increase accumulation of DNA damages such as misincorporated uracil and DNA strand breakage (212,225-229). Deficiency in folate reduces the formation of dTMP from dUMP resulting in accumulation and misincorporation of uracil into DNA (218,230). Apart from misincorporation, uracil can arise in DNA due to cytosine deaminations. Uracils in DNA are mutagenic

and are usually repaired by the base excision repair pathway. Any imbalance in the BER pathway results in the accumulation of toxic repair intermediates such as abasic sites and single strand breaks. Abasic sites and DNA single strand breaks can also appear in DNA directly due to spontaneous hydrolytic reactions and oxidative stress (231). In addition, abasic sites and single strand breaks are considered to be more toxic and mutagenic than misincorporated uracil. Here we evaluated the accumulation of these genomic damages during folate deficiency. As demonstrated previously by our lab (218) folate deficiency resulted in modest increase in uracil levels (~28%) in the liver genomic DNA as measured by an UDG-coupled ASB assay when compared to its folate adequate counterparts (Fig.5.2A).

Further, uracils in DNA are repaired by monofunctional glycosylases such as Uracil DNA glycosylase (UDG) leaving behind an abasic site. Using ASB assay we measured the abasic sites in our folate deficienct animals and observed ~ 33% reduction in them (Fig.5.2B). The abasic site left behind by UDG further processed by APE1/REF-1, an endonuclease. This endonuclease upon removal of the abasic site leaves behind single strand breaks, the substrate for DNA polymerase β (β-pol). We utilized a fast micromethod single strand break assay and measured the levels of single strand breaks as a decrease in fluorescence. Our data showed no significant difference in the level of single strand breaks between the folate adequate and deficient groups (Fig.5.2C). Our folate deficient condition showed only the accumulation of uracil whereas the other toxic damages were not significantly induced. This could be the result of reduction in spontaneous damage accumulation or efficient base excision repair pathway. Therefore, as the next series of experiment we characterized the effect of folate deficiency on the BER pathway.

Analysis of the BER pathway during folate deficiency in liver of C57BL/6 mice

Base excision repair becomes important during folate deficiency as all damages created by low folate are almost entirely repaired by the BER pathway. BER is a simple, dynamic, environmentally responsive DNA repair pathway (232-234) playing an important role in repairing alkylation and oxidative

damages. Cabelof et al, have previously reported the imbalance in the base excision repair pathway during folate deficiency despite the increase in single strand breaks observed during their study (211). Here again, in this study we observed no increase in the invitro G:U mismatch BER activity in response to folate deficiency (Fig. 5.3E). To further characterize the effect of folate deficiency on the individual enzymes in the BER pathway, we looked at the expression of the major enzymes involved in the repair of misincorporated uracil. Uracil DNA glycosylase, a monofunctional glycosylase is the primary enzyme involved in the removal of misincorporated uracil. Apart from UDG, SMUG, TDG and MBD4 act as backup glycosylases for the removal of uracil in DNA. Our folate deficient animals showed about 38% upregulation in the UDG protein (Fig.5.3A) as has been reported by other studies. In our previous study done on 8 weeks folate deficiency, we had reported a tight correlation between the increase in UDG protein and its activity (211). Here in this study with 12 weeks of folate deficiency we did not see a corresponding increase in UDG activity (Fig.5.3B). This lack of induction in the UDG activity potentially explains the increase in uracil levels in DNA during folate deficiency.

The next enzyme in the BER pathway is APE1/Ref-1, an endonuclease which can also act as a redox factor. Ape1/Ref-1, probably due to its redox activity functions as the rate limiting enzyme of the pathway when repairing an oxidative damage such as 8-OHdG (208). Ape1/Ref-1 endonuclease removes the abasic site leaving behind a single strand break.The protein level of this enzyme was significantly reduced by 59% in our folate deficient group (Fig. 5.3C). Inspite of this reduced APE1/Ref-1, the abasic sites in this condition were lower. However, the enzyme activity might be adequate enough to carry out its function. β-pol, the next enzyme in the pathway utilizes the single strand break with 3'-OH as its substrate and adds a new nucleotide. β-pol, is the rate determining enzyme during the removal uracil from DNA. β-pol, has dRPlyase activity which has been shown to be the rate limiting step in this pathway (205). In our previous study on folate deficiency where we had subjected the animals to 8 weeks of folate deficiency, a significantly higher level of single strand breaks corresponding to lower β-pol levels was observed (211). Since our single strand break levels in our 12 weeks folate deficient animals were not

different from its wildtype counterpart, we expected the β-pol protein levels to be similar or greater than the folate adequate group. To our surprise, the β-pol levels were significantly lowered (~45%) in the folate deficient animals (Fig.3D). Our findings clearly show that folate deficiency impairs the efficiency of the animals in processing the misincorporated uracil through the BER pathway. Since the repair efficiency of the folate deficient animals was reduced, it became important to look at the apoptotic capacity of the folate deficient animals.

Analysis of apoptosis during folate deficiency in the liver of C57BL/6 mice

Apoptosis acts as a protective mechanism during stress helping in eliminating the damaged DNA and cell (235). To characterize the effect of folate deficiency on cell cycle arrest and apoptosis, we analyzed three markers of apoptosis namely Gadd45g (growth arrest and DNA damage-inducible gene, γ), p53 and Caspase-3. Using real-time PCR we analyzed the mRNA expression of Gadd45g, a genotoxic stress-inducible gene associated with cell cycle arrest and apoptosis. Gadd45g mRNA level showed a lowering trend by ~38% during folate deficiency (Fig.5.4A). Since Gadd45g is a p53 responsive gene and because p53 is a well established regulator of cell cycle arrest and apoptosis, we next evaluated the stabilization of p53 protein in our folate deficient animals. A tight correlation existed between Gadd45g expression and p53 protein stabilization with p53 protein levels distinctly lowered by ~41 % in the folate deficient animals (Fig.5.4B). The result on p53 was in consensus with our data from a previous study conducted by our lab (211). We further determined the activity of one of the main final effectors of apoptosis, namely, Caspase-3. Following the Gadd45g and p53 levels, Caspase-3 activity was significantly reduced by ~26% during folate deficiency (Fig.5.4C). The folate deficient animal's display reduced apoptotic capacity despite the decrease in base excision repair efficiency. This phenomenon could be due to the reduced damage threshold perceived in the liver of the folate deficient animals observed as reduced abasic sites and single strand breaks. Therefore, the folate deficient animals display reduced repair and apoptotic efficiency, but at same time do not exhibit accumulation of detrimental DNA damages.

Analysis of the antioxidant response during folate deficiency in the liver of C57Bl/6 mice

Thioredoxin and glutathione are the two major cellular antioxidant systems. Thioredoxin is a 12 kda, oxidoreductase with a dithiol-disulfide active site. The reduced form of thioredoxin is regenerated by the enzyme thioredoxin reductase (TrxR) in a NADPH-dependent reaction. Thioredoxin reductase is the only identified enzyme that can regenerate reduced thioredoxins. There are three isoforms of thioredoxin reductase, TrxR1, TrxR2, TrxR3 and each isoform is found in the cytosol, mitochondria and testis respectively. The thioredoxin system is an important antioxidant in that loss of both copies of the thioredoxin gene is embryonically lethal in humans.

The other antioxidant Glutathione, is a tripeptide made of, L-cysteine,L-glutamate and glycine. This antioxidant is mainly synthesiszed through the transulfuration pathway of the folate cycle. Mice with deletions in the catalytic site of the enzyme, glutamate cysteine ligase which is involved in the synthesis of glutathione does not survive the first month of birth (236). The regeneration of the reduced form of glutathione is done by glutathione reductase which remains constitutively active in the cell. Glutathione peroxidase another enzyme part of the glutathione defense system helps in the conversion of lipid hydroperoxides to alcohols and also reduces hydrogen peroxide to water. Glutathione peroxidase uses reduced glutathione as the acceptor of electrons. Therefore, both the antioxidant system work efficiently to reduce the oxidative stress in normal cells.

Since folate deficiency has been implicated in creating oxidative stress and also has been demonstrated to generate hydrogen peroxide (237,238), we evaluated the thioredoxin system and glutathione peroxidase activity in our folate deficient animals. Thioredoxin-1 protein levels showed a moderate reduction by ~11% in the folate deficient group (Fig.5.5A). Thioredoxin reductase did not show any significant difference in its activity between the groups (Fig.5.5B). In similar terms, Glutathione peroxidase also did not show any significant difference in its activity during folate adequacy and deficiency (Fig.5.5C). Therefore, the folate deficient animals did not exhibit any robust upregulation in its antioxidants

compared to its folate adequate counterpart, suggesting that twelve weeks of folate deficiency did not sufficiently create any oxidative stress. Having evaluated the repair and apoptotic efficiency of the folate deficient animals, we further extended our study to determine if folate deficiency would make the animal more susceptible to an external DNA damaging agent such as a carcinogen.

Analysis of Aberrant crypt foci formation during folate deficiency and methionine restriction in response to DMH treatment in the colon of C57Bl/6 mice

Folate deficiency has been associated to many different kinds of cancer especially colon cancer which has high mortality. Preneoplastic lesions such as aberrant crypt foci induced by the administration of a carcinogen, is a well established early indicator of colon cancer in animal models (220-222). To determine if folate deficiency increased the predisposition to cancer in our animal model, we used 1,2-dimethylhydrazine (DMH), a potent colon carcinogen to induce formation of aberrant crypt foci. DMH is known to be a SN-1 alkylating agent known to generate methyl adducts such as O6Me-G and N7 MeA (239). The activation of DMH to its active metabolite, azoxymethane and methyldiazonium ion occurs in the liver and these metabolites are carried to the colon via bile and blood (240,241) . During its conversion to the active form, DMH also generates hydroxyl radicals and hydrogen peroxide in the presence of metal ions (241). Therefore, DMH is a potent carcinogen capable of generating both alkylation and oxidative stress.   At the outset of the present study, we randomly assigned c57BL/6 mice into four groups: the folate adequate/ methionine adequate (FA/MA), folate deficient (FD), methionine restricted (MR: 80% restriction) and combined folate deficient/methionine restricted (FD/MR) groups. One week into their respective diets the animals were injected with 30mg/Kg body weight of DMH, once a week for six weeks. Six weeks after the final injection, the mice were sacrificed and the colons were scored for aberrant crypt foci. As shown in Fig.5.6B &C., DMH treated folate deficient animals displayed significantly higher (~57% more) aberrant crypts as compared to its folate adequate counterparts (13 ± 1.8 for FA versus 30 ± 2.2 for FD respectively, p<0.01) in concurrence with other studies (30,31-Lisa,JBC). As observed in Fig.5.1B, folate deficiency by itself without any external factor

was not enough to induce aberrant crypts in the colon, but it definitely increases the susceptibility of the animals to DMH.

Methionine, the other essential component of the folate cycle ,has been shown to increase mean and maximum life span of laboratory animals (214-216). Further, methionine restriction in rat models has also been shown to reduce the occurrence of aberrant crypts when treated with azoxymethane (242). In order to dissect out the mechanism through which folate deficiency works and to test whether folate deficiency and methionine restriction show similar characteristics, we treated methionine restricted animals with DMH. To our surprise, methionine restricted animals showed increased predisposition to carcinogenesis compared to both folate adequate and folate deficient animals (Fig. 5.6B &C). Methionine restricted animals treated with DMH showed ~38% more aberrant crypts than folate deficient mice (46±2.9 for MR versus 28± 2.8 for FD, respectively, p<0.01). Intersetingly, methionine restricted animals displayed more advanced crypt multiplicity than folate deficient animals. The advanced aberrant crypts observed in methionine restricted animals presented a well defined elevation above the surrounding mucosa and appeared more like a microadenoma. This observation with methionine restriction is in contrast to a similar study conducted on rats (242). This observed difference could be due to the species difference and the difference in their metabolism and signaling.

Our fourth group, the combined folate deficient/methionine restricted animals potentially mimics, metabolically and physiologically, complete methyl donor deficient rodent models as two of the major methyl donors were restricted in this diet. These animals showed early signs of susceptibility to DMH with animals in the group dying by the fifth week of the last DMH injection. The animals that survived showed signs of Kyphosis, an indication for premature aging. Once the animals were sacrificed, the tissues such as the liver and brain appeared pale drained of blood. The colons appeared shrunk and presented difficulties under the microscope. Under the microscope, with methylene blue staining, the colons from the FD/MR animals showed overall abnormal morphology. Nevertheless, they displayed a dramatic increase in aberrant crypts compared to any other group studied (57±5.3 for FD/MR versus 46

±2.9 for MR versus 28±2.8 for FD, respectively, p<0.01). It would be interesting and also important to further study all the physiological changes in the FD/MR animals. Having observed greater predisposition to aberrant crypt foci and adenoma formation in the methionine restricted animals, we further analyzed the liver from all the groups studied.

Analysis of damages to DNA during folate deficiency and methionine restriction in response to DMH treatment in the liver of C57Bl/6 mice

Folate deficiency has always been implicated in the generation of DNA damages and has been shown to act synergistically with DNA damage inducing agents (226,243,244). DMH as mentioned previously becomes activated in the liver and in the process generates free radicals and methyl diazonium ions, which can cause damages to DNA (241). We analyzed our experimental groups sequentially for damages repaired via the base excision repair pathway to see if the dietary regimens predisposed the animals to greater DNA damage accumulation. The folate and methionine adequate animals treated with DMH did not show any significant difference in their uracil and abasic levels and showed significantly lower single strand breaks compared to its FA/MA counterpart without DMA treatment (Fig.5.7A, B&C). Interestingly, folate deficiency in concurrence with DMH showed a ~23% reduction in their uracil levels compared to their folate adequate counterparts (Fig .5.7A). On the other hand, the folate deficient animals showed significant increase in their abasic sites and single strand breaks in response to DMH (Fig.5.7B&C). Unlike the animals which were on just dietary folate manipulation, the folate deficient animals treated with DMH showed increased accumulation of highly mutagenic DNA damages.

Since the methionine restricted animals showed significant aberrant changes in their colon, we tested their liver for DNA damage accumulation. The methionine restricted animals, similar to the folate deficient animals, showed a decline in their uracil levels in response to DMH (Fig.5.7A). Correspondingly, the abasic sites in the MR DMH animals were significantly lower than the folate deficient DMH treated animals and remained at the basal level (Fig.5.7B). On the other hand, the single

strand breaks in the MR DMH although showed a lowering trend compared to the folate deficient animals remained significantly higher than the folate adequate/methionine adequate animals treated with DMH (Fig.5.7C). The combined folate deficient /methionine restricted animals as expected showed significantly higher uracil levels compared to folate deficient DMH and methionine restricted DMH groups individually (Fig.5.7A). Concurrently, they also showed significantly higher abasic sites similar to the folate deficient DMH group (Fig.5.7B). Interestingly, the FD/MR DMH group showed noticeably lower single strand breaks than the folate deficient DMH and methionine restricted DMH groups but the levels remained higher than the folate adequate DMH group. Herein, in contrast to what we observed in the colon, the folate deficient animals showed increased accumulation of damages in the liver compared to the methionine restricted group. Therefore to better understand the mechanism behind this accumulation, we next looked at the base excision repair pathway in these dietary regimes in response to DMH.

Analysis of the base excision repair pathway during folate deficiency and methionine restriction in response to DMH in the liver of C57Bl/6 mice

Base excision repair pathway, is a co-ordinated repair pathway with a series of enzymes functioning sequentially and are highly inducible to environmental stress (196,197,245,246). Imbalance in the base excision repair pathway leads to the accumulation of toxic repair intermediates. Misincorporated uracil, abasic sites and single strand breaks are examples of damages which would occur sequentially during impaired BER. Therefore, we looked at the overall efficiency of base excision repair in all our experimental groups by testing the invitro G:U mismatch BER activity initially. As expected, the BER activity was induced in all the DMH treated groups (Fig. 5.8D). As illustrated in Fig. 5.8D, FA/MA DMH animals showed about ~53% upregulation , FD DMH animals showed only ~40 % upregulation, MR DMH showed ~53% upregulation and the FD/MR DMH showed ~ 73% upregulation. Interestingly, the folate deficient DMH animals were the only group to show significantly lower induction in its BER activity.

In order to distinguish between the overall BER activity and the individual enzymes involved in this pathway, we looked at the expression and activity of the major BER enzymes involved in the removal of uracil from DNA. The monofunctional glycosylase involved in the removal of uracil from DNA, uracil DNA glycosylase (UDG) showed significant upregulation in the folate adequate group treated with DMH. The protein levels were upregulated by ~90% and the uracil excision activity was up by ~43% (Fig.5.8A,B), thereby reducing the uracil content to its basal level. Following UDG, the next enzyme in the pathway APE1/Ref-1, also showed an upward trend (~31%) in the FA/MA DMH group, providing an explanation for the reduced abasic sites in this condition (Fig.5.8B). The next enzyme in the pathway, β-pol also showed ~27% upregulation in its protein levels (Fig. 5.8D), thereby the reduction seen in the single strand breaks. On the other hand, the folate deficient animals treated with DMH did not show significant upregulation in its UDG protein (Fig. 5.8A) and uracil excision activity (Fig.5.8B). Based on the findings from our uracil measurement, we anticipated the UDG levels and activity to be upregulated. Interestingly, the UDG levels and activity were not sufficiently induced. Therefore it is inviting to suggest that, the decreased accumulation of uracils in DNA could be due to two reasons: (i) the increased activities of the backup glycosylase's such as MBD4 and TDG capable of removing uracil from DNA (247) and/or (ii) reduced misincorporation of uracil into DNA due to the increased hydrolysis of dUTP to dUMP by dUTPase (247,248). Direct testing of these notions is further warranted. Further, the folate deficient animals treated with DMH show markedly reduced APE1/Ref-1 by ~38% (Fig.5.8C) and reduced β-pol by ~33% (Fig.5.8D) showing loss of stress inducibility by these enzymes. This lack of induction displayed by APE1/Ref-1 and β-pol provide insights into the increased abasic sites and single strand breaks (substrates of the enzymes respectively) observed in the folate deficient DMH animals.

The next group of methionine restricted animals also did not show upregulation in its UDG protein (Fig.5.8A) and showed an increasing trend in its uracil excising activity compared to the folate deficient DMH animals, but remained lower than the FA/MA DMH group (Fig.5.8B). Here again, the lowered uracil levels could be due to the increased activities of the backup glycosylase's, but this part of

methionine restriction remains to be explored. The subsequent enzymes of the pathway, Ape1/Ref-1 and β-pol showed inductions by ~23% and 41% in the methionine restricted group treated with DMH compared to the folate deficient DMH animals. The moderate increase in APE1/Ref-1 might have been adequate enough to bring down the abasic sites to the levels observed in these animals, but interestingly, the single strand breaks remained high compared to FA/MA group despite the noticeable increase in its β-pol levels. Methionine restriction in synergism with DMH might be directly inducing the accumulation of single strand breaks in the genomic DNA, but again this phenomenon needs to be tested to be presented as a plausible mechanism. Furthermore, the combined folate deficient and methionine restricted animals treated with DMH showed very significant upregulation in its uracil excising activity, APE1/Ref-1 protein, and showed lowered β-pol levels (Fig. 5.8B, C, D). Despite the increase in BER enzymes and activity the FD/MR DMH group showed increased accumulation of DNA damages. Based on these findings, the folate deficient animals treated with DMH display significantly reduced BER efficiency compared to all other groups. Methionine restricted DMH animals although not optimal, showed better BER efficiency than the folate deficient animals. As the next series of experiment we looked at the apoptotic capacity of these dietary regimens in response to dimethyl hydrazine.

Analysis of apoptosis during folate deficiency and methionine restriction in response to DMH in the liver of C57Bl/6 mice

Having determined the reduced efficiency of base excision repair by the folate deficient animals in response to DMH, we ventured to evaluate their apoptotic response. As done previously, we analyzed the levels of three markers of apoptosis, Gadd45g, p53 and caspase-3. The folate adequate DMH treated animals show an up- regulating trend in their Gadd45g mRNA, p53 protein and caspase-3 activity (Fig.5.9A,B,C). As expected the folate adequate animals show ample apoptotic response when treated with DMH. Alternatively, the folate deficient DMH treated animals did not show upregulation in any of the factors tested (Fig.5.9A,B,C). Our lab had previously reported reduced apoptotic activity in the colon of folate deficient DMH treated animals, measured as TUNEL –positive staining cells (217).In line with

this data, the livers of folate deficient DMH treated animals, showed no significant induction in Gadd45g, p53 and caspase-3 activity, but rather showed a lowering trend in each of the factors (Fig.5.9A,B,C). To further determine whether methionine restricted animals would show robust apoptotic capacity in response to DMH, we repeated the same analysis in their liver samples. The MR DMH group, showed significant down-regulation in Gadd45g mRNA and p53 protein compared to the FD DMH mice (Fig.5.9 A, B) but their caspase-3 activity showed an increasing trend (Fing.5.9C). The final group, the folate deficient/methionine restricted animals treated with DMH, showed a very significant down-regulation in Gadd45g mRNA, p53 protein and caspase-3 activity (Fig.5.9 A,B,C). The reduction in apoptosis in the liver of FD/MR DMH animals may possibly be due to the robust DNA repair seen as increased BER activity. In conclusion, folate deficiency in conjunction with DMH seems to reduce the efficiency of base excision repair and apoptosis thereby increasing the accumulation of toxic repair intermediates, which could potentially result in the development of cancer. Conversely, the methionine restricted animals show a moderately better base excision repair and apoptotic capacity compared to the folate deficient counterparts, but remain below optimum compared to the folate adequate/methionine adequate mice.

Analysis of the antioxidant response during folate deficiency and methionine restriction in response to DMH in the liver of C57Bl/6 mice

To further determine the antioxidant response of the experimental groups to DMH treatment, we looked at three factors associated to the antioxidant system. As illustrated in Fig. 5.10 A,B,C, all the dietary groups showed significant induction in their antioxidants when treated with DMH. Folate adequate animals showed an increasing trend in their thioredoxin protein levels and significant upregulation in thioredoxin reductase and glutathione peroxidase activities (Fig. 5.10 A,B,C). The folate deficient DMH treated mice also show an increasing trend in their thioredoxin protein, but show significant upregulation in thioredoxin reductase and glutathione peroxidase activity when compared to their folate adequate counterparts (Fig. 5.10 A,B,C). Further, the methionine restricted animals show an increasing trend in response to DMH treatment in their thioredoxin protein levels and thioredoxin

reductase activity and significant upregulation in their glutathione peroxidase activity when compared to the folate deficient DMH mice (Fig. 5.10 A,B,C). On the other hand, the FD/MR DMH group show very high thioredoxin protein levels that are even higher than the methionine restricted animals, but their thioredoxin reductase activity showed a reducing trend compared to the MR DMH group and remained significantly higher or equivalent to other dietary groups (Fig. 5.10 A,B). Furthermore, FD/MR DMH group showed significantly lower glutathione peroxidase activity than the MR group treated with DMH (Fig.5.10C). Since the FD/MR animals potentially should have their folate cycle rate nearly shut down since they have both folate and methionine limiting in their diet, it would be interesting to evaluate the biosynthesis of glutathione through the trans-sulfuration pathway.

The antioxidant systems, both thioredoxin and glutathione have anti-apoptotic effects in normal conditions. Thioredoxin-1 is the physiological inhibitor of apoptosis signal-regulatory kinase 1 (Ask1) (249). Ask I via the JNK and p38 MAP kinase pathway act as inducers of apoptosis and increased expression of thioredoxin-1 inhibits Ask1 activity thereby inhibiting apoptosis (249). Moreover, inhibitors to thioredoxin have been shown to inhibit apoptosis and are effectively used in cancer treatment (250). Similarly glutathione peroxidase also plays role in inhibition of apoptosis and has been used in anti-cancer treatment for several years. Specifically , glutathione peroxidase 1 prevents apoptosis via two mechanisms, (i) scavenges hydroperoxides efficiently thereby inhibiting ROS mediated apoptosis and (ii) inhibits hydroperoxide mediated stabilization of p53 (251). Based on these studies, it is inviting to suggest that the reduced p53 levels and caspase-3 activity observed in the folate deficient and methionine restricted mice subjected to DMH is possibly due to the increase in their antioxidant activities.

Discussion

Nutritional intervention studies have gained importance in the field of research paving roads for newer design of therapy and prevention of disease. Dietary manipulations such as caloric restriction and methionine restriction are proven strategies for lifespan extension and decreased susceptibility to diseases

in rodents. In addition research on functional components of foods such as curcumin and garcinol have been providing insights into the different pathways that can be targeted for treatments such as anti-cancer treatments (252-254). Currently, nutritional studies are concentration on understanding the mechanism behind aging and age-related diseases which would help in the prevention and treatment of the same. Similarly, folic acid an essential component required for the normal functioning and maintenance of the cell has been targeted in many anti-cancer strategies. Anti-folate drugs such as methotrexate and pemetrexed are well known and commonly used anti-cancer agents (255,256). Folic acid chemically, is an essential water soluble vitamin which takes part in one carbon metabolism. Since folate acts as a carbon donor it plays a central role in almost all metabolic reactions. As can be deciphered from the folate cycle, folic acid plays an important role in DNA synthesis and its maintainence, DNA methylation and epigenetics and redox cycling. Impairment in any segment of the folate cycle could lead to accumulation of damages in the DNA, increased mutation frequency, genomic instability and eventually cancer.

Folate deficiency has always been associated to the development of many types of cancer especially colorectal cancer. Individuals with single nucleotide polymorphism in the methylene tetyrahydrofolate reducatse gene and low plasma folates are epidemiologically shown to be more at risk for the development of colorectal cancer (257,258). However, studies conducted on folate deficiency and supplementations are inconsistent and suggest that the effect of folate on cancer depends on the time period of the dietary regimen and the exposure to external agents such as carcinogens (259-263). Our data shows that folate deficiency by itself without any external agent does not induce the development of preneoplastic lesions, i.e, aberrant crypt foci, in the colon of mice. This distinctly shows that at least 12 weeks of folate deficiency is a low penetrance event and does not induce preneoplastic lesions in the colon and emphasizes the requirement of a carcinogen.

Apart from cancer risk, folate deficiency has also been reported to incapacitate DNA repair pathways and result in accumulation of DNA damages (211-213,264). Folate deficiency induces accumulation of damages such as uracil misincorporation, which are primarily repaired via the BER

pathway. Our lab has previously demonstrated and published that eight weeks of folate deficiency imbalances the base excision repair pathway and leads to accumulation of damages such as aldehydic lesions and single strand breaks (211). In line with our earlier findings, we here report the loss of co-ordination in the critical BER enzymes with twelve weeks of folate deficiency. We observed an upregulation in the expression of the initial glycosylase UDG, but this increase in the protein level did not correlate with an increased activity. As a consequence of this attenuated activity ,we observed an increase in uracil levels in the folate deficient animals. Subsequently, the next enzyme in the pathway, Ape1/ref-1 failed to show upregulation, but was in actual fact significantly lower in the folate deficient animals. Despite this reduction in APE1/Ref-1 protein, its substrate, abasic site did not show any appreciable increase. Our lab has previously reported that abasic sites do not accumulate even when one allele of APE1/Ref-1 is knocked out (265). Therefore, the reduction in abasic sites could be due to adequate APE1/Ref-1 endonuclease activity i.e. adequate processing of abasic sites or be a consequence of reduced glycosylase activity in this case the UDG activity.

The next enzyme in the pathway, β-pol, the rate determining enzyme for the removal of uracil, also was observed to be significantly lowered at its protein level during folate deficiency. Inadequate β-pol response has been shown to increase the level of its substrate, single strand breaks (198,211). On the contrary, in this study we did not observe any substantial increase in single strand breaks during folate deficiency. This lack of accumulation of single strand break emphasizes the reduced processing of the abasic sites or increased β-pol activity. Alternatively, unrepaired single strand break during replication can become double strand breaks which subsequently would induce homologous recombination (HR) via parp-1 which would eventually repair the double strand break (266,267). In other words, an increase in single strand breaks increases parp-1 activity and parp-1 in turn helps in completing BER but in the absence of adequate BER response initiates cross-talk with homologous recombination (266,267). Therefore, it is inviting to suggest that this cross-talk with homologous recombination could have removed any accumulating single strand breaks, if any, during folate deficiency. All the more, direct

testing of this cross-talk during folate deficiency is necessary to suggest this as a plausible mechanism. Further, the overall invitro G:U mismatch BER activity was also attenuated during folate deficiency. Our data clearly demonstrates that the base excision repair enzymes were down-regulated during folate deficiency and the removal of uracil was absolutely not initiated. This is interesting as folate deficient animals did not show any adverse signs except for the increased uracil levels when compared to its folate adequate counterparts.

After establishing the DNA repair capacity i.e., BER capacity of the folate deficient, it was important to look at the other tip of the balance, apoptosis. Microarray analysis performed on colon cancer cells show that folate deficiency alters expression of genes involved in apoptosis along with DNA repair genes (268). Previous data from our lab show that folate deficiency induces apoptosis in the colon of mice treated with carcinogen when base excision repair is compromised genetically (217). Our current data from the wildtype animals showed that the apoptotic system was not adequately induced during folate deficiency despite the lowered BER enzymes, in other words p53, Gadd45g and caspase3 did not show any significant upregulation. This lack of stimulation in apoptosis could be due to the lack of accumulation of toxic intermediates such as abasic sites and single strand breaks. Uracil was the only measured damage which showed accumulation but uracil is considered less cytotoxic than the other two damages measured. Therefore, our data states that folate deficiency independently reduces the DNA repair and the apoptotic capacity but does not lead to significant accumulation of cytotoxic DNA damages.

Folate deficiency has been reported to act synergistically with DNA-damaging agents to increase damages such as DNA strand breaks, mutation frequency and chromosomal aberrations (226,243,244). These damage accumulations have been suggested to be the consequence of impaired DNA repair. Therefore, in this study we determined the effects of folate deficiency on the repair and apoptotic capacity of the liver and ACF development in the colon of mice when exposed to a potent carcinogen such as 1,2-dimethylhydrazine. In addition, we also studied the effects of methionine

restriction on the colon and liver of mice when treated with dimethylhydrazine since many studies have shown the beneficial effects of methionine restriction and also because methionine is an integral part of the folate cycle. After restricting the folate pathway either via folate deficient diet or methionine restricted diet, we further analyzed the consequence of a combined deficiency in folate and methionine restriction on these pathways.

Folate deficiency in conjunction with β-pol haploinsufficiency showed reduced occurrence of aberrant crypt foci, a preneoplastic lesion when exposed to dimethylhydrazine, but folate deficiency in wild type animals increased the potency of the carcinogen and showed significantly larger number of aberrant crypts in the colon (217). In our current study we show markedly increased aberrant crypts in our DMH treated folate deficient wildtype animals, confirming the earlier data obtained by Lucente et al. This exacerbation of the system could be due to the underlying functional BER deficiency created by low folate levels. In line with this notion, folate deficiency has been shown to increase the mutagenicity of the alkylating agent N-ethyl-N-nitrosurea (269). Human colon epithelial cells inefficiently repaired the damages created by methyl methanesulfonate and hydrogen peroxide when folate was limiting in its medium (226). Further, colonocytes grown in low folate conditions exhibited poor excision repair capability (264). In order to confirm this phenomenon, we examined the BER capacity of these animals in the liver. Similar to what we saw earlier, dimethylhydrazine failed to mount adequate BER response during folate deficiency. The UDG protein levels and activity were attenuated in the folate deficient animals and the subsequent enzymes in the pathway, APE1/Ref-1 and β-pol also showed lack of induction. The G:U mismatch BER was also not adequately induced during folate deficiency compared to its folate deficient counterparts. This is interesting as the BER pathway is a stress inducible pathway. This lack of induction observed in the base excision repair enzymes could be due to the direct regulation of expression of these genes at the transcriptional level by folate deficiency. We have previously provided evidence for this, wherein the upregulation of β-pol expression in response to 2-nitropropane induced oxidative stress was inhibited during folate deficiency (270). We further showed increased binding of

negative regulatory factor to the folic acid response region of β-pol encompassed in its CREB binding site, during oxidative stress (270).

Folate deficiency, as was demonstrated previously, markedly impaired the base excision repair pathway during carcinogen exposure. As a direct consequence of this lack of BER response, toxic repair intermediates such as abasic sites and single strand breaks, which formerly did not show any increase with folate deficiency alone, were significantly augmented. Here again, it is inviting to suggest that, the cross talk between BER and HR could be impaired during the synergistic actions of folate deficiency and DMH, leading to the accumulation of single strand breaks. In support of this, parp-1 mRNA levels did not show significant upregulation during folate deficiency in response to DMH treatment suggestive of the loss of the cross talk (data not shown). Abasic sites are highly mutagenic whereby an adenine would be added against it during replication leading to substitution or frameshift mutations (271). These accumulating abasic sites and single strand breaks could potentially lead to increased mutation frequency and chromosomal instability, which are the common characteristics of folate deficiency. These findings are in line with many other studies conducted on folate efficiency. Observing the lack of base excision repair response and increased accumulation of toxic DNA damages during folate deficiency, we studied the expression and activity of factors involved in apoptosis. Lucente et al had previously demonstrated the increase in apoptosis in folate deficient, β-pol haploinsufficient animals when treated with dimethylhydrazine, explaining the reduction in aberrant crypts in the colon of animals studied (217). Lucente et al, also reported significantly reduced apoptotic activity in their colon, measured as TUNEL-positive staining cells in the wildtype animals exposed to folate deficiency and carcinogen (217). In concurrence with this information, we saw reduced apoptotic response in the liver of our folate deficient animals in response to dimethylhydrazine. The mRNA expression of Gadd45g, a cell cycle arrest gene was significantly reduced in the folate deficient animals. Gadd45g has been shown to promote apoptosis via the p38K-JunNH$_2$-terminal kinase pathway when stimulated by stress (272,273). Therefore, its reduction signifies reduced promotion of apoptosis. In addition, the induction of p53 tumor suppressor

protein and marker of apoptosis was prevented during folate deficiency and dimethylhydrazine treatment. Finally, the activity of Caspase-3 the effector, molecule of the apoptotic pathway was also not adequately induced. In normal conditions, lack of DNA repair response and increased accumulation of DNA damages triggers the apoptotic machinery to eliminate the damaged cells, but folate deficiency not only reduces the DNA repair capacity but also brings down the apoptotic ability of these animals predisposing them to the development of cancer.

The restriction of the other segment of the folate cycle, i.e., methionine restriction, has been reported to increase mean and maximum life-span in laboratory animals when restricted by about 80 % from the controls (214-216). Methionine restriction has also been demonstrated to reduce free radical leak and oxidative DNA damage and provide resistance to oxidative stress in laboratory rodents which has been suggested as a potential mechanism behind the life-span extension (214,274). Furthermore, methionine restriction has been shown to reduce the incidence of aberrant crypt foci in rats exposed to azoxymethane (242). Depletion of methionine has been shown to induce apoptosis in cancer cells (275,276). Methionine restriction has also been shown to reduce the susceptibility of mice to oxidative stress created by acetaminophen (216). Based on these studies, we anticipated seeing significantly lower aberrant crypts in our DMH treated methionine restricted animals. To our surprise, the methionine restricted animals showed significantly more aberrant crypts and crypt multiplicity. With exactly the same strategy of experiment used for folate deficiency, methionine restriction showed the development of microadenomas. In addition, although our data from liver showed better repair activity and apoptotic efficiency than the folate deficient animals, the repair and apoptotic response was not relatively very different from the folate adequate/methionine adequate DMH treated animals. Given the fact that methionine restriction reduces ROS generations, increases stress resistance and apoptosis, the repair and apoptotic activities in our methionine restricted DMH treated animals should have been far greater than the FA/MA animals. All the more, methionine restricted animals showed more accumulation of single strand breaks in DNA than the folate adequate/methionine adequate group.

This marked difference that we see in our methionine restricted animals compared to other studies which portray its beneficial effects might be due to the difference in the time period of the dietary and carcinogen exposure. In this study, we exposed the animals to the experimental diets and dimethylhydrazine treatment simultaneously without giving the animals sufficient time for adjustment in the specific diets. Maybe with sufficient time for adjustment in the respective diets, the animals might exhibit different characteristics similar to the lifespan extending interventions. The study conducted to demonstrate increased stress resistance to acetaminophen by methionine restricted animals, exposed the animals to ~9 months of methionine restriction before treating them with acetaminophen (216). The notion that longer dietary period for adjustment might be beneficial is further supported by the study conducted by Leu et al, wherein they expose the animals to 4 weeks of (277,278). They observed a significant reduction in the number of aberrant crypt foci in the colon of their folate deficient group compared to the folate adequate ones (277). Leu et al further demonstrated that these animals, given time for adjustment in the diet also displayed reduced incidence and number of colonic tumors in folate deficient animals exposed to AOM (278). In conclusion, the only experimental group in our current study which actually depicted true failure of the folate cycle is the combined folate deficient and methionine restricted group. In the other two groups, folate deficient DMH and methionine restricted DMH , although these animals were exposed to the respective diets for a longer term, the carcinogen treatment was conducted without giving sufficeint time for adaptation. Therefore in order to dissect out the exact mechanism behind folate deficiency and methionine restriction, additional studies allowing an ample period of time for adaptation in the respective dietary condition prior to carcinogen exposure is critical.

In conclusion dietary interventions such as folate deficiency alter stress response genes altering the balance of DNA repair such as base excision repair. This imbalance in DNA repair causes inefficient repair of damages leading to its persistence through replication and transcription, becoming permanent mutations and genomic instability. And this instability drives the enhancement of aging phenotypes and age related diseases such as cancer.
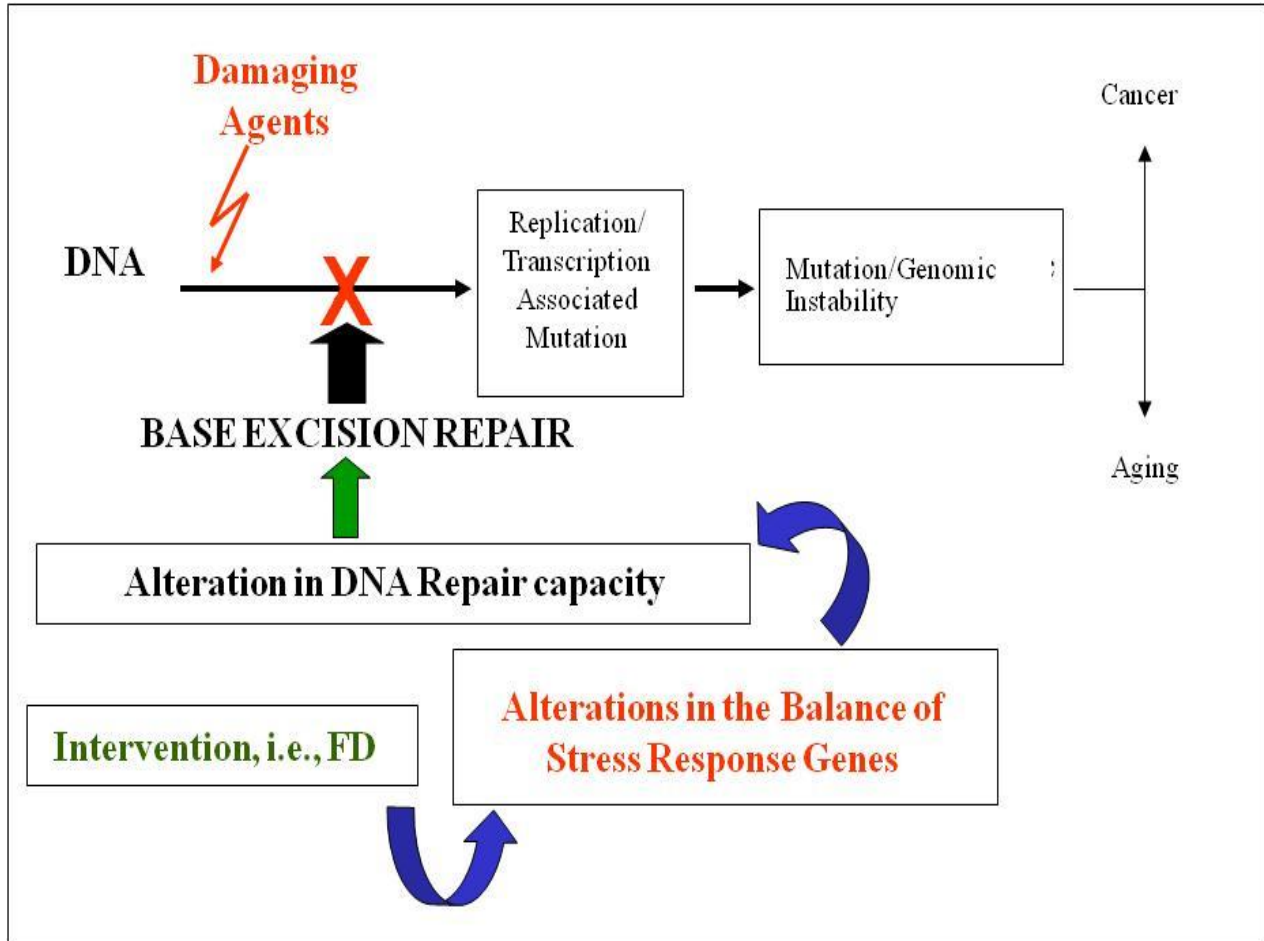
Figure Legends

Figure5.1. Effect of the folate deficient diet on ACF formation in the colon of C57Bl/6 mice. A, experimental design: c57Bl/6 mice were fed folate adequate (2mg/kg, FA) or a folate deficient (0mg/kg, FD) diet for 12 weeks. After 12 weeks of ingestion of the respective diets, mice were sacrificed by CO_2 asphyxiation. B, exemplary methylene blue stained colons, showing the normal crypts from both FA and FD mice.
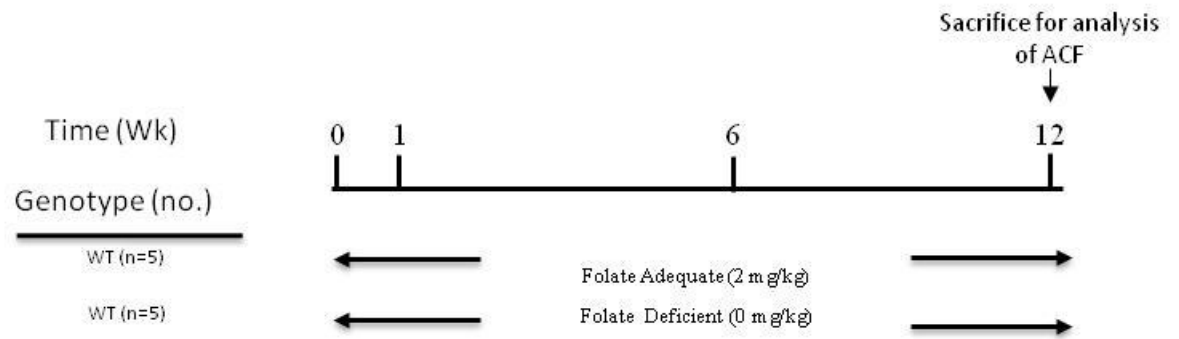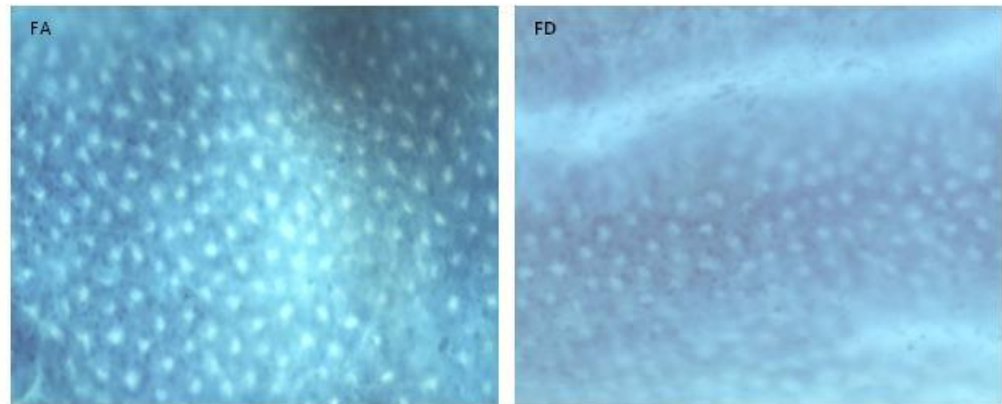
A

B

Figure5.2.Effect of folate deficiency on the formation of DNA damages such as uracil misincorporation, abasic site and single strand break in the liver of C57Bl/6 mice. A, DNA was isolated from the liver of mice fed FA and FD diets using DNeasy kit from Qiagen and the levels of uracil were measured using UDG coupled- ASB assay as described under experimental procedures. The data are expressed as the I.D.V. of the band/ug of DNA loaded. B, DNA was isolated from the liver of mice fed FA and FD diets using DNeasy kit from Qiagen and the levels of uracil were measured using ASB assay as described under experimental procedures. The data are expressed as the I.D.V. of the band/ug of DNA loaded. C, Levels of single strand break was measured using fast micromethod fluorescence assay as described under experimental procedures. The data are expressed as fluorescence units at 538 nm. Values represent an average ± S.E. for data obtained five mice in each group. Values with * indicate significant differences at $P<0.05$. FA, folate adequate: FD, folate deficient.

A
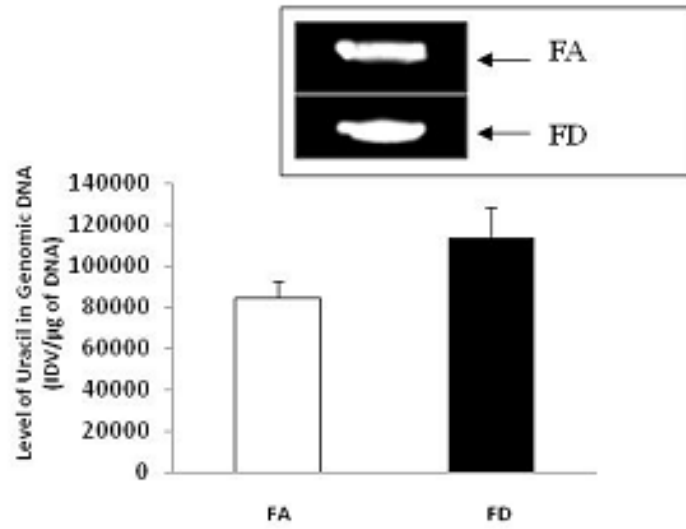
B
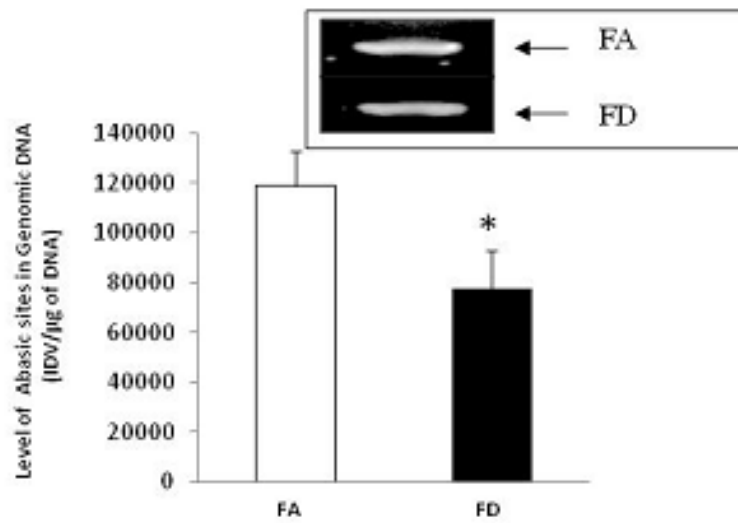
C
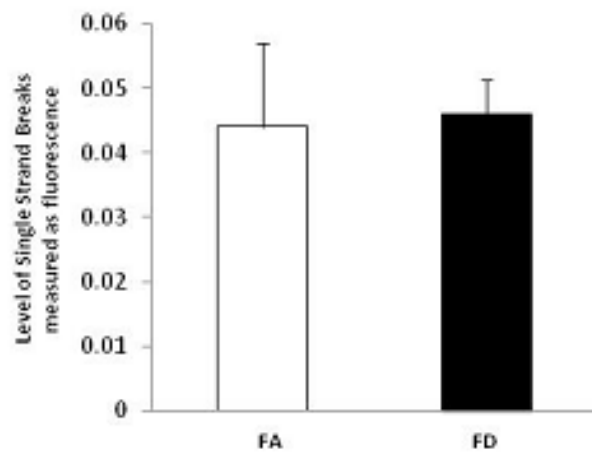
Figure5.3. Effects of folate deficiency on the expression of the enzymes in the BER pathway and the G:U mismatch repair activity in the liver of C57Bl/6 mice. A, C, D, The levels of UDG, APE1/Ref-1 and β-pol protein respectively, in 100 μg of liver nuclear extract obtained from mice fed FA and FD diet were determined by western blot analysis. The levels of each protein were normalized with the levels of β-actin. The data is expressed as the integrated density value corresponding to the level of each protein as quantified by a Bio-Rad chemiImager system and normalized to β-actin. B, The Uracil excision activity was conducted using whole cell extracts obtained from livers of mice fed FA and FD diet as described in the experimental procedures. The reaction products were resolved on a sequencing gel. Uracil excision activity was visualized by the appearance of a 11-base fragment. The relative level of this activity was quantified using a Bio-Rad Molecular Imager system. The data were normalized based on the amount of protein used in each reaction and expressed as integrated density. Values represent an average ± S.E. for data obtained five mice in each group. E, The invitro G:U mismatch BER activity was conducted using nuclear extracts obtained from livers of mice fed FA and FD diet as described in the experimental procedures. The reaction products were resolved on a sequencing gel. Repair activity was visualized by the appearance of a 16-base fragment. The relative level of BER was quantified using a Bio-Rad Molecular Imager system. The data were normalized based on the amount of protein used in each reaction and expressed as integrated density value. Values represent an average ± S.E. for data obtained five mice in each group. Values with * indicate significant differences at P<0.05. FA, folate adequate: FD, folate deficient. PC, Positive control: NC, Negative control.
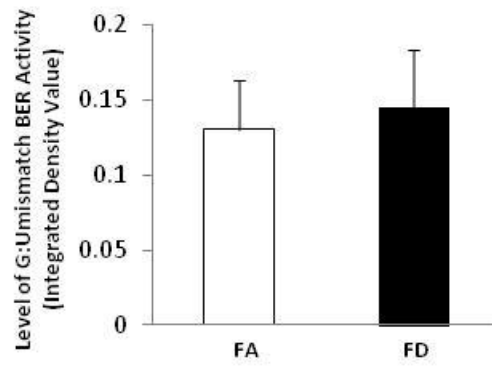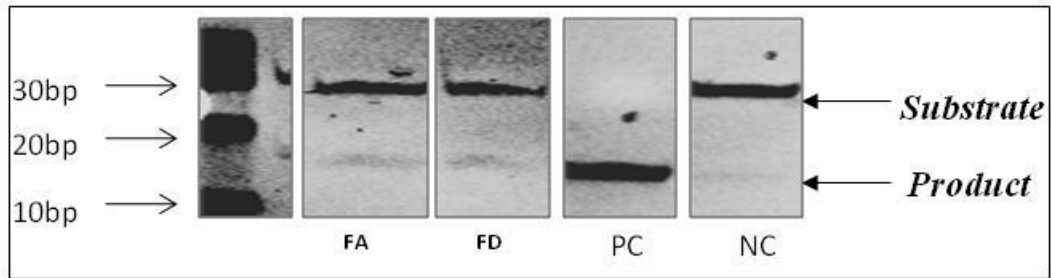
A
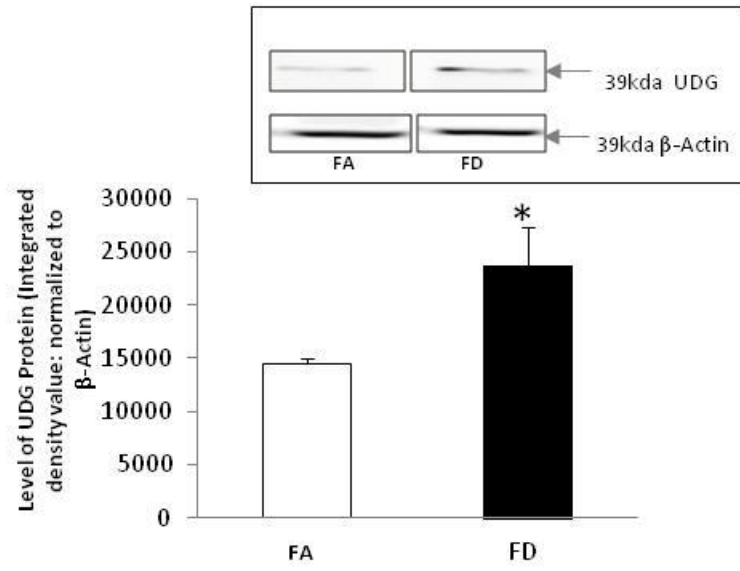
B
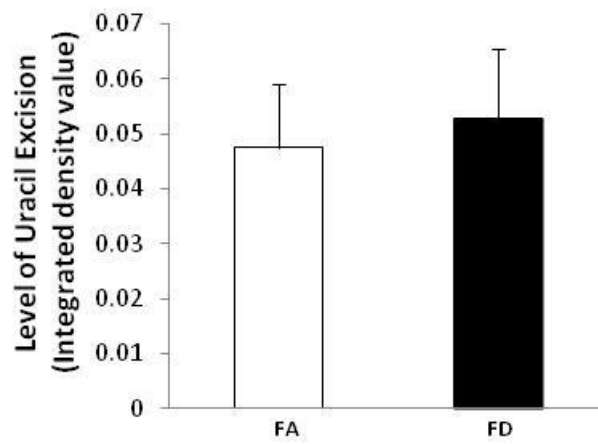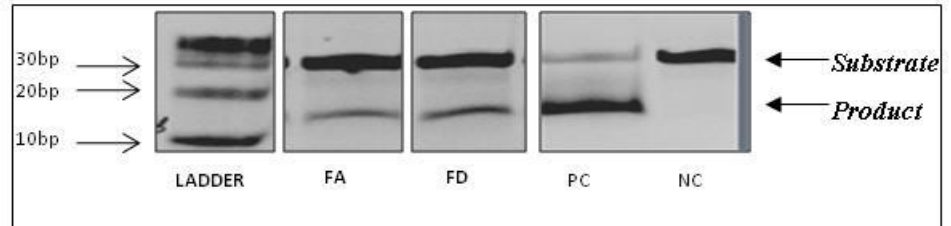
C
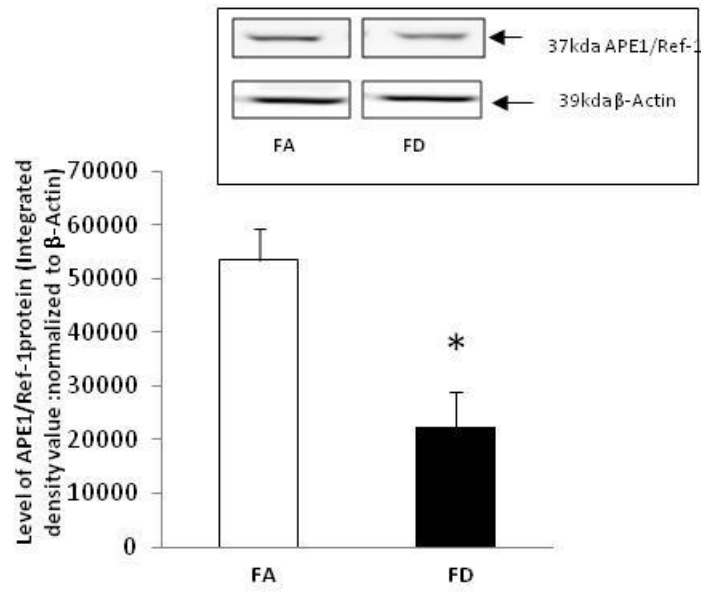
D
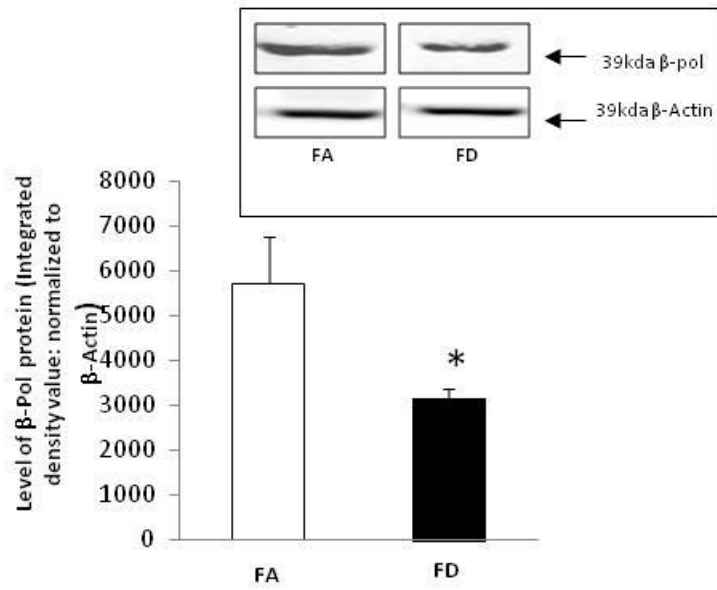
E

Figure5.4. Impact of folate deficiency on apoptosis in the liver of C57Bl/6 mice. A, Gadd45g mRNA expression level was quantified using real-time PCR and normalized with RPLO. B, The level of p53 protein, in 100 µg of liver nuclear extract obtained from mice fed FA and FD diet were determined by western blot analysis. The levels of p53 protein were normalized with the levels of β-actin. The data is expressed as the integrated density value corresponding to the level of each protein as quantified by a Bio-Rad chemiImager system and normalized to β-actin. C, The level of caspase-3 activity in liver cytosolic extract was determined using Enzchek Caspase-3 assay from molecular probes. Values represent an average ± S.E. for data obtained five mice in each group. Values with * indicate significant differences at P<0.05. FA, folate adequate: FD, folate deficient.
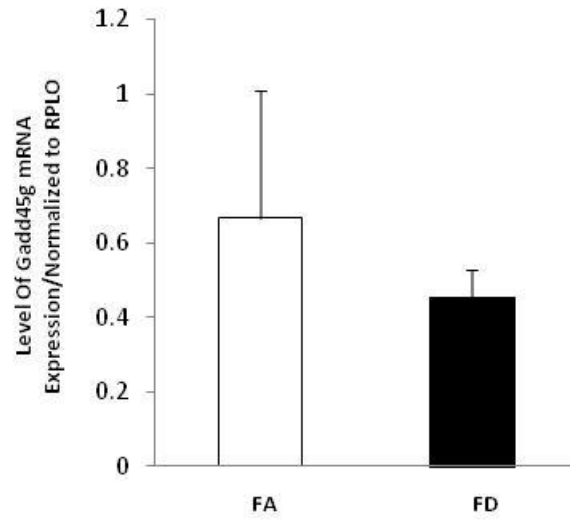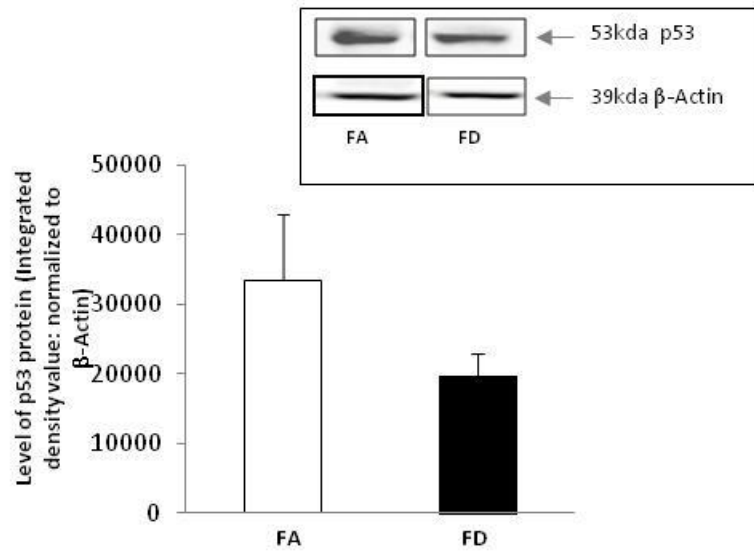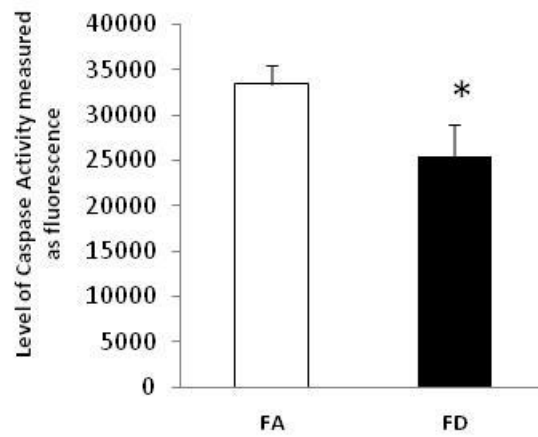
A

B

C

Figure5.5. The effect of folate deficiency on the antioxidant status of the liver of C57Bl/6 mice. A, The level of Thioredoxin-1 (Trx-1) protein, in 100 µg of liver cytosolic extract obtained from mice fed FA and FD diet were determined by western blot analysis. The levels of p53 protein were normalized with the levels of β-actin. The data is expressed as the integrated density value corresponding to the level of each protein as quantified by a Bio-Rad chemiImager system and normalized to β-actin. B, The level of thioredoxin reductase activity in liver whole cell extract was determined using the assay kit from Cayman chemicals. The data is expressed as absorbance measured at 405-414nm. C, The level of glutathione peroxidase activity in liver whole cell extract was determined using the assay kit from Cayman chemicals. The data is expressed as absorbance measured at 340nm. Values represent an average ± S.E. for data obtained five mice in each group. Values with * indicate significant differences at $P<0.05$. FA, folate adequate: FD, folate deficient.
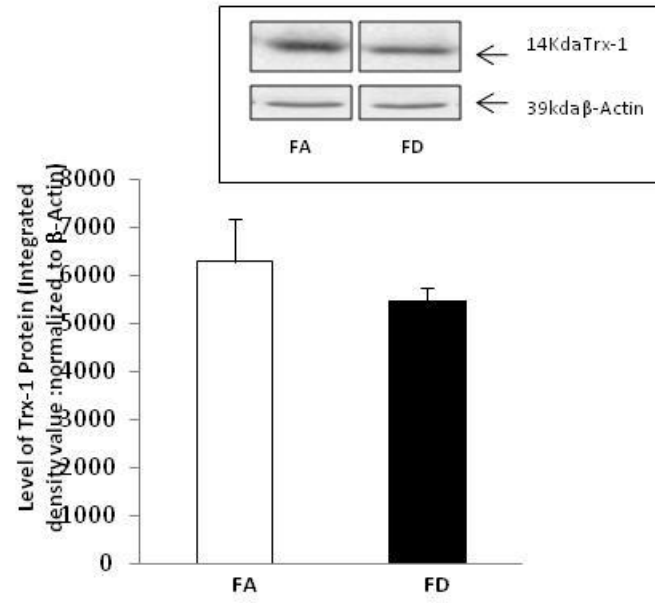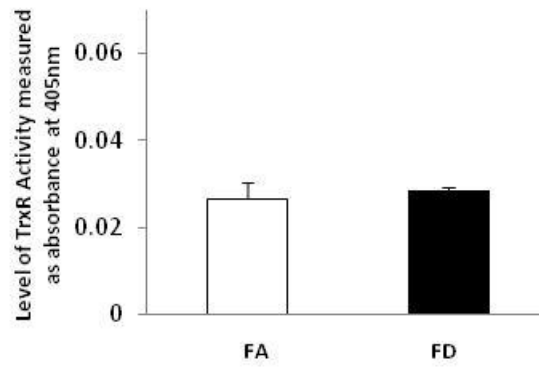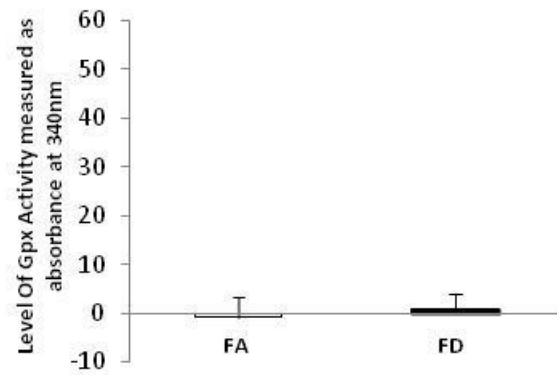
A

B

C

Figure5.6. Effect of the folate deficiency and methionine restriction on ACF formation in response to Dimethylhydrazine (DMH). A, experimental design: c57Bl/6 mice were fed different experimental diets: folate adequate/methionine adequate (2mg/kg, foltae/8.2mg/kg of methionine, FA/MA), folate deficient (0mg/kg, FD), methionine restricted (1.64mg/kg, MR) and Folate deficient/Methionine restricted (0mg/kg folate and 1.64 mg/kg methionine, FD/MR) diet for 12 weeks. After 1 week of ingestion of the respective diets, mice were injected with 30mg/kg body weight of DMH for 6 weeks. Six weeks after the final injection, animals were sacrificed by CO_2 asphyxiation. B,and C, ACF formation in the colon of mice from the different dietary FA/MA, FA/MA DMH, FD DMH, MR DMH and FD/MR DMH groups. The colons from the mice on sacrifice were processed as described in the experimental procedures. The methylene blue stained colons were analyzed under light microscopy to visualize the number of Aberrant crypts expressed as aberrant crypt foci/mouse. Values represent an average $\pm$ S.E. for data obtained five mice in each group. Data expressed as relative fold difference compared to FD DMH. Values with different superscripts indicate significant differences at $P<0.05$. FA, folate adequate: FD, folate deficient: MR, methionine restriction: FA/MA, folate adequate/methionine adequate: FD/MR, folate deficient/ methionine restricted: DMH, dimethylhydrazine.

A

DMH Treatment
(30 mg/kg)

Sacrifice for analysis
of ACF

Sacrifice for analysis of
cancer

Time (Wk)   0   1   6   12   46

Genotype (no.)

WT (n=5)   Folate (2 mg/kg) & Methionine(8.2 mg/kg)

WT (n=5)   Folate (0 mg/kg)

WT (n=5)   Methionine (1.64mg/kg)

WT (n=5)   Folate (0mg/kg) & Methionine (1.64mg/kg)
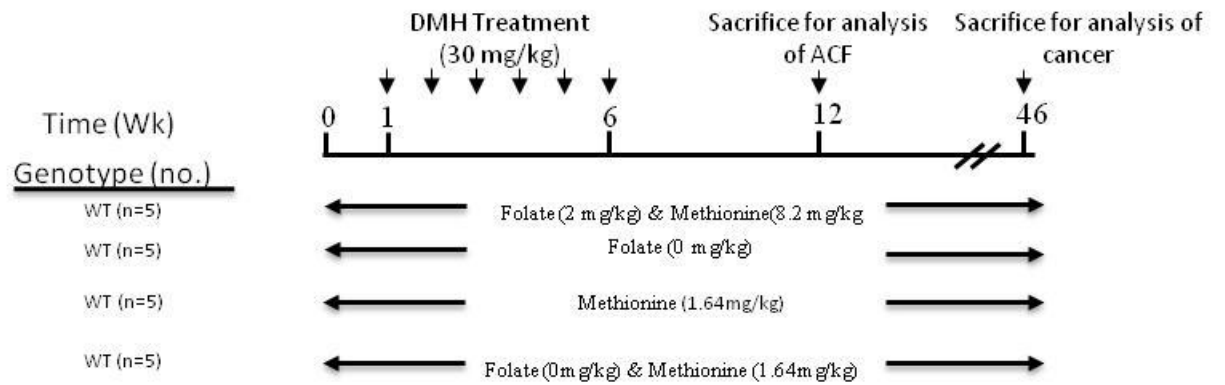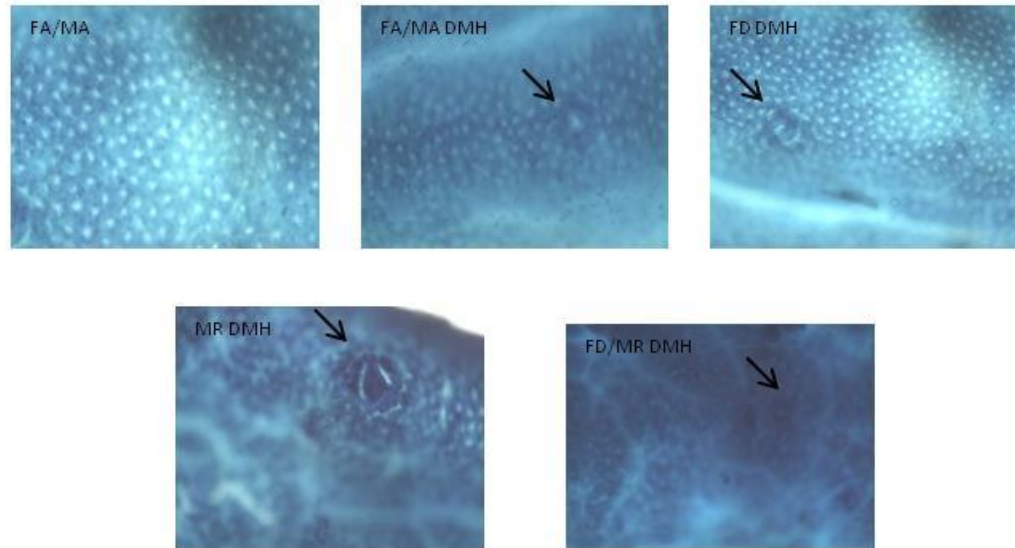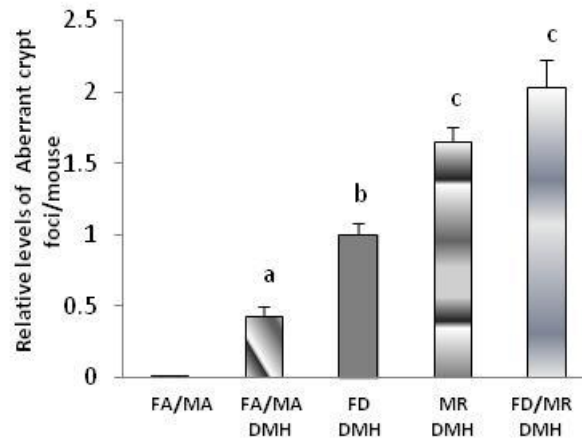
B

C

Figure5.7. Effect of folate deficiency and methionine restriction on the formation of DNA damages such as uracil misincorporation, abasic site and single strand break in response to DMH. A, DNA from the liver of mice from each group was isolated using DNeasy kit from Qiagen and the levels of uracil were measured using UDG coupled- ASB assay as described under experimental procedures. The data are expressed as the I.D.V. of the band/ug of DNA loaded. B, DNA from the liver of mice from each group was isolated using DNeasy kit from Qiagen and the levels of uracil were measured using ASB assay as described under experimental procedures. The data are expressed as the I.D.V. of the band/ug of DNA loaded. C, Levels of single strand break was measured using fast micromethod fluorescence assay as described under experimental procedures. The data are expressed as fluorescence units at 538 nm. Values represent an average ± S.E. for data obtained five mice in each group. Data expressed as relative fold difference compared to FD DMH. Values with different superscripts indicate significant differences at P<0.05. FA, folate adequate: FD, folate deficient: MR, methionine restriction: FA/MA, folate adequate/methionine adequate: FD/MR, folate deficient/ methionine restricted: DMH, dimethylhydrazine
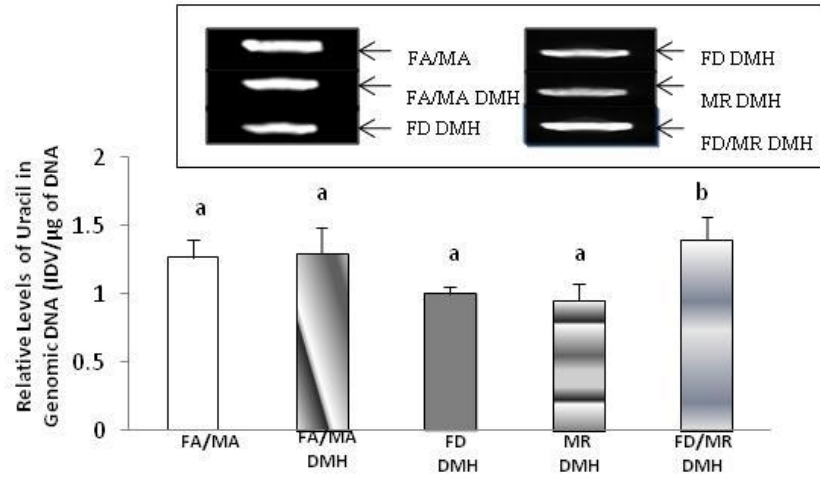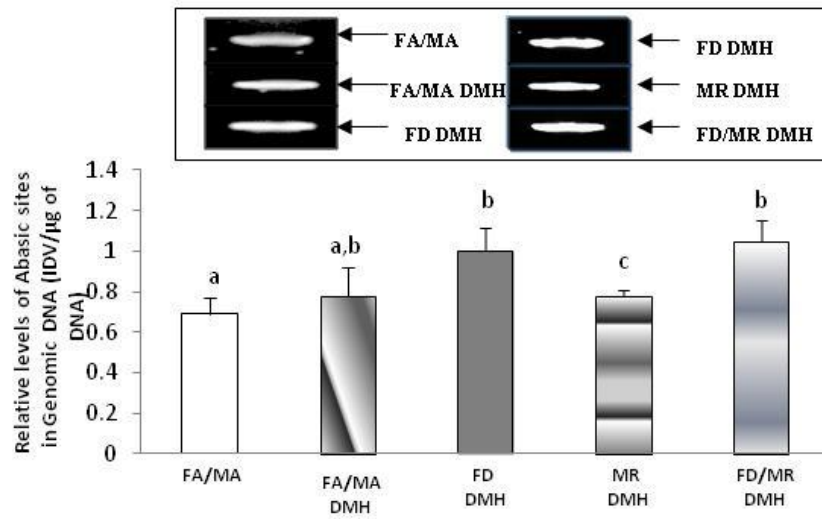
Figure5.8. . Effect of folate deficiency and methionine restriction on the expression of the enzymes in the BER pathway and the G:U mismatch repair activity in response to DMH. A, C, D, The levels of UDG, APE1/Ref-1 and β-pol protein respectively, in 100 μg of nuclear extract obtained from the liver of mice from all the dietary groups were determined by western blot analysis. The levels of each protein were normalized with the levels of β-actin. The data is expressed as the integrated density value corresponding to the level of each protein as quantified by a Bio-Rad chemiImager system and normalized to β-actin. B, The Uracil excision activity was conducted using whole cell extracts obtained from livers of mice from all the dietary groups as described in the experimental procedures. The reaction products were resolved on a sequencing gel. Uracil excision activity was visualized by the appearance of a 11-base fragment. The relative level of this activity was quantified using a Bio-Rad Molecular Imager system. The data were normalized based on the amount of protein used in each reaction and expressed as integrated density. Values represent an average ± S.E. for data obtained five mice in each group. E, The invitro G:U mismatch BER activity was conducted using nuclear extracts obtained from livers of mice from all the dietary groups as described in the experimental procedures. The reaction products were resolved on a sequencing gel. Repair activity was visualized by the appearance of a 16-base fragment. The relative level of BER was quantified using a Bio-Rad Molecular Imager system. The data were normalized based on the amount of protein used in each reaction and expressed as integrated density value. Values represent an average ± S.E. for data obtained five mice in each group. Data expressed as relative fold difference compared to FD DMH. Values with different superscripts indicate significant differences at P<0.05. FA, folate adequate: FD, folate deficient: MR, methionine restriction: FA/MA, folate adequate/methionine adequate: FD/MR, folate deficient/ methionine restricted: DMH, dimethylhydrazine. PC, Positive control: NC, Negative control.
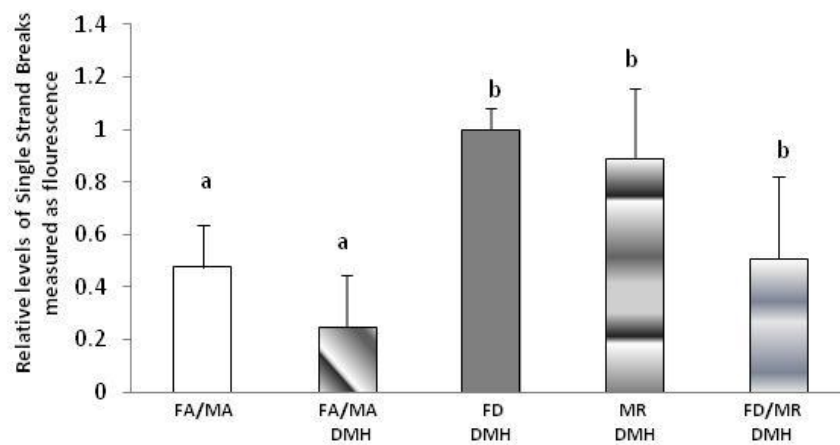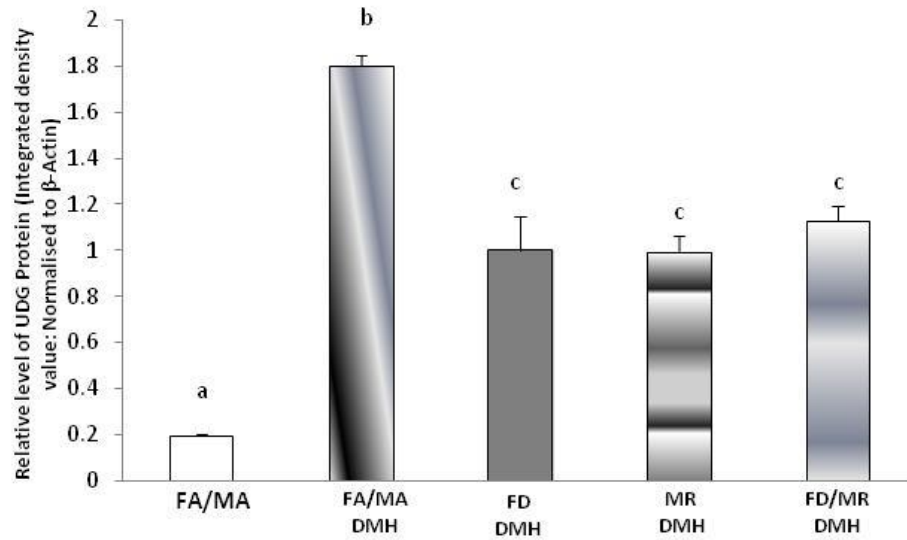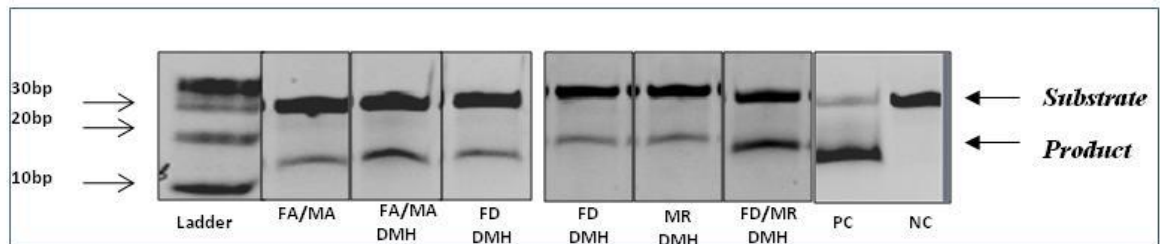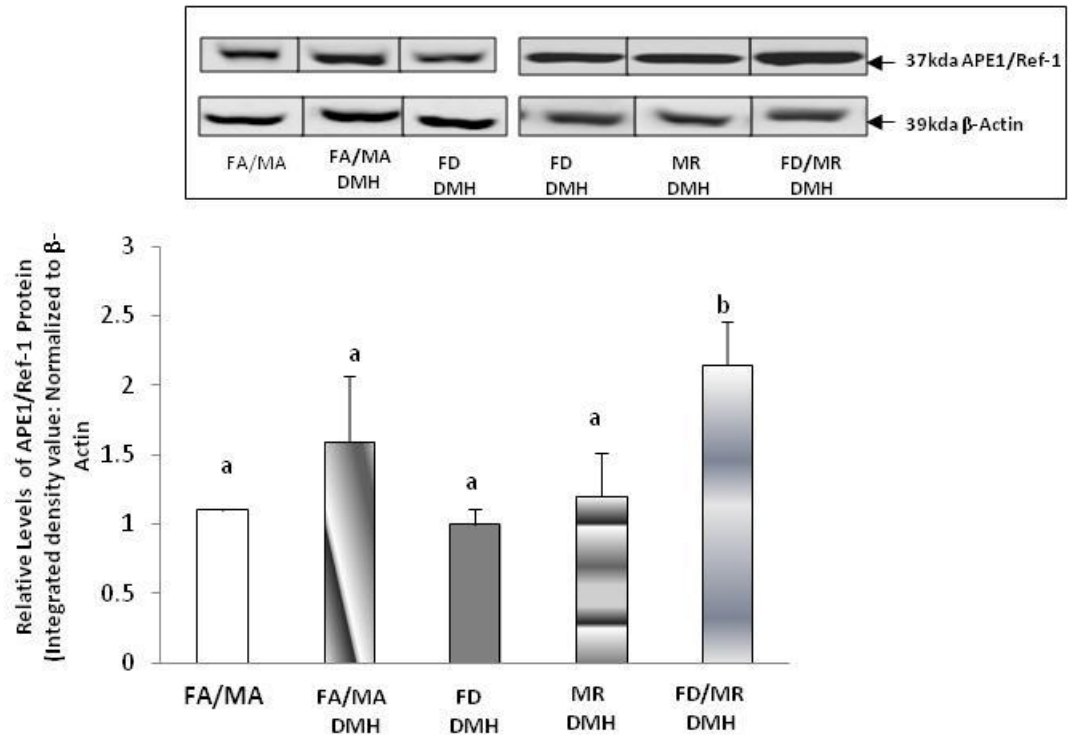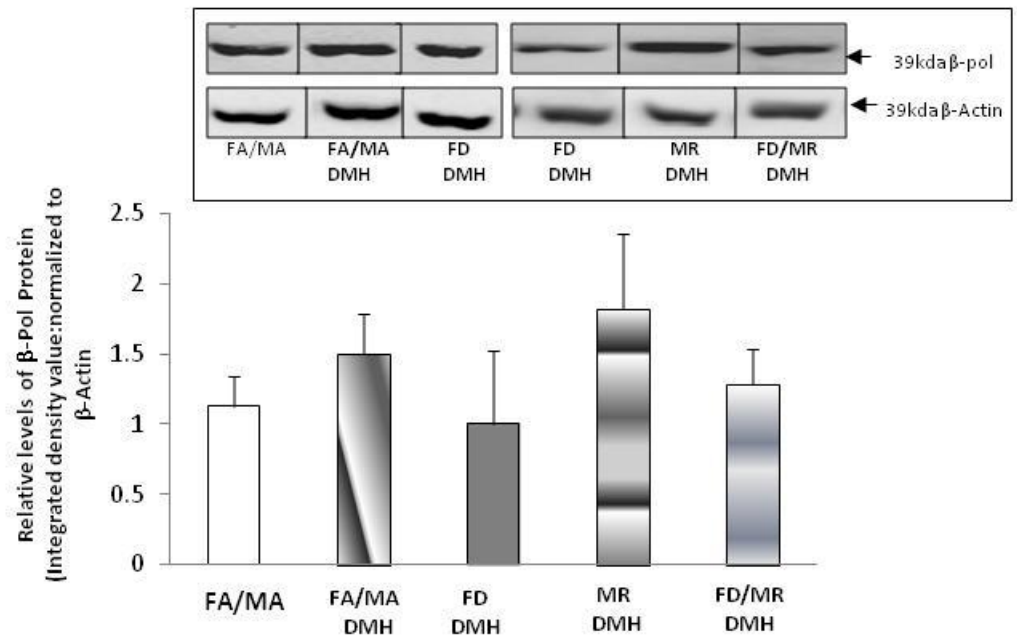
A
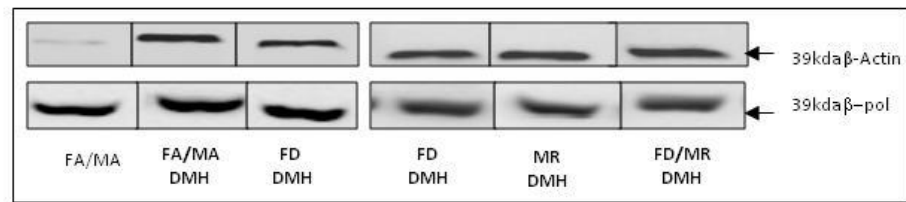
B
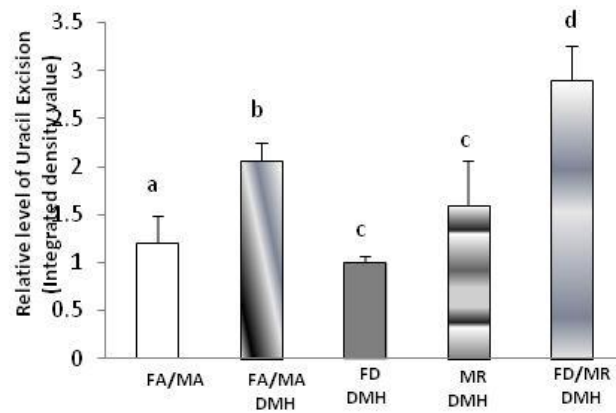
C

d

E
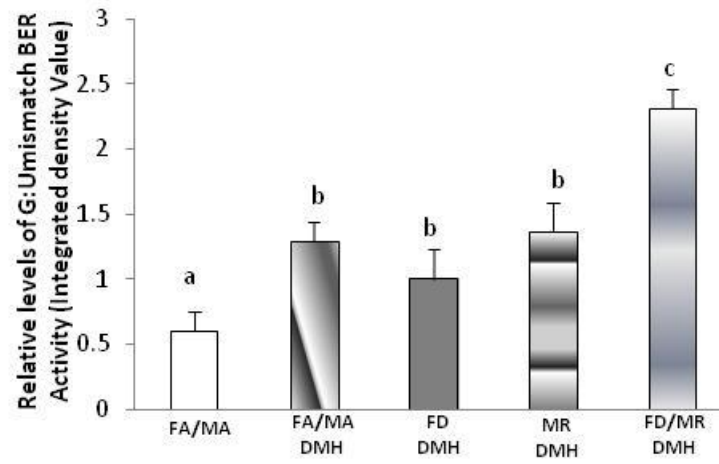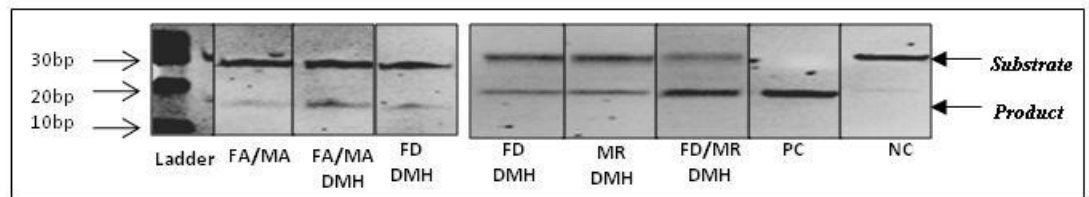
Figure5.9. Impact of folate deficiency and methionine restriction on apoptosis in response to DMH. A, Gadd45g mRNA expression level was quantified using real-time PCR and normalized with RPLO. B, The level of p53 protein, in 100 µg of nuclear extract obtained from livers of mice from all the dietary groups were determined by western blot analysis. The levels of p53 protein were normalized with the levels of β-actin. The data is expressed as the integrated density value corresponding to the level of each protein as quantified by a Bio-Rad chemiImager system and normalized to β-actin. C, The level of caspase-3 activity in liver cytosolic extract was determined using Enzchek Caspase-3 assay from molecular probes. Values represent an average ± S.E. for data obtained five mice in each group. Data expressed as relative fold difference compared to FD DMH. Values with different superscripts indicate significant differences at P<0.05. FA, folate adequate: FD, folate deficient: MR, methionine restriction: FA/MA, folate adequate/methionine adequate: FD/MR, folate deficient/ methionine restricted: DMH, dimethylhydrazine.

A

B

C

Figure5.10. The effect of folate deficiency and methionine restriction on the antioxidant status in response to DMH. A, The level of Thioredoxin-1 (Trx-1) protein, in 100 µg of cytosolic extract obtained from livers of mice from all the dietary groups were determined by western blot analysis. The levels of p53 protein were normalized with the levels of β-actin. The data is expressed as the integrated density value corresponding to the level of each protein as quantified by a Bio-Rad chemiImager system and normalized to β-actin. B, The level of thioredoxin reductase activity in liver whole cell extract was determined using the assay kit from Cayman chemicals. The data is expressed as absorbance measured at 405-414nm. C, The level of glutathione peroxidase activity in liver whole cell extract was determined using the assay kit from Cayman chemicals. The data is expressed as absorbance measured at 340nm. Values represent an average ± S.E. for data obtained five mice in each group. Data expressed as relative fold difference compared to FD DMH. Values with different superscripts indicate significant differences at P<0.05. FA, folate adequate: FD, folate deficient: MR, methionine restriction: FA/MA, folate adequate/methionine adequate: FD/MR, folate deficient/ methionine restricted: DMH, dimethylhydrazine.
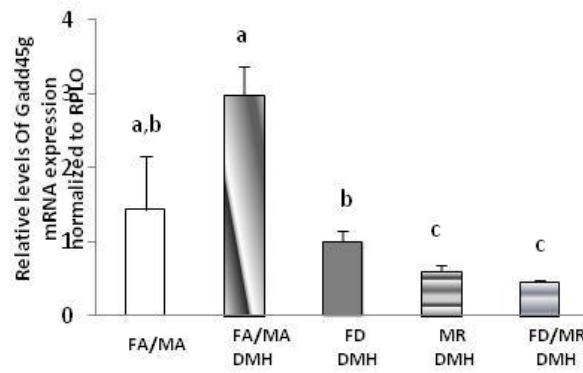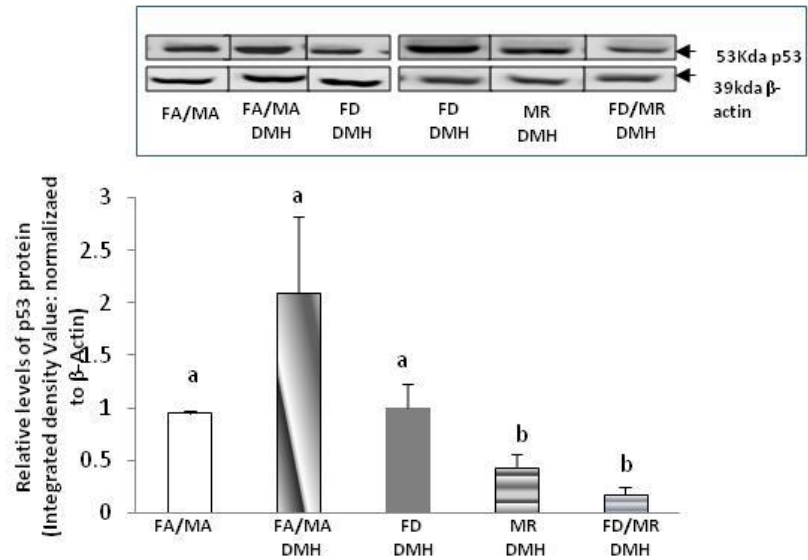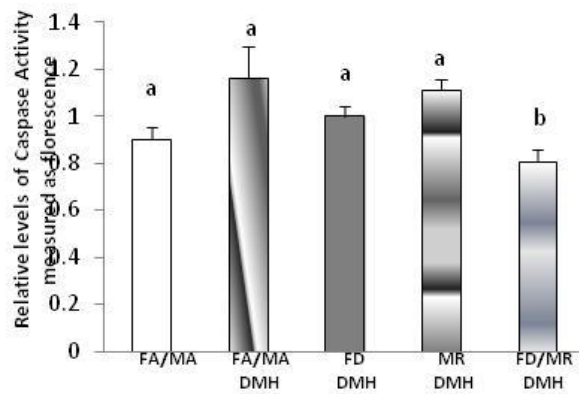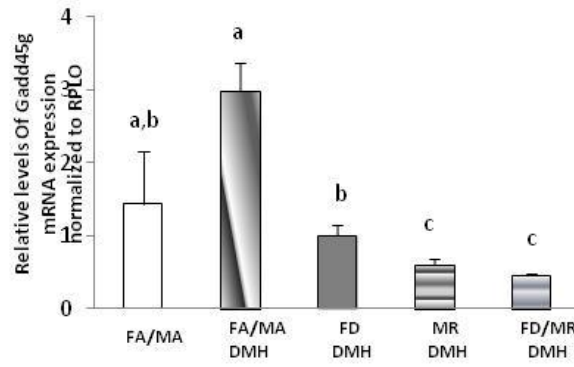
A

B

C

Chapter 6

Summary and Future Directions

Study 1: Base excision repair is integral to the maintenance of genomic stability. Imbalance in this repair process results in accumulation of toxic repair intermediates which are mutagenic and would lead to the development of cancer. Base excision repair pathway is central in removing oxidative and alkylation damages. And our study on APE1/Ref-1 haploinsufficient animals has further provided support for the critical role played by APE1/Ref-1 during oxidative stress. We show that heterozygosity in APE1/Ref-1 attenuates the optimal balance between stress response factors such as NF-kB and DNA repair when exposed to oxidative stress. Reduction in the redox activity of APE1/Ref-1 is responsible for the reduced DNA binding activity of NF-kB. This loss in survival signaling leads to cell cycle arrest and apoptosis. This notion is supported by our data which shows increased expression of Gadd45g, a cell cycle arrest gene, p53 tumor suppressor protein and Caspase-3 activity, the final effecter of apoptosis. This study demonstrates that haploinsufficiency in APE1/Ref-1 and thereby base excision repair pathway will make the animal model more susceptible to oxidative stress. Furthermore, our data distinctly shows that APE/Ref-1 is the rate determining enzyme during bifunctional glycosylase mediated base excision repair and β-pol is the rate determining factor during monofunctional glycosylase initiated base excision repair. This has important translational significance as polymorphisms in the BER genes have been observed within the human population. Further these findings have important implications in cancer therapy. Many types of tumor cells have been shown to have increased levels of APE1/Ref-1, therefore, knocking down APE1/Ref-1 in these cancer cells would potentially increase their apoptotic response which might bring about a positive outcome in cancer therapy.

Future Directions: Having characterized the effect of folate deficiency on β-pol haploinsufficient animals (Cabelof, et JBC: 2004 and Lisa et al, JBC:2010) it would be interesting to study the impact of folate deficiency on APE1/Ref-1 haploinsufficiency. Future studies would evaluate the development of

preneoplastic lesions in the colon of the haploinsufficient mice in response to a carcinogen treatment. We expect to see dramatic results in the APE1/Ref-1 haploinsufficient mice similar to the β-pol haploinsufficient ones in response to 1,2-dimethylhydrazine treatment. It would be intriguing to see if APE1/Ref-1 haploinsufficiency also would reduce the incidence of aberrant crypt foci during folate deficiency and carcinogen exposure. And this study will also focus on evaluating the combined effect of folate deficiency and APE1/Ref-1 haploinsufficiency on the expression of genes involved in other DNA repair pathways and the apoptotic capacity. These studies as mentioned above will have important implications in the development of new strategies for cancer treatment.

Study 2: Our subsequent studies on folate deficiency demonstrated the impact of this dietary intervention on the base excision repair pathway. Our study demonstrates that folate deficiency has differential effect on the expression of the genes involved in base excision repair pathway. We show that folate deficiency regulates the expression of β-pol, the key enzyme involved in the removal of uracil from DNA, at the level of transcription. We identified specific hot spot regions in the promoter of β-pol using foot printing analysis which are specifically affected during folate deficiency (FARR). Further the negative regulation on of β-pol was associated to this hot spot and through the interplay of cis-and trans-acting regulatory factors. Our data provide evidence for the involvement of negative- regulatory factors which keeps the expression of □-pol at its basal level and inhibits its DNA damage inducibility during oxidative stress.

Future Directions: The future studies will include experimental designs to determine the negative regulatory factor involved in the inhibition of of β-pol. We propose to isolate the negative regulatory complex that binds to the folate responsive region (FARR) of the of β-pol promoter and further analyze it using the proteomics approach. And also we would perform in vitro transcription assays to establish the vital role played by the FARR element in β-pol expression. And our future studies will also include experiments to determine the methylation status of the promoter of other genes involved in the base

excision repair pathway. These studies will provide more insights into mechanism by which folate deficiency incapacitates the DNA repair pathways.

Study 3: Our study on folate deficiency and methionine restriction shows that these dietary restrictions increase the incidence of preneoplastic lesions in the colon of mice treated with dimethylhydrazine. Further, our study shows that folate deficiency and methionine restriction impairs the efficiency of base excision repair pathway on exposure to the carcinogen. We also show that the apoptotic efficiency of the mouse models used is affected during these dietary restrictions and carcinogen exposure. The intriguing fact about these findings are that methionine restriction, an intervention established to extend life-span and decrease oxidative stress also showed increase in cancer incidence. Further, methionine restricted animals showed reduced DNA repair and apoptotic efficiency. This differential effect of methionine restriction could be due to the difference in dietary exposure time used by us and other labs which show the beneficial effects of methionine restriction. If this is true for methionine restriction, folate deficiency also might show differential responses when the experimental strategy is modified.

Future Directions:: The future studies, will design an experimental strategy to provide long term exposure to the folate deficient diet before exposing the animals to the carcinogen. We will evaluate whether the long term exposure to the diet provides the animals enough time to get adjusted to the stress created by the dietary intervention. Further, we will determine, if this long term dietary exposure reduces the incidence of cancer when exposed to the carcinogen. We will also evaluate the DNA repair and apoptotic efficiency of this long term dietary exposure. This study will have very important implications as folate deficiency has been considered to be a global health concern and folate fortifications would be viewed with a different perspective.

REFERENCES

1. Friedberg, E.C.; Walker, G.C.; Siede, W.; Wood, R. D.; Schultz, R. A.; Ellenberger, T. DNA repair and Mutagenesis. pp.169-226, Washington D.C: ASM Press; 2006.

2. Heydari, A.R., Unnikrishnan, A., Ventrella-Lucente, L., and Richardson, A. Caloric restriction and genomic stability. Nucleic Acids Res. 35, 7485-7496; 2007.

3. Duthie SJ, Naryanan S, Sharp L, Little J, Basten G, Powers H. Folate DNA stability and colo-rectal neoplasia. Proc Nutr Soc. 2004 Nov;63(4):571-8. Review.

4. Yi P, Melnyk S, Pogribna M, Pogribny IP, Hine RJ, James SJ. Increase in plasma homocysteine associated with parallel increases in plasma S-adenosylhomocysteine and lymphocyte DNA hypomethylation. J Biol Chem. 2000 Sep 22;275(38):29318-23.

5. Branda RF, Blickensderfer DB. Folate deficiency increases genetic damage caused by alkylating agents and gamma-irradiation in Chinese hamster ovary cells. Cancer Res. 1993 Nov 15;53(22):5401-8.

6. Finkelstein JD. Methionine metabolism in mammals. J Nutr Biochem. 1990 May;1(5):228-37.

7. Kim YI. Nutritional epigenetics: impact of folate deficiency on DNA methylation and colon cancer susceptibility. J Nutr. 2005 Nov;135(11):2703-9.

8. Shen, J.C., Rideout, W.M., 3d and Jones, P.A. High frequency mutagenesis by a DNA methyltransferase. Cell *71:*1073-1080, 1992.

9. Duthie SJ, Narayanan S, Brand GM, Pirie L, Grant G. Impact of folate deficiency on DNA stability. J Nutr. 2002 Aug;132(8 Suppl):2444S-2449S.

10. Fowler B. The folate cycle and disease in humans. Kidney Int Suppl. 2001 Feb;78:S221-9. Review

11. Jennings, E. Folic acid as a cancer-preventing agent. Med. Hypotheses, 45: 297-303, 1995.

12. Friedberg,E.C. Out of the shadows and into the light: the emergence of DNA repair. Trends Biochem. Sci.. 1995; 20:381.

13. Yebra MJ, Bhagwat AS. A cytosine methyltransferase converts 5-methylcytosine in DNA to thymine. Biochemistry. 1995 Nov 14;34(45):14752-7.

14. Duthie, S.J. and Hawdon, A. DNA instability (strand breakage, uracil misincorporation, and defective repair) is increased by folic acid depletion in human lymphocytes in vitro. FASEB J. *12:*1491-1497, 1998.

15. MacGregor, J.T., Wehr, C.M., Hiatt, R.A., Peters, B., Tucker, J.D., Langlois, R.G., Jacob, R.A., Jensen, R.H., Yager, J.W., Shigenaga, M.K., Frei, B., Eynon, B.P. and Ames, B.N. 'Spontaneous' genetic damage in man: evaluation of interindividual variability, relationship among markers of damage, and influence of nutritional status. Mutation Res. *377:*125-135, 1997.

16. Everson, R.B., Wehr, C.M., Erexson, G.L. and MacGregor, J.T. Association of marginal folate depletion with increased human chromosomal damage in vivo: demonstration by analysis of micronucleated erythrocytes. J.Natl.Cancer Inst. *80:*525-529, 1988

17. Reidy, J.   A. role of deoxyuridine incorporation and DNA repair in the expression of human chromosomal fragile sites. Mutat. Res. 1988k 211: 215-220.

18. Blount BC, Mack MM, Wehr CM, MacGregor JT, Hiatt RA, Wang G, Wickramasinghe SN, Everson RB, Ames BN. Folate deficiency causes uracil misincorporation into human DNA and chromosome breakage: implications for cancer and neuronal damage. Proc Natl Acad Sci U S A. 1997 Apr 1;94(7):3290-5.

19. Mason JB, Choi SW. Folate and carcinogenesis: developing a unifying hypothesis. Adv Enzyme Regul. 2000;40:127-41. Review.

20. Ames BN, Wakimoto P. Are vitamin and mineral deficiencies a major cancer risk? Nat Rev Cancer. 2002 Sep;2(9):694-704. Review.

21. Rader, J.I. Folic acid fortification, folate status and plasma homocysteine. J Nutr. *132(8 Suppl)*:2466S-2470S, 2002

22. Choi, S.W. and Mason, J.B. Folate and carcinogenesis: an integrated scheme. J.Nutr. 130:129-132 2000.

23. Lucock, M. Folic acid: nutritional biochemistry, molecular biology, and role in disease processes. Mol.Genet.Metab. 71:121-138, 2000.

24. Glynn, S.A. and Albanes, D. Folate and cancer: a review of the literature. Nutrition and Cancer *22:*101-119, 1994.

25. Butterworth, C.E., Jr. Folate status, women's health, pregnancy outcome, and cancer. J.Am.Coll.Nutr. *12:*438-441, 1993

26. Zhang, S., Hunter, D.J., Hankinson, S.E., Giovannucci, E.L., Rosner, B.A., Colditz, G.A., Speizer, F.E. and Willett, W.C. A prospective study of folate intake and the risk of breast cancer. JAMA. *281:*1632-1637, 1999.

27. Kamei, T., Kohno, T., Ohwada, H., Takeuchi, Y., Hayashi, Y. and Fukuma, S. Experimental study of the therapeutic effects of folate, vitamin A, and vitamin B12 on squamous metaplasia of the bronchial epithelium. Cancer *71:*2477-2483, 1993.

28. Janerich, D.T., Mayne, S.T., Thompson, W.D., Stark, A.D., Fitzgerald, E.F. and Jacobson, H.I. Familial clustering of neural tube defects and gastric cancer. Int.J.Epidemiol. *19:*516-521, 1990.

29. Cravo, M.L., Mason, J.B., Dayal, Y., Hutchinson, M., Smith, D., Selhub, J. and Rosenberg, I.H. Folate deficiency enhances the development of colonic neoplasia in dimethylhydrazine-treated rats. Cancer Res. *52:*5002-5006, 1992.

30. Kim YI, Salomon RN, Graeme-Cook F, Choi SW, Smith DE, Dallal GE, Mason JB. Dietary folate protects against the development of macroscopic colonic neoplasia in a dose responsive manner in rats. Gut. 1996 Nov;39(5):732-40.

31. Song, J., Medline, A., Mason, J.B., Gallinger, S. and Kim, Y.I. Effects of dietary folate on intestinal tumorigenesis in the apcMin mouse. Cancer Res. *60:*5434-5440, 2000.

32. Khosraviani K, Weir HP, Hamilton P, Moorehead J, Williamson K. Effect of folate supplementation on mucosal cell proliferation in high risk patients for colon cancer. Gut. 2002 Aug;51(2):195-9.

33. Le Leu, R.K., Young, G.P. and McIntosh, G.H. Folate deficiency reduces the development of colorectal cancer in rats. Carcinogenesis *21:*2261-2265, 2000.

34. Kim, YI, Folate, Colorectal Carcinogenesis and DNA Methylation: Lessons From Animal Studies, Environmental and Molecular Mutagenesis. 2004;44:10-25.

35. Bird RP. Role of aberrant crypt foci in understanding the pathogenesis of colon cancer. Cancer Lett. 1995 Jun 29;93(1):55-71. Review

36. M.Valko, C.J. Rhodes, J. Moncol, M. Izakovic, M. Mazur. Free radicals, metals and antioxidants in oxidative stress-induced cancer. Chemico-Biological Interactions 160 (2000) 1-40.

37. Hankey, G. J. & Eikelboom, J. W. (1999) Homocysteine and vascular disease. Lancet 354: 407–413.

38. Pietrzik, K. & Bronstrup, A. (1997) Folate in preventive medicine: A new role in cardiovascular disease, neural tube defects and cancer. Ann. Nutr. Metab. 41: 331-343.

39. Bora Akoglu, Vladan Milovic, Wolfgang F. Caspary and Dominik Faust. European journal of Nutrition 43:93-99: 2004.

40. Stephanie J. W, Regina G. Z, Jacob S, Thomas R.F, Howard D.S, Louise A.B, Richard F. H, Robert S. L, Katherine M and Paul D. S. Cancer causes and control 12:317-324:2001.

41. Starkebaum, G. & Harlan, J. M. (1986) Endothelial cell injury due to copper-catalyzed hydrogen peroxide generation from homocysteine. J. Clin. Invest.77: 1370-1376.

42. Chern CL, Huang RFS, Chen YH, Cheng JT, Liu TZ. Folate deficiency-induced oxidative stress and apoptosis are mediated via Homocysteine dependant overproduction of hydrogen peroxide and enhanced activation of NF-κB in human Hep G2 cells. Biomedicine and Pharmacotherapy, 2001 Oct, 55(8); 432-442.

43. Rwei-Fen S. Huange, Yu-Chin Hsu, Hsiu-Ling Lin and Feili L. Yang. Folate depletion and elevated plasma Homocysteine promote oxidative stress in rat livers. J. Nutr. 131:33-38,2001.

44. Moat, S. J., Doshi, S. N., Lang, D., McDowell, I. F. W., Lewis, M.J., and Goodfellow, J. Treatment of coronary heart disesase with folic acid: is there a future? Am J Physiol Heart Circ Physiol, 287, H1-H7; 2004.

45. Robertson, K.D. and Jones, P.A. DNA methylation: past, present and future directions. Carcinogenesis *21:*461-467, 2000.

46. Wickramasinghe, S.N. and Fida, S. Bone marrow cells from vitamin B12- and folate-deficient patients misincorporate uracil into DNA. Blood *83:*1656-1661, 1994.

47. Duthie, S.J., Grant, G. and Narayanan, S. Increased uracil misincorporation in lymphocytes from folate- deficient rats. Br.J.Cancer *83:*1532-1537, 2000.

48. Frederico, L.A., Kunkel, T.A., and Shaw, B.R. A sensitive genetic assay for the detection of cytosine deamination: determination of rate constants and the activation energy. Biochemistry *29:*2532-7, 1990.

49. Zingg, J.M., Shen, J.C., Yang, A.S., Rapoport, H. and Jones, P.A. Methylation inhibitors can increase the rate of cytosine deamination by (cytosine-5)-DNA methyltransferase. Nucleic Acids.Res. *24:*3267-3275, 1996.

50. Holmquist, F.P. Mutat. Res. Endogenous lesions, S-phase-independent spontaneous mutations, and evolutionary strategies for base excision repair. *400*: 59-68, 1998.

51. Lindahl, T. Suppression of spontaneous mutagenesis in human cells by DNA Base Excision-Repair. Mutation Research *462:*129-135, 2000.

52. Cabelof, DC., Raffoul, JJ., Nakamura, J., Kapoor, D., Abdalla, H., and Heydari, AR. Imbalanced base excision repair in response to folate deficiency is accelerated by polymerase beta haploinsufficiency. J Biol Chem. 2004 Aug 27;279(35):36504-13.

53. Alberto Sanz, Pilar Caro, Victoria Ayala, Manuel Portero-otin, Reinald Pamplona and Gustavo Barja. The Faseb Journal. 20: 1064-13: 2006.

54. Reinald Pamplona and Gustavo Barja. Biochemica et Biophysica Acta. 1757: 496-508: 2006.

55. Despina Komninou, Yvonne Leutzinger, Bandaru S. Reddy, and John P. Richie Jr. Methionine restriction inhibits colon carcinogenesis. Nutrition and Cancer. 2006,54(2), 202-208.

56. Shan Lu, Sara M. Hoestje, Eugene M. Choo, Daniel E. Epner. Methionine restriction induces apoptosis of prostate cancer cells via the c-Jun N-terminal kinase-mediated signaling pathway. Cancer Letter. 2002; 51-58.

57. Xin L, Cap WX, Fei XF, Want Y, Liu Wt, Liu BY, Zhu Zg. Applying proteomic methodologies to analyze the effect of methionine restriction on proliferation of human gastric cancer SGC7901 cells. Clin Chim Acta. 2007 Feb;377(1-2):206-12.

58. Earl R Stadtman, Holly Van Remmen, Arlan Richardson, Nancy B. Wehr, Rodney L. Levine. Biochemica et Biophysica Aeta. 2005. 135-140.

59. Levine, R.L. Carbonyl modified proteins in cellular regulation, aging, and disease. Free Radic. Biol. Med. 1, 790-6, 2002.

60. Earl R. Stadtman, Jackob Moskovitz, Barbara S. Berlett and Rodney L. Levine. Cyclic oxidation and reduction of protein methionine residues is an important antioxidant mechanism. Molecular and Cellular Biochemistry. 2002; 234-235.

61. Duthie, S.J., Narayanan, S., Blum, S., Pirie, L. and Brand, G.M. Folate deficiency in vitro induces uracil misincorporation and DNA hypomethylation and inhibits DNA excision repair in immortalized normal human colon epithelial cells. Nutr.Cancer 37:245-251, 2000.

62. Evans, M.D.; Dizdaroglu, M.; Cooke, M.S. Oxidative DNA damage and disease: induction, repair and significance. Mutat. Res. **567:** 1-61; 2004.

63. Mullaart, E.; Lohman, P.H.M.; Berends, F.; Vijg, J. DNA damage metabolism and aging. Mutat. Res. **237:** 189-210; 1990.

64. Jackson, A.L.; Loeb, L.A. The contribution of endogenous sources of DNA damage to the multiple mutations in cancer. Mutat. Res. **477 :** 7-21 ;2001.

65. Sancar, A.; Lindsey-Boltz, L.A.; Unsal-Kacmaz, K.; Linn, S. Molecular mechanisms of mammalian DNA repair and the DNA damage checkpoints. Annu. Rev. Biochem.**73:** 39-85; 2004.

66. Slupphaug, G.; Kavli, B.; Krokan, H.E. The interacting pathways for prevention and repair of oxidative DNA damage. Mutat. Res. **531:** 231-251; 2003.

67. Friedberg, E.C.; Walker, G.C.; Siede, W.; Wood, R. D.; Schultz, R. A.; Ellenberger, T. DNA repair and Mutagenesis. pp.169-226, Washington D.C: ASM Press; 2006.

68. Ljungquist, S.; Lindahl T. A mammalian endonuclease specific for apurinic sites in double-stranded deoxyribonucleic acid. I. Purification and general properties. J. Biol. Chem. **249:** 1530-1535; 1974.

69. Ljungquist, S.; Andersson, A.; Lindahl, T. A mammalian endonuclease specific for apurinic sites in double-stranded deoxyribonucleic acid. II. Further studies on the substrate specificity. J. Biol. Chem. **249:** 1536-1540; 1974.

70. Lindahl, T. Inroads into base excision repair I: The discovery of apurinic/apyrimidinic [AP] endonuclease. DNA Repair **3:** 1521-1530; 2004.

71. Xanthoudakis, S.; Curran, T. Identification and characterization of Ref-1, a nuclear protein that facilitates AP-1 DNA-binding activity. EMBO J. **11 :** 653-665 ; 1992.

72. Xanthoudakis, S.; Miao, G.; Wang, F.; Pan, Y.C.; Curran, T. Redox activation of Fos-Jun DNA binding activity is mediated by a DNA repair enzyme. EMBO J. **11:** 3323-3335; 1992.

73. Evans, A.R.; Limp-Foster, M.; Kelley, M.R. Going APE over Ref-1. Mutat. Res. **461:** 83-108; 2000.

74. Shimizu, N.; Sugimoto, K.; Tang, J.; Nishi, T.; Sato, I.; Hiramoto, M.; Aizawa, S.; Hatakeyama, M.; Ohba, R.; Hatori, H.; Yoshikawa, T.; Suzuki, F.; Oomori, A.; Tanaka, H.; Kawaguchi, H.; Watanabe, H.; Handa, H. High-performance affinity beads for identifying drug receptors. Nat. Biotechnol. **18:** 877-881; 2000.

75. Nishi, T.; Shimizu, N.; Hiramoto, M.; Sato, I.; Yamaguchi, Y.; Hasegawa, M.; Aizawa, S.; Tanaka, H.; Kataoka, K.; Watanabe, H.; Handa, H. Spatial redox regulation of a critical cysteine residue of NF-kappa B in vivo. J. Biol .Chem. **277:** 44548-44556; 2002.

76. Hall, J.L.; Wang, X.; Adamson, V.; Zhao, Y.; Gibbons, G.H. Overexpression of Ref-1 inhibits hypoxia and tumor necrosis factor-induced endothelial cell apoptosis through nuclear factor-κB-independent and -dependent pathways .Circ. Res. **88:** 1247-1253; 2001.

77. Guan, Z.; Basi, D.; Li, Q.; Mariash, A.; Xia, Y.F.; Geng, J.G.; Kao, E.; Hall, J.L. Loss of redox factor 1 decreases NF-kappaB activity and increases susceptibility of endothelial cells to apoptosis. Arterioscler. Thromb. Vasc. Biol. **25:** 96-101; 2005.

78. Lindahl, T. Keynote: past, present, and future aspects of base excision repair. Nucleic Acid Res. Mol Biol. **68:** xvii-xxx; 2001.

79. Parikh, S.S.; Mol, C.D.; Hosfield, D.J.; Tainer, J.A. Envisioning the molecular choreography of DNA base excision repair. Curr. Opin. Struct. Biol. **9:** 37-47; 1999.

80. Wilson, S.H.; Kunkel, T.A. Passing the baton in base excision repair. Nature Struct. Biol. **7:** 176-178; 2000.

81. Wilson III, D.M.; Sofinowski, T.M.; McNeill, D.R. Repair mechanisms for oxidative DNA damage. Front. Biosci. **8:** d963-981; 2003.

82. Izumi, T.; Wiederhold, L.R.; Roy, G.; Roy, R.; Jaiswal, A.; Bhakat, K.K.; Mitra, S.; Hazra, T.K. Mammalian DNA base excision repair proteins: their interactions and role in repair of oxidative DNA damage .Toxicology **193:** 43-65; 2003.

83. Cabelof, D.C.; Raffoul, J.J.; Yanamadala, S.; Guo, Z.; Heydari, A.R. Induction of DNA polymerase β-dependent base excision repair in response to oxidative stress *in vivo*. Carcinogenesis **23:** 1419-1425; 2002.

84. Grosch, S.; Fritz, G.; Kaina, B. Apurinic endonuclease [Ref-1] is induced in mammalian cells by oxidative stress and is involved in clastogenic adaptation. Cancer Res. **58:**4410-4416; 1998.

85. Ramana, C.V.; Boldogh, I.; Izumi, T.; Mitra, S. Activation of apurinic/apyrimidinic endonuclease in human cells by reactive oxygen species and its correlation with their adaptive response to genotoxicity of free radicals. Proc. Natl. Acad. Sci. U.S.A. **95:** 5061-5066; 1998.

86. Ono, Y.; Furuta, T.; Ohmoto, T.; Akiyama, K.; Seki, S. Stable expression in rat glioma cells of sense and antisense nucleic acids to a human multifunctional DNA repair enzyme, *APEX* nuclease. Mutat. Res. **315:** 55-63; 1994.

87. Meira, L.B.; Devaraj, S.; Kisby, G.E.; Burns, D.K.; Daniel, R.L.; Hammer, R.E.; Grundy, S.; Jialal, I.; Friedberg, E.C. Heterozygosity for the mouse *Apex* gene results in phenotypes associated with oxidative stress . Cancer Res. **61:** 5552-5557; 2001.

88. Walker, L.J.; Craig, R.B.; Harris, A.L.; Hickson, I.D. A role for the human DNA repair enzyme HAP1 in cellular protection against DNA damaging agents and hypoxic stress. Nucleic Acids Res **22:** 4884-4889; 1994.

89. Fung, H.; Demple, B. A vital role for Ape1/Ref1 protein in repairing spontaneous DNA damage in human cells. Mol. Cell **17:** 463-470; 2005.

90. Izumi, T.; Brown, D.B.; Naidu, C.V.; Bhakat, K.K.; MacInnes, M.A.; Saito, H.; Chen, D.J.; Mitra, S. Two essential but distinct functions of mammalian abasic endonuclease. Proc. Natl. Acad. Sci. U.S.A**. 102:** 5739-5743; 2005.

91. Vasko, M.R.; Guo, C.; Kelley, M.R. The multifunctional DNA repair/redox enzyme Ape1/Ref-1 promotes survival of neurons after oxidative stress. DNA Repair **4:** 367-379; 2005.

92. Raffoul, J.J.; Cabelof, D.C.; Nakamura, J.; Meira, L.B.; Friedberg, E.C.; Heydari, A.R. Apurinic/apyrimidinic endonuclease [APE/REF-1] haploinsufficient mice display tissue-specific differences in DNA polymerase beta-dependent base excision repair. J. Biol. Chem. **279:** 18425-18433; 2004.

93. Hadi, M.Z.; Coleman, M.A.; Fidelis, K.; Mohrenweiser, H.W.; Wilson III, D.M. Functional characterization of Ape1 variants identified in the human population. Nucleic Acids Res. **28:** 3871-3879; 2000.

94. De Boer, J.G. Polymorphisms in DNA repair and environmental interactions. Mutat. Res. **509:** 201-210; 2002.

95. Mohrenweiser, H.W.; Wilson III, D.M.; Jones, I.M. Challenges and complexities in estimating both the functional impact and the disease risk associated with the extensive genetic variation in human DNA repair genes. Mutat. Res. **526:** 93-125; 2003.

96. Hou, E.W.; Prasad, R.; Asagoshi, K.; Masaoka, A.; Wilson, S.H. Comparative assessment of plasmid and oligonucleotide DNA substrates in measurement of in vitro base excision repair activity. Nucleic Acids Res. **35:** 1-10; 2007.

97. Cabelof, D.C.; Raffoul, J.J.; Nakamura, J.; Kapoor, D.; Abdalla, H.; Heydari, A.R. Imbalanced base excision repair in response to folate deficiency is accelerated by polymerase beta haploinsufficiency. *J. Biol. Chem.* **279:** 36504-36513; 2004.

98. Nakamura, J.; Walker, V.E.; Upton, P.B.; Chiang, S.Y.; Kow, Y.W.; Swenberg, J.A. Highly sensitive apurinic/apyrimidinic site assay can detect spontaneous and chemically induced depurination under physiological conditions. Cancer Res. **58:** 222-225; 1998.

99. Sokal, R.R.; Rohlf, F.J. Biometry, New York, NY: W.H. Freeman and Company; 1981.

100. Sakano, K.; Oikawa, S.; Murata, M.; Hiraku, Y.; Kojima, N.; Kawanishi, S. Mechanisms of metal-mediated DNA damage induced by metabolites of carcinogenic 2-nitropropane. Mutat. Res. **479:** 101-111; 2001.

101. Andrae, U.; Homfeldt, H.; Vogl, L.; Lichtmannegger, J.; Summer, K.H. 2-Nitropropane induces DNA repair synthesis in rat hepatocytes *in vitro* and *in vivo.* Carcinogenesis **9:** 811-815; 1988.

102. Izumi, T.; Hazra, T.K.; Boldogh, I.; Tomkinson, A.E.; Park, M.S.; Ikeda, S.; Mitra, S. Requirement for human AP endonuclease 1 for repair of 3'-blocking damage at DNA single-strand breaks induced by reactive oxygen species. Carcinogenesis **21:** 1329-1334; 2000.

103. Wiederhold, L.; Leppard, J.B.; Kedar, P.; Karimi-Busheri, F.; Rasouli-Nia, A.; Weinfeld, M.; Tomkinson, A.E.; Izumi, T.; Prasad, R.; Wilson, S.H.; Mitra, S.; Hazra, T.K. AP endonuclease-independent DNA base excision repair in human cells. Mol. Cell **15:** 209-220; 2004.

104. Sabine, G.; kaina, B. Transcriptional activation of Apurinic/Apyrimidinic endonuclease [Ape,Ref-1] by oxidative stress requires CREB. Biochem. and Biophy. Res. Communications. **261:** 859-863; 1999.

105. Yau-Jan, C.; Rawson, T.Y.; Wilson, S.H. Cloning and characterization of a novel member of the human ATF/CREB family: ATF2 deletion, a potential regulator of the human DNA polymerase β promoter. Gene **312:** 117-124; 2003.

106. Fornance Jr, A.J.; Zmudzka, B.; Hollander, M.C.; Wilson, S.H. Induction of beta-polymerase mRNA by DNA-damaging agents in Chinese hamster ovary cells. Mol. Cell. Biol. **9:** 851-853; 1989.

107. Hazra, T.K.; Izumi, T.; Maidt, L.; Floyd, R.A.; Mitra, S. The presence of two distinct 8-oxoguanine repair enzymes in human cells: their potential complementary roles in preventing mutation. Nuc. Acids Res. **26:** 5116-5122; 1998.

108. Nilsen, H.; Rosewell, I.; Robins, P.; Skjelbred, C.F.; Andersom, S.; Slupphaug, G.; Daly, G.; Krokan, H. E.; Lindahl, T.; Barnes, D.E. Uracil-DNA Glycosylase [UNG]-deficient mice reveal a primary role of the enzyme during DNA replication. Mol. Cell **5:** 1059-1065; 2000.

109. Endres, M.; Biniszkiewicz, D.; Sobol, R.B.; Harms, C.; Ahmadi, M.; Lipski, A.; Katchanov, J.; Mergenthaler, P.; Dirnagl, U.; Wilson, S.H.; Meisel, A.; Jaenisch, R. Increased potischemic brain injury in mice deficienct in uracil-DNA glycosylase. J Clin Invest. **113:** 1711-1721; 2004.

110. Dizdaroglu, M.; Karakaya, A.; Jaruga, P.; Slupphaug, G.; Krokan, H.E. Novel activities of human uracil DNA N-glycosylase for cytosine derived products of oxidative DNA damage. Nuc. Acids Res. **24:** 418-422; 1996.

111. Fritz, G.; Grosch, S.; Tomicic, M.; Kaina, B. APE/Ref-1 and the mammalian response to genotoxic   stress. Toxicology **193:** 67-78; 2003.

112. Hsieh, M.M.; Hegde, V.; Kelley, M.R.; Deutsch, W.A. Activation of APE/Ref-1 redox activity is mediated by reactive oxygen species and PKC phosphorylation. Nuc. Acids Res. **29:** 3116-3122; 2001.

113. Pines, A.; Perrone, L.; Bivi, N.; Romanello, M.; Damante, G.; Gulisano, M.; Kelley, M.R.; Quadrifoglio, F.; Tell, G. Activation of APE1/Ref-1 is dependent on reactive oxygen species generated after purinergic receptor stimulation by ATP. Nuc. Acids Res. **33:** 4379-4394; 2005.

114. Ludwig, D.L.; MacInnes, M.A.; Takiguchi, Y.; Purtymun, P.E.; Henrie, M.; Flannery, M.; Meneses, J.; Pederson, R.A.; Chen, D.J. A murine AP-endonuclease gene-targeted deficiency with post-implantation embryonic progression and ionizing radiation sensitivity. Mutat.Res**. 409:** 17-29; 1998.

115. Xanphoudakis, S.; Smeyne, R.J.; Wallace, J.D.; Curran, T. The redox/DNA repair protein, Ref-1, is essential for early embryonic development in mice. Proc. Natl. Acad. Sci.U.S.A **93:** 8919-8923; 1996.

116. Huamani, J.; McMahan, C.A.; Herbert, D.C.; Reddick, R.; McCarrey, J.R.; MacInnes, M.I.; Chen D.J.; Walter, C.A. Spontaneous mutagenesis is enhanced in *Apex* heterozygous mice. Mol. Cell. Biol. **24:** 8145-8153; 2004.

117. Friedberg, E.C.; Meira, L.B. Database of mouse strains carrying targeted mutations in genes affecting biological responses to DNA damage version 7, DNA repair 5 . DNA repair **5:** 189-209; 2006.

118. Kohl, C.; Morgan, P.; Gescher, A. Metabolism of the genotoxicant 2-nitropropane to a nitric oxide species. Chemico-Biological Interactions 97. Chemico-Biological Interactions **97:** 175-184, 1995.

119. Wink, D.A.; Kasprzak, K.S.; Maragos, C.M.; Elespuru, R.K.; Misra, M.; Dunams, T. M.; Cebula, T.A.; Koch, W.H.; Andrews, A.W.; Allen, J.S.; Keefer, L.K. DNA deaminating ability and genotoxicity of nitric oxide and its progenitors. Science **254:** 1001-1003; 1991.

120. Carrero, P.; Okamoto, K.; Coumailleau, P.; O'Brien, S.; Tanaka, H.; Poellinger, L. Redox-regulated recruitment of the transcriptional coactivators CREB-binding protein and SRC-1 to hypoxia-inducible factor 1alpha. Mol. Cell Biol. **20:** 402-415; 2000.

121. Ziel, K.A.; Campbell, C.C.; Wilson, G.L.; Gillespie, M.N. Ref-1/Ape is critical for formation of the hypoxia-inducible transcriptional complex on the hypoxic response element of the rat pulmonary artery endothelial cell VEGF gene. FASEB J. **18:** 986-988; 2004.

122. Raffoul, J.J.; Banerjee, S.; Singh-Gupta, V.; Knoll, Z.E.; Fite, A.; Zhang, H.; Abrams, J.; Sarkar, F.H.; Hillman, G.G. Down-regulation of apurinic/apyrimidinic endonuclease 1/redox-factor 1 expression by soy isoflavones enhances prostate cancer radiotherapy *in vitro* and *in vivo.* Cancer Res. **67:** 2141-2149; 2007.

123. Raffoul, J.J.; Wang, Y.; Kucuk, O.; Forman, J.D.; Sarkar, F.H.; Hillman, G.G. Genistein inhibits radiation-induced activation of NF-κB in prostate cancer cells promoting apopstosis and G2/M cell cycle arrest. BMC Cancer **6:**107; 2006.

124. Baldwin Jr, A.S. The transcription factor NF-κB and human disease. The Journal of Clinical Investigation **107:** 3-6; 2001.

125. Srivastava, D.K.; Vande Berg, B.J.; Prasad, R.; Molina, J.T.; Beard, W.A.; Tomkinson, A.E.; Wilson S.H. Mammalian abasic site base excision repair. Identification of the reaction sequence and rate-determining steps. J.Boil.Chem **273:** 21203-21209; 1998.

126. Cabelof, D.C.; Raffoul, J.J.; Yanamadala, S.; Ganir, C.; Guo, Z.; Heydari, A.R. Attenuation of DNA polymerase beta-dependent base excision repair and increased DMS-induced mutagenicity in aged mice. Mutat. Res. **500:** 135-145; 2002.

127. Cabelof, D.C.; Guo, Z.; Raffoul, J.J.; Sobol, R.W.; Wilson, S.H.; Richardson, A.; Heydari, A.R. Base excision repair deficiency caused by polymerase beta haploinsufficiency: accelerated DNA damage and increased mutational response to carcinogens. Cancer Res. **63:** 5799-5807; 2003.

128. Cabelof, D.C.; Yanamadala, S.; Raffoul, J.J.; Guo, Z.; Soofi, A.; Heydari, A.R. Caloric restriction promotes genomic stability by induction of base excision repair and reversal of its age-related decline. DNA Repair **2:** 295-307; 2003.

129. Suh, D.; Wilson, D.M.; Povirk, L.F. 3'-phosphodiesterase activity of human apurinic/apyrimidinic endonuclease at DNA double-strand break ends. Nuc. Acids Res. **25:** 2495-2500; 1997.

130. Bernstein, C.; Bernstein, C H.; Payne, C.M.; Garewal, H. DNA repair/pro-apoptotic dual-role proteins in five major DNA repair pathways: fail-safe protection against carcinogenesis. Mut. Res. **511:** 145-178; 2002.

131. Zhou, J.; Ahn, J.; Wilson, S.H.; Prives, C. A role of P53 in base excision repair. EMBO. J. **20:** 914-923; 2001.

132. Saitoh, T.; Shinmura, K.; Yamaguchi, S.; Tani, M.; Seki, S.; Murakami, H.; Nojima, Y.; Yokota, J. Enhancement of OGG1 protein AP lyase activity by increase of Apex protein. Mutation Research **486:** 31-40; 2001.

133. Huang, D.; Shenoy, A.; Cui, J.; Huang, W.; Liu, P.K. In situ detection of AP sites and DNA strand breaks bearing 3'-phosphate termini in ischemic mouse brain. FASEB J. **14:** 407-417; 2000.

134. Mokkapati, S.K.; Wiederhold, L.; Hazra, T.K.; Mitra, S. Stimulation of DNA glycosylase activity of OGG1 by NEIL1: functional collaboration between two human DNA glycosylases. Biochemistry **43:** 11596-11604; 2004.

135. Das,A.; Hazra, T.K..; Boldogh, I.; Mitra, S.; Bhakat, K.K. Induction of the human oxidized base-specific DNA glycosylase NEIL1 by reactive oxygen species. J. Biol. Chem. **280:** 35272-35280; 2005.

136. Ying, J.; Srivastava, G.; Hsieh, W.S.; Gao, Z.; Murray, P.; Liao, S.K.; Tao, Q. The stress-responsive gene GADD45g is a functional tumor suppressor, with its response to environmental stresses frequently disrupted epigenetically in multiple tumors. Clin. Cancer Res. **18:** 6442-6449; 2005.

137. Takekawa, M.; Saito, H. A family of stress-inducible GADD45-like proteins mediate activation of the stress-responsive MTK1/MEKK4/MAPKKK. Cell **95:** 521-530; 1998.

138. Fishel, M.L.; Kelley, M.R. The DNA base excision repair protein Ape1/Ref-1 as a therapeutic and chemopreventive target. Molecular aspects of Medicine **28:** 375-395; 2007.

139. Cindy, C.D.; Milner, J. Frontiers in Nutrigenomics, proteomics, metabolomics and cancer prevention. Mut.Res. **551,** 51-64; 2004.

140. Trujillo, E.; Davis, C.; Milner, J. Nutrigenomics, Proteomics, Metabolomics, and the practice of dietetics. J. Am. Diet Assoc. **106,** 403-413; 2006.

141. Cravo, M.L.; Mason, J.B.; Dayal, Y.; Hutchinson, M.; Smith, D.; Selhub, J.; Rosenberg, I.H. Folate deficiency enhances the development of colonic neoplasia in dimethylhydrazine-treated rats. Cancer Res. **52**, 5002-5006; 1992.

142. James, S.J.; Miller, B. J.; Basnaknian, A.G.; Pogribny, I.P.; Pogribna, M.; Muskhelishvili, I. Apoptosis and proliferation under conditions of deoxynucleotide pool imbalance in liver of folate/methyl deficient rats. Carcinogenesis **18**, 287-293; 1997.

143. Kim, Y-I.; Pogribny, I. P.; Basnakian, A.G.; Miller, J.W.; Selhub,J.; James, S.J.; Mason, J.B. Folate deficiency in rats induces DNA strand breaks and hypomethylation within the p53 tumor suppressor gene. Am J Clin Nutr. **65**, 46-52; 1997.

144. Duthie, S.J.; Hawdon, A. DNA instability [strand breakage, uracil misincorporation, and defective repair] is increased by folic acid depletion in human lymphocytes in vitro. Faseb J. **12**, 1491-1497; 1998.

145. Melnyk, S.; Pogribna, M.; Miller, B. J.; Basnakian, A. G.; Pogribny, I.P.; James, S.J. Uracil misincorporation, DNA strand breaks, and gene amplification are associated with tumorigenic cell transformation in folate deficient/repleted Chinese hamster ovary cells. Cancer Letters **146**, 35-44; 1999.

146. James, S. J.; Basnakian, A. G.; Miller, B.J. In vitro folate deficiency induces deoxynucleotide pool imbalance, apoptosis, and mutagenesis in Chinese hamster ovary cells. Cancer Res. **54**, 5075-5080; 1994.

147. Kim, Y-I. Folate and DNA methylation: A mechanistic link between folate deficiency and colorectal cancer? Cancer Epidemiol. Biomarkers Prev. **13**, 511-519; 2004.

148. Ventrella-Lucente, L.F.; Unnikrishnan, A.; Pilling, A. B.; Patel, H.V.; Kushwaha, D.; Dombkowski, A.A.; Schmelz, E. M.; Cabelof, D.C.; Heydari, A.R. Folate deficiency provides

protection against colon carcinogenesis in DNA polymerase beta haploinsufficiency mice. J.Biol.Chem. **285**, 19246-51928; 2010.

149. Cabelof, D.C.; Raffoul, J.J.; Nakamura, J.; Kapoor, D.; Abdalla, H.; Heydari, A.R. Imbalanced base excision repair in response to folate deficiency is accelerated by polymerase □ haploinsufficiency. J. Biol.Chem. **279**, 36504-36513; 2004.

150. Friedberg, E.C.; Walker, G.C.; Siede, W.; Wood, R.D.; Schultz, R.A.; Ellenberger, T. Base excision repair. In: DNA Repair and Mutagenesis, 2nd edition. Washington D.C.: ASM press; 2006: 169-226.

151. Wilson III, D.M.; Sofinowski, T.M.; McNeill, D.R. Repair mechanisms for oxidative DNA damage. Front. Biosci. **8**, d963-d981; 2003.

152. Izumi, T.; Wiederhold, L.R.; Roy, G.; Roy, R.; Jaiswal, A.; Bhakat, K.K.; Mitra, S.; Hazra, T.k. Mammalian DNA base excision repair repair proteins: their interactions and role in repair of oxidative DNA damage. Toxicology **193**, 43-65; 2003.

153. Cabelof, D.C.; Raffoul, J.J.; Yanamadala, S.; Guo, Z.; Heydari, A.R. Induction of DNA polymerase □-dependent base excision repair in response to oxidative stress in vivo. Carcinogenesis **23**, 1419-1425; 2002.

154. Cabelof, D.C.; Guo, Z.; Raffoul, J.J.; Sobol, R.W.; Wilson, S.H.; Richardson, A.; Heydari, A.R. Base excision repair deficiency caused by polymerase □ haploinsufficiency: Accelerated DNA damage and increased mutational response to carcinogens. Cancer Res. **63**, 5799-5807; 2003.

155. Unnikrishnan, A.; Raffoul, J.J.; Patel, H.V.; Prychitko, T.M.; Anyangwe, N.; Meira, L.B.; Friedberg, E.C.; Cabelof, D.C.; Heydari, A.R. Oxidative stress alters base excision repair pathway and increases apoptotic response in apurinic/apyrimidinic endonuclaese 1/redoxfactor-1 haploinsufficient mice. Free Rad. Biol. Med. **49**, 1488-1499; 2009.

156. Raffoul, J.J.; Cabelof, D.C.; Nakamura, J.; Meira, L.B.; Friedberg, E.C.; Heydari, A.R. Apurinic/apyrimidinic endonuclease [APE/REF-1] haploinsufficient mice display tissue specific differences in DNA polymerase beta-dependent base excision repair. J. Biol. Chem. **279**, 18425-18433; 2004.

157. Srivastava, D.K.; VandeBerg, B.J.; Prasad, R.; Molina, J.T.; Beard, W.A.; Tomkinson, A.E.; Wilson, S.H. Mammalian abasic site base excision repair: identification of the reaction sequence and rate-determining steps. J. Biol. Chem. **273**, 21203-21209; 1998.

158. Li, L.C.; Dahiya, R. MethPrimer: designing primers for methylation PCRs. Bioinformatics **11**, 1427-1431; 2002.

159. Sohn, K-J.; Stempak, J.M.; Reid, S.; Shirwadkar, S.; Mason, J. B.;Kim, Y-I. The eefect of dietary folate on genomic and p53-specific DNA methylation in rat colon. Carcinogensis **24**, 81-90; 2003.

160. Briggs, M.R.; Kadonaga, J.T.; Bell, S.P.; Tjian, R. Purification and biochemical characterization of the promoter specific transcription factor, Sp1. Science **234**, 47-52; 1986.

161. Englander, E.W.;Wilson, S.H. Protein binding elements in the human □-polymerase promoter. Nucleic acids Res. **18**, 919-928; 1990.

162. He, F.; Yang, X-P.; Srivastava, D.K.;Wilson, S.H. DNA polymerase □ gene expression: The promoter activator CREB-1 is upregulated in Chinese hamster ovary cells by DNA alkylating agent-induced stress. Biol. Chem. **384**, 19-23; 2003.

163. Chyan, Y-J.; Rawson, T.Y.;Wilson, S.H. Cloning and characterization of a novel member of the human ATF/CREB family: ATF2 deletion, a potential regulator of the human DNA polymerase □ promoter. Gene **312**, 117-124; 2003.

164. Fornance Jr, A. J.; Zmudzka, B.; Hollander, M.C.; Wilson, S.H. Induction of b-polymerase mRNA by DNA-damaging agents in Chinese hamster ovary cells. Mol. Cell Biol. **9**, 851-853; 1989.

165. Kim, Y-I. Folate, colorectal carcinogenesis, and DNA methylation: Lessons from Animal studies. Environ. Mol. Mutagen. **44**, 10-25; 2004.

166. Linhart, H. G.; Troen, A.; Bell, G.W.; Cantu, E.; Chao, W-H.; Moran, E.; Steine, E.; He, T.; Jaenisch, R. Folate deficiency induces genomic uracil misincorporation and hypomethylation but does not increase DNA point mutations. Gasteroenterology **136**, 227-235; 2009.

167. Logan, R.F.; Grainge, M.J.; Shepherd, V.C.; Armitage, N.C.;Muir, K.R. Aspirin and folic acid for the prevention of recurrent colorectal adenomas. Gastroenterology **134**, 29-38; 2008.

168. Cole, B.F.; Baron, J.A.; Sandler, R.S.; Haile, R.W.; Ahnen, D.J.; Bresalier, R.S.; Eyssen, G.M.; Summers, R.W.; Rothstein, R.I.; Burke, C.A.; Snover, D.C.; Church, T.R.; Allen, J.I.; Robertson, D.J.; Beck, G.J.; Bond, J.H.; Byers, T.; Mandel, J.S.; Mott, L.A.; Perason, L.H.; Barry, E.L.; Rees, J.R.; Marcon, N.; Saibil, F.; Ueland, P.M.; Greenberg, R. Folic acid for the prevention of colorectal adenomas: a randomized clinical trial. JAMA **297**, 2351-2359; 2007.

169. Van Guelpen, B.; Hultdin, J.; Johansson, I.; Hallmans, G.; Stenling, R.; Riboli, E.; Winkvist, A.; Palmqvist, R. Low folate levels may protect against colorectal cancer. Gut **55**, 1461-1466; 2006.

170. Eussen, S.J.P.M.; Vollset, S. E.; Igland, J.; Meyer, K.; Fredriksen, A.; Ueland, P.M.; Jenab, M.; Slimani, N.; Boffetta, P.; Overvad, K.; Tjonneland, A.; Olsen, A.; Clavel-Chapelon, F.; Boutron-Ruault, M-C.; Morois, S.; Weikert, C.; Pischon, T.; Linseisen, J.; Kaaks, R.; Trichopoulou, A.; Zilis, D.; Katssoulis, M.; Palli, D.; Berrino, F.; Vineis, P.; Tumino, R.; Panico, S.; Peeters, P.H.M.; Bueno-de-Mesquita, H.B.; Duijnhoven, F.J.B.V.; Gram, I.T.; Skeie, G.; Lund, E.; Gonzalez, C.A.; Martinez, C.; Dorronsoro, M.; Ardanaz, E.; Navarro, C.; Rodriguez, L.; Guelpen, B.V.; Palmqvist, R.; Manjer, J.; Ericson, U.; Bingham, S.; Khaw, K-T.; Norat, T.; Riboli, E. Plasma folate, related

genetic variants and colorectal cancer risk in EPIC. Cancer Epidemiol Biomarkers Prev **19**, 1328-1340; 2010.

171. Choi, S-W.; Kim, Y-I.; Weitzel, J.N.;Mason, J.B. Folate depletion impairs DNA excision repair in the colon of the rat. Gut **43**, 93-99; 1998.

172. Borchers, A.H.; Kennedy, K. A.; Straw, J.A. Inhibition of DNA excision repair by methotrexate in Chinese hamster ovary cells following exposure to ultraviolet irradiation or ethylmethanesulfonate. Cancer Res. **50**, 1786-1789; 1990.

173. Chen, K.H.; Yakes, F.M.; Srivastava, D.K.; Singhal, R.K.; Sobol, R.W.; Horton, J. K.; vanHouten, B.; Wilson, S.H. Upregulation of base excision repair correlates with enhanced protection against a DNA damaging agent in mouse cell lines. Nucleic Acids Res. **26**, 2001-2007; 1998.

174. Lin, L. H.; Cao, S.; Yu, L.; Cui, J.; Hamilton, W.J.; Liu, P.K. Upregulation of base excision repair activity for 8-hydroxy-2'deoxyguanosine in the mouse brain after forebrain ischemia reperfusion. J. Neurochem. **74**, 1098-1105; 2000.

175. Novakovic, P.; Stempak, J. M.; Sohn, K-J.; Kim, Y-I. Effects of folate deficiency on gene expression in the apoptosis and cancer pathways in colon cancer cells. Carcinogenesis 27, 916-924; 2006

176. Chanson, A.; Sayd, T.; Rock, E.; Chambon, C.; Sante-Lhoutellier, V.; Potier de Courcy, G.; Brachet, P. Proteomic analysis reveals changes in the liver protein pattern of rats exposed to dietary folate deficiency. J.Nutr. **135**, 2524-2529; 2005.

177. Asagoshi, K.; Liu, Y.; Masaoka, A.; Lan, L.; Prasad, R.; Horton, J.K.; Brown, A.R.; Wang, X-H.; Bdour, H.M.; Sobol, R.W.; Taylor, J-S.; Yasui, A.; Wilson S.H. DNA polymerase □-dependent long patch base excision repair in living cells. DNA Repair **9**, 109-119; 2010.

178. Horton, J.K.; Prasad, R.; Hou, E.; Wilson, S.H. protection against methylation-induced cytotoxicity by DNA polymerase □-dependent long patch base excision repair. J.Biol. Chem. 275, 2211-2218; 2000.

179. Gu, H.; Marth, J.D.; Orban, P.C.; Mossmann, H.; Rajewsky, K. Deletion of a DNA polymerase beta gene segment in T cells using cell type-specific gene targeting. Science **265**, 103-106; 1994.

180. Sobol, R.W.; Wilson, S.H. Mammalian DNA polymerase □ in base excision repair of alkylation damage. Prog. Nucleic Acid Res. Mol. Biol. 68, 57-74; 2001.

181. Horton, J.K.; Joyce-Gray, D.F.; Pachkowski, B.F.; Swenberg, J.A.; Wilson, S.H. Hypersensitivity of DNA polymerase □ null mouse fibroblasts refelects accumulation of cytotoxic repair intermediates from site-specific alkyl DNA lesions. DNA Repair **2**, 27-48; 2003.

182. Choi, S-W.; Mason, J.B. Folate and Carcinogenesis: An integrated Scheme. J.Nutr. **130**,129-132; 2000.

183. Gaudet, F.; Hodgson, J.G.; Eden, A.; Jackson-Grusby, L.; Dausman, J.; Gray, J.W.; Leonhardt, H.; Jaenisch, R. Induction of tumors in mice by genomic hypomethylation. Science **300**, 489-492; 2003.

184. Eden, A.; Gaudet, F.; Waghmare, A.; Jaenisch, R. Chromosomal instability and tumors promoted by DNA hypomethylation. Science **300**, 455; 2003.

185. Goelz, S.E.; Vogelstein, B.; Hamilton, S.R.; Feinberg, A.P. Hypomethylation of DNA from benign and malignant human colon neoplasms. Science **228**, 187-190; 1985.

186. Clark, S. J.; Melki, J. DNA methylation and gene silencing in cancer: which is the guilty party? Oncogene **21**, 5380-5387; 2002.

187. Narayan, S.; Wilson, S.H. Kinetic analysis of Sp1-mediated transcriptional activation of the human DNA polymerase □ promoter. Oncogene **19**, 4729-4735; 2000.

188. Yang, X-P.; He, F.; Rawson, T.Y.; Wilson, S.H. Human DNA polymerase-□ promter: Phorbol ester activation is mediated through the cAMP response element and cAMP-response-element-binding protein. J. Biomed. Sci. **4**, 279-288; 1997.

189. Yamaguchi, M.; Hayashi, Y.; Hirose, F.; Shiroki, K.; Matsukage, A. Activation of the mouse DNA polymerase □ gene promoter by adenovirus type 12 E1A proteins. Nucleic Acids Res. **20**, 2321-2325; 1992.

190. Lamph, W.W.; Dwarki, V.J.; Ofir, R.; Montminy, M.; Verma, I.M. Negative and positive regulation by transcription factor cAMP response element-binding protein is modulated by phosphorylation. Proc. Natl. Acad. Sci. **87**, 4320-4324; 1990.

191. Montminy, M.R.; Sevarino, K. A.; Wagner, J.A.; Mandel, G.; Goodman, R.H. Identification of a cyclic-AMP-responsive element within the rat somatostatin gene. Proc. Natl. Acad. Sci. **83**, 6682-6686; 1986.

192. Schule, R.; Umesono, K.; Mangelsdorf, D.J.; Bolado, J.; Pike, J.W.; Evans, R.M. Jun-Fos and receptors for Viatmins A and D recognize a common response element in the human osteocalcin gene. Cell **61**, 497-504; 1990.

193. Schule, R.; Rangarajan, P.; Kliewer, S.; Ransone, L.J.; Bolado, J.; Verma, I.M.;Evans, R.M. Functional antagonism between oncoprotein c-Jun and the glucocorticoid receptor. Cell **62**, 1217-1226; 1990.

194. Diamond,M.I.; Miner,J.N.; Yoshinaga, S.K.; Yamamoto, K.R. Transcription factor interactions: Selectors of positive or negative regulation from a single DNA element. Science **249**, 1266-1272; 1990.

195. Pedraza-Alva, G.; Zingg, J-M.; Jost, J-P. Ap-1 binds to a putative cAMP response element of the MyoD1 promoter and negatively modulates MyoD1 expression in dividing myoblasts. J. Biol. Chem. **269**, 6978-6985; 1994.

196. Wilson III, D.M.; Sofinowski, T.M.; McNeill, D.R. Repair mechanisms for oxidative DNA damage. Front. Biosci. **8**, d963-d981; 2003.

197. Izumi, T.; Wiederhold, L.R.; Roy, G.; Roy, R.; Jaiswal, A.; Bhakat, K.K.; Mitra, S.; Hazra, T.k. Mammalian DNA base excision repair repair proteins: their interactions and role in repair of oxidative DNA damage. Toxicology **193**, 43-65; 2003.

198. Cabelof, D.C.; Raffoul, J.J.; Yanamadala, S.; Guo, Z.; Heydari, A.R. Induction of DNA polymerase b-dependent base excision repair in response to oxidative stress in vivo. Carcinogenesis **23**, 1419-1425; 2002.

199. Fornance Jr, A. J.; Zmudzka, B.; Hollander, M.C.; Wilson, S.H. Induction of b-polymerase mRNA by DNA-damaging agents in Chinese hamster ovary cells. Mol. Cell Biol. **9**, 851-853; 1989.

200. Chen, K.H.; Yakes, F.M.; Srivastava, D.K.; Singhal, R.K.; Sobol, R.W.; Horton, J. K.; vanHouten, B.; Wilson, S.H. Upregulation of base excision repair correlates with enhanced protection against a DNA damaging agent in mouse cell lines. Nucleic Acids Res. **26**, 2001-2007; 1998.

201. Lin, L. H.; Cao, S.; Yu, L.; Cui, J.; Hamilton, W.J.; Liu, P.K. Upregulation of base excision repair activity for 8-hydroxy-2'deoxyguanosine in the mouse brain after forebrain ischemia reperfusion. J. Neurochem. **74**, 1098-1105; 2000.

202. Lindahl, T. Inroads into base excision repair I: The discovery of apurinic/apyrimidinic [AP] endonuclease. DNA Repair **3:** 1521-1530; 2004.

203. Xanthoudakis, S.; Curran, T. Identification and characterization of Ref-1, a nuclear protein that facilitates AP-1 DNA-binding activity. EMBO J. **11 :** 653-665 ; 1992.

204. Xanthoudakis, S.; Miao, G.; Wang, F.; Pan, Y.C.; Curran, T. Redox activation of Fos-Jun DNA binding activity is mediated by a DNA repair enzyme. EMBO J. **11:** 3323-3335; 1992.

205. Srivastava, D.K.; Vande Berg, B.J.; Prasad, R.; Molina, J.T.; Beard, W.A.; Tomkinson, A.E.; Wilson S.H. Mammalian abasic site base excision repair. Identification of the reaction sequence and rate-determining steps. J.Boil.Chem **273:** 21203-21209; 1998.

206. Meira, L.B.; Devaraj, S.; Kisby, G.E.; Burns, D.K.; Daniel, R.L.; Hammer, R.E.; Grundy, S.; Jialal, I.; Friedberg, E.C. Heterozygosity for the mouse *Apex* gene results in phenotypes associated with oxidative stress . Cancer Res. **61:** 5552-5557; 2001.

207. Ludwig, D.L.; MacInnes, M.A.; Takiguchi, Y.; Purtymun, P.E.; Henrie, M.; Flannery, M.; Meneses, J.; Pederson, R.A.; Chen, D.J. A murine AP-endonuclease gene-targeted deficiency with post-implantation embryonic progression and ionizing radiation sensitivity. Mutat.Res**. 409:** 17-29; 1998.

208. Unnikrishnan, A.; Raffoul, J.J.; Patel, H.V.; Prychitko, T.M.; Anyangwe, N.; Meira, L.B.; Friedberg, E.C.; Cabelof, D.C.; Heydari, A.R. Oxidative stress alters base excision repair pathway and increases apoptotic response in apurinic/apyrimidinic endonuclaese 1/redoxfactor-1 haploinsufficient mice. Free Rad. Biol. Med. **49**, 1488-1499; 2009.

209. Gu, H.; Marth, J.D.; Orban, P.C.; Mossmann, H.; Rajewsky, K. Deletion of a DNA polymerase beta gene segment in T cells using cell type-specific gene targeting. Science **265**, 103-106; 1994.

210. Cabelof, D.C.; Guo, Z.; Raffoul, J.J.; Sobol, R.W.; Wilson, S.H.; Richardson, A.; Heydari, A.R. Base excision repair deficiency caused by polymerase □ haploinsufficiency: Accelerated DNA damage and increased mutational response to carcinogens. Cancer Res. **63**, 5799-5807; 2003.

211. Cabelof, D.C.; Raffoul, J.J.; Nakamura, J.; Kapoor, D.; Abdalla, H.; Heydari, A.R. Imbalanced base excision repair in response to folate deficiency is accelerated by polymerase □ haploinsufficiency. J. Biol.Chem. **279**, 36504-36513; 2004.

212. Duthie, S.J.; Hawdon, A. DNA instability [strand breakage, uracil misincorporation, and defective repair] is increased by folic acid depletion in human lymphocytes in vitro. Faseb J. **12**, 1491-1497; 1998.

213. James, S. J.; Basnakian, A. G.; Miller, B.J. In vitro folate deficiency induces deoxynucleotide pool imbalance, apoptosis, and mutagenesis in Chinese hamster ovary cells. Cancer Res. **54**, 5075-5080; 1994.

214. Alberto Sanz, Pilar Caro, Victoria Ayala, Manuel Portero-otin, Reinald Pamplona and Gustavo Barja. The Faseb Journal. 20: 1064-13: 2006.

215. Reinald Pamplona and Gustavo Barja. Biochemica et Biophysica Acta. 1757: 496-508: 2006.

216. Miller, R. A., Buehner, G., Chang, Y., Harper, J.M., Sigler, R., and Smith-Wheelock, M. Methionine-deficient diet extends mouse life-span, slows immune and lens aging, alters glucose, T4, IGF-1 and insulin levels, and increases hepatocyte MIF levels and stress resistance. Aging Cell, 4, 119-25, 2005.

217. Ventrella-Lucente, L.F.; Unnikrishnan, A.; Pilling, A. B.; Patel, H.V.; Kushwaha, D.; Dombkowski, A.A.; Schmelz, E. M.; Cabelof, D.C.; Heydari, A.R. Folate deficiency provides protection against colon carcinogenesis in DNA polymerase beta haploinsufficiency mice. J.Biol.Chem. **285**, 19246-51928; 2010.

218. Cabelof DC, Nakamura J, Heydari AR: A sensitive biochemical assay for the detection of uracil. *Environ Mol Mutagen* , **47**(1):31-37; 2006.

219. Hou, E.W.; Prasad, R.; Asagoshi, K.; Masaoka, A.; Wilson, S.H. Comparative assessment of plasmid and oligonucleotide DNA substrates in measurement of in vitro base excision repair activity. Nucleic Acids Res. **35:** 1-10; 2007.

220. Bird RP. Role of aberrant crypt foci in understanding the pathogenesis of colon cancer. Cancer Lett. Jun 29;93(1):55-71;1995.

221. mcLellan, E, A., Medline, A., and Bird, R,P. Cancer Res. 51, 5270-5274; 1991.

222. Fenoglio-Preiser, c.M., and Noffsinger, A. Toxicol.Pathol. 27, 632-642; 1999.

223. James, S.J.; Miller, B. J.; Basnaknian, A.G.; Pogribny, I.P.; Pogribna, M.; Muskhelishvili, I. Apoptosis and proliferation under conditions of deoxynucleotide pool imbalance in liver of folate/methyl deficient rats. Carcinogenesis **18**, 287-293; 1997

224. Duthie, S.J., Grant, G. and Narayanan, S. Increased uracil misincorporation in lymphocytes from folate- deficient rats. Br.J.Cancer *83:*1532-1537, 2000.

225. Kim YI, Shirwadkar S, Choi SW, Puchyr M, Wang Y, Mason JB: Effects of dietary folate on DNA strand breaks within mutation-prone exons of the p53 gene in rat colon. *Gastroenterology* , **119**(1):151-161; 2000.

226. Pogribny IP, Muskhelishvili L, Miller BJ, James SJ: Presence and consequence of uracil in preneoplastic DNA from folate/methyl-deficient rats. *Carcinogenesis* , **18**(11):2071-2076; 1997.

227. Duthie, S.J., Narayanan, S., Blum, S., Pirie, L. and Brand, G.M. Folate deficiency in vitro induces uracil misincorporation and DNA hypomethylation and inhibits DNA excision repair in immortalized normal human colon epithelial cells. Nutr.Cancer 37:245-251, 2000.

228. Melnyk, S.; Pogribna, M.; Miller, B. J.; Basnakian, A. G.; Pogribny, I.P.; James, S.J. Uracil misincorporation, DNA strand breaks, and gene amplification are associated with tumorigenic cell transformation in folate deficient/repleted Chinese hamster ovary cells. Cancer Letters **146**, 35-44; 1999.

229. Kim,Y,I., Shirwadkar, S., Choi, S.W., Puchyr, M., Wang, Y., and Mason, J. B. Gastroenterology 119, 151-161; 2000.

230. Blount BC, Mack MM, Wehr CM, MacGregor JT, Hiatt RA, Wang G, Wickramasinghe SN, Everson RB, Ames BN: Folate deficiency causes uracil misincorporation into human DNA and chromosome breakage: implications for cancer and neuronal damage. *Proc Natl Acad Sci U S A*, **94**(7):3290-3295; 1997.

231. Lindahl, T. Instability and decay of the primary structure of DNA: Nature, 362, 709-715; 1993.

232. Lindahl T: Keynote: past, present, and future aspects of base excision repair. *Prog Nucleic Acid Res Mol Biol*, **68**:xvii-xxx; 2001.

233. Parikh, S.S.; Mol, C.D.; Hosfield, D.J.; Tainer, J.A. Envisioning the molecular choreography of DNA base excision repair. Curr. Opin. Struct. Biol. 9: 37-47; 1999.

234. Wilson, S.H.; Kunkel, T.A. Passing the baton in base excision repair. Nature Struct. Biol. **7:** 176-178; 2000.

235. Kerr, J.F., Winterford, C.M., and Harmon, B.V. Apoptosis: its significance in cancer and cancer therapy. Cancer, 73, 2013-2026; 1994.

236. Chen, Y., Yang, Y., et al. Hepatocyte-specific Gclc deletion leads to rapid onset of steatosis with mitochondrial injury and liver failure. Hepatology; 45, 1118-28; 2007.

237. Starkebaum, G. & Harlan, J. M. (1986) Endothelial cell injury due to copper-catalyzed hydrogen peroxide generation from homocysteine. J. Clin. Invest.77: 1370-1376.

238. Chern CL, Huang RFS, Chen YH, Cheng JT, Liu TZ. Folate deficiency-induced oxidative stress and apoptosis are mediated via Homocysteine dependant overproduction of hydrogen peroxide and enhanced activation of NF-κB in human Hep G2 cells. Biomedicine and Pharmacotherapy, 2001 Oct, 55(8); 432-442.

239. Choudhary G, Hansen H: Human health perspective on environmental exposure to hydrazines: a review. *Chemosphere* , **37**(5):801-843; 1998.

240. No, H., Kwon, H., Park, Y., Cheon, C., Park, J., Park, T., Aruoma, O., and Sung, M. Nutr. Res. 27, 659-664; 2007.

241. Khan, R., and Sultana, S. Farnesol attenuates 1,2-dimethylhydrazine induced oxidative stress, inflammation and apoptotic responses in the colon of wistar rats. Chemico-Biological Interactions 192, 193-200; 2011.

242. Despina Komninou, Yvonne Leutzinger, Bandaru S. Reddy, and John P. Richie Jr. Methionine restriction inhibits colon carcinogenesis. Nutrition and Cancer.,54(2), 202-208; 2006.

243. Branda, R, F., Lafayette, A.R., O'Neill, J. P., and Nicklas, J.A. Mutation Res. 427, 79-87; 1999.

244. Duthie, S. J., and Hawdon, A. FASEB J, 12, 1491-1497; 1998.

245. Parikh, S.S.; Mol, C.D.; Hosfield, D.J.; Tainer, J.A. Envisioning the molecular choreography of DNA base excision repair. Curr. Opin. Struct. Biol. **9:** 37-47; 1999.

246. Wilson, S.H.; Kunkel, T.A. Passing the baton in base excision repair. Nature Struct. Biol. **7:** 176-178; 2000.

247. Krokan, H.E., Drablos, F., and Slupphaug. Uracil in DNA-occurrence, consequences and repair. Oncogene, 21, 8935-8948; 2002.

248. Mcintosh, E, M., and Haynes, R, H. dUTP pyrophosphatase as a potential target for chemotherapeutic drug development. Acta Biochemica Polonica. 44, 159-172; 1997.

249. Saitoh, M., Nishitoh, H., et al. Mammalian thioredoxin is a direct inhibitor of apoptosis signal-regulating kinase (ASK) 1. The EMBO Journal. 17, 2596-2606; 1998.

250. Tonissen, K, F., and Di Trapani. Thioredoxin system inhibitors as mediators of apoptosis for cancer therapy. Mol Nutr Food Res, 53, 87-103; 2009.

251. Brigelius-Flohe, R and Kipp, A. Glutathione peroxidases in different stages of carcinogenesis. Biochimica et Biophysica Acta, 1790, 1555-1568; 2009.

252. Padhye, S., Ahmad, A., Oswal, N., and Sarkar, F. Emerging role of garcinol, the antioxidant chalcone from garcinia indica choisy and its synthetic analogs. Journal of Hematology & Oncology, 2; 2009.

253. Anand, P., Sundaram, C., Jhurani, S., Kunnumakkara, A., and Aggarwal, B. Curcumin and cancer: An 'old-age' disease with an 'age-old solution. Cancer Letters, 267, 133-164; 2008.

254. Wilken, R., veena, M., Wang, M., and Srivatsan, E. Curcumin: A review of anti- cancer properties and therapeutic activity in head and neck squamous cell carcinoma. Mol. Cancer, 10, 2011.

255. Goldman, I.D., Chattopadhyay, S., Zhao, R., and Moran R. The antifolates: evolution, new agents in the clinic, and how targeting delivery via specific membrane transporters is driving the development of a next generation of folate analogs. Curr Opin Investig Drugs, 11, 1409-23; 2010.

256. Exinger, D., Exinger, F., Mennecier, B et al. Multitargeted antifolate (Pemetrexed): A comprehensive review of its mechanisms of action, recent results and future prospects. Cancer Therapy, 1, 315-322; 2003.

257. Cindy, C.D.; Milner, J. Frontiers in Nutrigenomics, proteomics, metabolomics and cancer prevention. Mut.Res. **551,** 51-64; 2004.

258. Eussen, S.J.P.M.; Vollset, S. E.; Igland, J.; Meyer, K.; Fredriksen, A.; Ueland, P.M.; Jenab, M.; Slimani, N.; Boffetta, P.; Overvad, K.; Tjonneland, A.; Olsen, A.; Clavel-Chapelon, F.; Boutron-Ruault, M-C.; Morois, S.; Weikert, C.; Pischon, T.; Linseisen, J.; Kaaks, R.; Trichopoulou, A.; Zilis, D.; Katsoulis, M.; Palli, D.; Berrino, F.; Vineis, P.; Tumino, R.; Panico, S.; Peeters, P.H.M.; Bueno-de-Mesquita, H.B.; Duijnhoven, F.J.B.V.; Gram, I.T.; Skeie, G.; Lund, E.; Gonzalez, C.A.; Martinez, C.; Dorronsoro, M.; Ardanaz, E.; Navarro, C.; Rodriguez, L.; Guelpen, B.V.; Palmqvist,

R.; Manjer, J.; Ericson, U.; Bingham, S.; Khaw, K-T.; Norat, T.; Riboli, E. Plasma folate, related genetic variants and colorectal cancer risk in EPIC. Cancer Epidemiol Biomarkers Prev **19**, 1328-1340; 2010.

259. Kim, Y-I. Folate, colorectal carcinogenesis, and DNA methylation: Lessons from Animal studies. Environ. Mol. Mutagen. **44**, 10-25; 2004.

260. Linhart, H. G.; Troen, A.; Bell, G.W.; Cantu, E.; Chao, W-H.; Moran, E.; Steine, E.; He, T.; Jaenisch, R. Folate deficiency induces genomic uracil misincorporation and hypomethylation but does not increase DNA point mutations. Gasteroenterology **136**, 227-235; 2009.

261. Logan, R.F.; Grainge, M.J.; Shepherd, V.C.; Armitage, N.C.;Muir, K.R. Aspirin and folic acid for the prevention of recurrent colorectal adenomas. Gastroenterology **134**, 29-38; 2008.

262. Cole, B.F.; Baron, J.A.; Sandler, R.S.; Haile, R.W.; Ahnen, D.J.; Bresalier, R.S.; Eyssen, G.M.; Summers, R.W.; Rothstein, R.I.; Burke, C.A.; Snover, D.C.; Church, T.R.; Allen, J.I.; Robertson, D.J.; Beck, G.J.; Bond, J.H.; Byers, T.; Mandel, J.S.; Mott, L.A.; Perason, L.H.; Barry, E.L.; Rees, J.R.; Marcon, N.; Saibil, F.; Ueland, P.M.; Greenberg, R. Folic acid for the prevention of colorectal adenomas: a randomized clinical trial. JAMA **297**, 2351-2359; 2007.

263. Van Guelpen, B.; Hultdin, J.; Johansson, I.; Hallmans, G.; Stenling, R.; Riboli, E.; Winkvist, A.; Palmqvist, R. Low folate levels may protect against colorectal cancer. Gut **55**, 1461-1466; 2006.

264. Choi, S-W.; Kim, Y-I.; Weitzel, J.N.;Mason, J.B. Folate depletion impairs DNA excision repair in the colon of the rat. Gut **43**, 93-99; 1998.

265. Raffoul, J.J.; Cabelof, D.C.; Nakamura, J.; Meira, L.B.; Friedberg, E.C.; Heydari, A.R. Apurinic/apyrimidinic endonuclease [APE/REF-1] haploinsufficient mice display tissue-specific differences in DNA polymerase beta-dependent base excision repair. J. Biol. Chem. **279:** 18425-18433; 2004.

266. Yang, Z., Waldman, A.S., and Wyatt, M.D. DNA damage and homologous recombination signaling induced by thymidylate deprivation. Biochem Pharmacol. 76, 987-996;2008.

267. Novakovic, P.; Stempak, J. M.; Sohn, K-J.; Kim, Y-I. Effects of folate deficiency on gene expression in the apoptosis and cancer pathways in colon cancer cells. Carcinogenesis 27, 916-924; 2006.

268. Branda,R.F., Hacker,M., Lafayette,A., Nigels,E., Sullivan,L., Nicklas,J,A., and O'Neill,J,P. Environ.Mol.Mutagen 32,33-38; 1998.

269. Unnikrishnan, A., Prychitko, T., Patel, H., Choedhury, M., Pilling, A., Ventrella-Lucente, L., Papakonstantinou, E.., Cabelof, D and Heydari, A. Folate deficiency regulates expression of DNA polymerase b in response to oxidative stress. Free Radical Biology & Medicine. 50, 270-280; 2011.

270. Otterlei, M., Kavli, B., Standahl, R., Skjelbred, C., Bharati, S., and Krokan, H, Einar. Repair of chromosomal abasic sites in vivo involves at least three different repair pathways. The EMBO Journal, 19, 5542-5551; 2000.

271. Ying, J.; Srivastava, G.; Hsieh, W.S.; Gao, Z.; Murray, P.; Liao, S.K.; Tao, Q. The stress-responsive gene GADD45g is a functional tumor suppressor, with its response to environmental stresses frequently disrupted epigenetically in multiple tumors. Clin. Cancer Res. **18:** 6442-6449; 2005.

272. Takekawa, M.; Saito, H. A family of stress-inducible GADD45-like proteins mediate activation of the stress-responsive MTK1/MEKK4/MAPKKK. Cell **95:** 521-530; 1998.

273. Sanchez-Roman., Gomez, A., Gomez, J et al. Forty percent methionine restriction lowers DNA methylation, complex I ROS generation, and oxidative damage to mtDNA nd mitochondrial proteins in rat heart. J Bioenerg Biomembr, 2011.

274. Shan Lu, Sara M. Hoestje, Eugene M. Choo, Daniel E. Epner. Methionine restriction induces apoptosis of prostate cancer cells via the c-Jun N-terminal kinase-mediated signaling pathway. Cancer Letter. 2002; 51-58.

275. Xin L, Cap WX, Fei XF, Want Y, Liu Wt, Liu BY, Zhu Zg. Applying proteomic methodologies to analyze the effect of methionine restriction on proliferation of human gastric cancer SGC7901 cells. Clin Chim Acta. 2007 Feb;377(1-2):206-12.

276. Xin L, Cap WX, Fei XF, Want Y, Liu Wt, Liu BY, Zhu Zg. Applying proteomic methodologies to analyze the effect of methionine restriction on proliferation of human gastric cancer SGC7901 cells. Clin Chim Acta. Feb;377(1-2):206-12; 2007.

277. Le Leu,, R. K., Young, G.P. and McIntosh, G.H. Folate deficiency diminishes the occurrence of aberrant crypt foci in the rat colon but does not alter global DNA methylation status. J Gastroenterology Hepatol, 15, 1158-64; 2000.

278. Le Leu, R.K., Young, G.P. and McIntosh, G.H. Folate deficiency reduces the development of colorectal cancer in rats. Carcinogenesis *21:*2261-2265, 2000.

ABSTRACT

BASE EXCISION REPAIR, FOLATE DEFICIENCY AND CANCER

by

ARCHANA UNNIKRISHNAN

December 2011

Advisor: Dr Ahmad R. Heydari

Major: Nutrition and Food Science

Degree: Doctor of philosophy

Folate, an essential water soluble vitamin has been implicated in the etiology of many types of cancer especially colorectal cancer. Folate deficiency has been reported to incapacitate DNA repair pathways and thereby affect the genomic stability. Our lab has reported previously and here again through this research that folate deficiency affects the DNA damage inducibility of base excision repair pathway. Our study shows the differential effect folate deficiency has on the expression of the genes involved in this pathway. Further, our study shows the increase in preneoplastic lesions in the colon of mice exposed to folate deficiency in response to dimethylhydrazine, a colon and liver carcinogen. This study further supports our findings from previous studies from our lab that folate deficiency increases the susceptibility to cancer by deregulating DNA repair pathways, base excision repair in this scenario. Similarly, methionine restriction also, increases accumulation of preneoplastic lesions and incapacitates base excision repair in mice exposed to dimethylhydrazine. Since methionine restriction has shown to produce beneficial effects in laboratory rodents when the animals are exposed to long term restrictions, it would be interesting to put our animal models on methionine restriction and folate deficient diets for longer periods to test whether long term adaptations would bring about any beneficial effects.

AUTOBIOGRAPHICAL STATEMENT

ARCHANA UNNIKRISHNAN

Education

April 2000 Master of Science in Biochemistry
     University of Madras, India
April 1998 Bachelor of Science in Biochemistry
     University of Madras, India

Professional Experience:

2009-Present Research Assistant/Part-time faculty, Department of Nutrition and Food Science
     Wayne State University, Detroit, MI
2005-2009 Graduate Teaching Assistant, Department of Nutrition and Food Science
     Wayne State University, Detroit, MI
2004-2005 Graduate Research Assistant, Department of Nutrition and Food Science
     Wayne State University, Detroit, MI
2000-2002 Lecturer, Department of Biochemistry
     University of Madras, India

Publications:

Heydari AR, Unnikrishnan A, Lucente LV, Richardson A. Caloric restriction and DNA repair. Nucleic Acids Res. 2007;35 (22):7485-96.

Unnikrishnan A, Raffoul JJ, Patel H, Prychitko TM, Anyangwe N, Meira LB, Friedberg EC,. Cabelof DC and Heydari AR. Oxidative stress alters base excision repair pathway and increases apoptotic response in Apurinic/apyrimidinic endonuclease 1/Redox factor-1 haploinsufficient mice. Free Radic. Biol. Med. 2009 Jun 1:46(11):1488-99.

Ventrella-Lucente L, Unnikrishnan A, Pilling AB, Patel HV, Kushwaha D, Dombkowski A, Schmelz EV, Cabelof DC and Heydari AR. Folate Deficiency provides protection against colon carcinogenesis in DNA polymerase □ haploinsufficient mice. Journal of Biol. Chem. 2010 Jun 285: 19246-19256.

Unnikrishnan A, Prychitko TM, Patel HV, Chowdhury ME, Pilling AB, Ventrella-Lucente L, Papakonstantinou EV, Cabelof DC and Heydari AR. Folate Deficiency regulates expression of DNA polymerase -β in response to oxidative stress. Free Radic. Biol. MED. 2010.

Presentations:

Apurinic/apyrimidinic endonuclease 1/Redox factor-1 (APE1/Ref-1) Haploinsufficient Mice are Hypersensitive to Oxidative DNA Damage. Midwest DNA repair symposium (Ohio State University, Ohio). May 2007. Poster Presentation.

Differential effect of 2-NP on gene expression of enzymes involved in DNA repair pathways in response to folate deficiency. Midwest DNA repair symposium (Indiana State University, Indianapolis). May 2006. Poster presentation.

Deregulation of polymerase β expression by folate deficiency: Role of DNA methylation. Midwest DNA repair symposium (Wayne State University, Michigan). May 2005. Poster presentation.

Protective effect of α-tocopherol on carbon tetra chloride induced lipid peroxidation in rat liver homogenates. Science symposium (University of Madras, India). March 2002. Platform presentation.